

**The Structural Basis of the p50:p50:HDAC1 Anti-inflammatory  
Corepressor Complex**

Tyrell Neko Cartwright

Doctor of Philosophy

Submitted: September 2018





## Abstract

---

Protein-protein interactions between NF- $\kappa$ B subunits and many transcriptional regulatory proteins have been discussed and in some cases well understood, however, the structural basis of the previously described p50:p50-Histone Deacetylase 1 (HDAC1) inflammatory repressor complex is poorly characterized. Understanding the mechanism of this interaction will be invaluable in the search for therapeutics that exploit this complex to attenuate inflammation in a potentially IKK-independent manner.

We have combined *in silico* analysis along with *in vitro* peptide arrays, co-expression and co-immunoprecipitation assays to verify potential sites of interaction between the p50 homodimer and HDAC1. Multiple sites of interest on the p50 structure determined from *in silico* predictions were combined with peptide array data to reveal clear regions of potential interaction between p50 and HDAC1. Detailed directed mutagenesis of one such region (the nuclear localization sequence) resulted in a loss of the interaction between p50 and HDAC1 in co-immunoprecipitation experiments. Additionally, loss of this HDAC1 interaction appears to induce a greater pro-inflammatory response in both resting and stimulated conditions. These results provide the first structural evidence of a direct interaction and points to a specific region of p50 as the key region for p50 protein-protein interaction.

Establishing the rules governing this critical complex will undoubtedly assist in further exploration of its properties *in vivo* and shed light on the complex interactions of NF- $\kappa$ B transcription factors and their co-regulators. Further studies have the potential to identify novel tailored therapeutic targets in diseases characterized by both acute and chronic inflammation unencumbered by the drawbacks associated with the ubiquitous actions of therapeutic kinase inhibitors.



## Dedication

---

This thesis is dedicated to my mother Debra D. Cartwright for her self-sacrifice to ensure that any dream I had could be achieved often at the expense of her own comfort. Who gave every moment of her life wanting nothing more than my happiness. While she may never get to see me achieve this milestone I am grateful for her memory and all that she has done for me. None of this would have been possible without her.



## Acknowledgements

---

I would like to thank and acknowledge the numerous people who have in some way assisted me through this project. My collaborators Professor Patrick Kiely and Dr Catriona Dowling from the University of Limerick and Professor Tom Edwards and Dr Sarah Harris from Leeds University all of who's expertise has greatly enhanced this project. I would also like to thank the additional coauthors on the published manuscript that has arisen from this work for their dedication and hard work needed during all stages of the publication process. Namely Dr. Julie Worrell, Ms Letizia Marchetti, Professor Jelena Mann and Ms Amber Knox. I would also like to thank the Faculty of Medical sciences and the Newcastle University Overseas Research Studentship Fund for funding this PhD as well as Prof. Neil Perkins and Prof. Jane Endicott for their valuable insight through this project as members of my progression panel. I would also like to thank my supervisors Professor Derek Mann and Dr Caroline Wilson for their overall insight and mentoring as well as unwavering support through more difficult personal circumstances. I will forever be grateful for the knowledge you have passed on and kindness you have shown.

Finally, I would like to thank my family whose constant guidance and support regardless of distance allowed me to complete this PhD. Thank you!



## Publications

---

Work from this thesis has directly lead to the publication of the following articles:

Borthwick LA, Suwara MI, Carnell SC, Green NJ, Mahida R, Dixon D, Gillespie C, **Cartwright TN**, Horabin J, Walker A, et al. (2015) *Pseudomonas aeruginosa* induced airway epithelial injury drives fibroblast activation: a mechanism in chronic lung allograft dysfunction. *Am J Transplant*.

**Cartwright T**, Perkins ND, L. Wilson C (2016) NFKB1: a suppressor of inflammation, ageing and cancer. *FEBS J* 283: 1812–1822.

**Cartwright TN**, Worrell JC, Marchetti L, Dowling CM, Knox A, Kiely P, Mann J, Mann DA, and Wilson CL (2018). HDAC1 Interacts with the p50 NF- $\kappa$ B Subunit via its Nuclear Localization Sequence to Constrain Inflammatory Gene Expression. *BBA Gene Regulatory Mechanisms*. Accepted for publication 6, September 2018.



# Table of Contents

---

Abstract .....	iii
Dedication .....	v
Acknowledgements .....	vii
Publications .....	ix
<b>Chapter 1 Introduction .....</b>	<b>8</b>
1.1 p50: A Canonical Member of the NF- $\kappa$ B Family .....	8
1.1.1 The NF- $\kappa$ B Family .....	8
1.1.2 NF- $\kappa$ B Activation .....	10
1.1.3 Deactivation of NF- $\kappa$ B Signaling .....	13
1.1.4 NF- $\kappa$ B Interactions and Modifications .....	14
1.1.4.1 RelA/p65 .....	14
1.1.4.2 c-Rel .....	15
1.1.4.3 RelB:p52 .....	17
1.1.5 NFKB1 - The p105/p50 Subunit .....	18
1.1.6 Interactions and Modifications of p50 .....	20
1.1.6.1 Posttranslational Modifications .....	20
1.1.6.2 Mutations .....	22
1.1.6.3 Protein-protein Interactions .....	23
1.2 HDAC1 and p50: Repressors of Inflammation .....	25
1.2.1 Nuclear Genetic Organization .....	25
1.2.2 Epigenetic Modification of Histones .....	26
1.2.3 HDAC1: A Class 1 Histone Deacetylase .....	28
1.2.4 Repression of Active NF- $\kappa$ B .....	30
1.2.5 Evidence for the p50:p50:HDAC1 Interaction .....	31
1.3 Aims .....	32
<b>Chapter 2 Materials and Methods .....</b>	<b>33</b>
2.1 Cell Culture .....	33
2.2 Cell Harvest and Protein Lysate Preparation .....	33
2.3 Western Blot .....	33
2.4 Proteasome Inhibition .....	34
2.5 Transient Transfection .....	34

2.6 Luciferase Assay.....	34
2.7 Molecular Dynamics Simulations .....	34
2.8 Multiple Sequence Alignment and Evolutionary Analysis.....	35
2.9 Immunofluorescence Microscopy.....	35
2.9.1 Endogenous Immunofluorescence.....	35
2.9.2 Nuclear Localization Immunofluorescence Microscopy .....	36
2.10 Flag, Endogenous and Co-Immunoprecipitation.....	36
2.11 GRAMM-X Protein Interaction Prediction and Visualization .....	37
2.12 Solvent Accessibility Calculations.....	37
2.13 PCR, Hi-Fidelity PCR and DNA Gel Purification.....	37
2.14 RNA Isolation, Quantitative Real Time PCR and General PCR Conditions.....	38
2.15 Generation of Mutant p50-FLAG Constructs.....	38
2.16 Generation of Chemically-competent DH5 $\alpha$ <i>E.coli</i> .....	39
2.17 Generation of petM30 protein expression constructs.....	39
2.18 DNA Ligation, Bacterial Transformation and Protein Expression.....	40
2.19 Bacterial DNA MiniPrep, MaxiPrep and Restriction Enzyme Digestion .....	41
2.20 Protein Purification.....	41
2.21 Coomassie Blue and Silver Stains .....	42
2.22 Peptide Arrays .....	42
2.23 Nuclear and Cytoplasmic Extracts .....	42
2.24 Chromatin Immunoprecipitation (ChIP) .....	43
2.25 TNF $\alpha$ Treatment .....	44
2.26 Enzyme Linked Immunosorbent Assay.....	44
2.27 Neutrophil Isolation and Chemotaxis Assay.....	44
2.28 Statistical Analysis .....	45

**Chapter 3 p50 Dimerization: Residues Critical to p50 Stability and Partner Selection..... 46**

3.1 Introduction.....	46
3.2 Aims .....	48
3.3 Results .....	49
3.3.1 Phosphorylation of p50 S343 as a master regulator of p50 homo-dimerization.....	49
3.3.2 Serine 343 of p50 is critical for protein stability .....	55
3.3.3 p50 Dimerization: Evolutionary Insights into Dimer Selection.....	62
3.4 Discussion .....	72

3.4.1 Post-Translational Modification as a Mechanism for Dimer Selection.....	72
3.4.2 Evolutionary Distinctiveness as the Major Control Mechanism of Dimer Assembly .....	73
3.4.3 Co-factors, Post-translational Modifications and Evolutionary Differences: The complexity of dimerization. ....	74
<b>Chapter 4 Determining the Structural Basis of the p50:HDAC1 Interface ....</b>	<b>76</b>
4.1 Introduction.....	76
4.2 Aims.....	77
4.3 Results .....	78
4.3.1 p50 associates with HDAC1 in resting cells.....	78
4.3.2 Predicting the p50:HDAC1 Interaction and Generation of Recombinant Proteins.....	84
4.3.3 Peptide Arrays Identify the Nuclear Localization Signal of p50 as the Primary Motif of Interaction with HDAC1.....	89
4.3.4 Mutation of the p50 NLS Ablates its Interaction with HDAC1 .....	96
4.4 Discussion.....	102
4.4.1 Nuclear p50 interacts with HDAC1 in resting cells in a Sin3A independent manner .....	102
4.4.2 Loss of p50's NLS Leads to a loss of HDAC1 Interaction.....	103
<b>Chapter 5 Function of p50<sup>Mu</sup> Mutant in the Context of a Loss of HDAC1 Interaction .....</b>	<b>105</b>
5.1 Introduction.....	105
5.2 Aims.....	106
5.3 Results .....	107
5.3.1 Mutation of p50 which causes a loss of HDAC1 Interaction Has no Effect on Canonical p50 Interactions .....	107
5.3.2 Mutation of p50 which causes a loss of HDAC1 Interaction Does not Inhibit Nuclear Localization.....	110
5.3.3 p50 <sup>Mu</sup> Does not alter DNA binding but increases $\kappa$ B Promoter Acetylation .....	112
5.3.4 p50 <sup>Mu</sup> recapitulates the pro-inflammatory phenotype observed when p50 homodimers are lost.....	116
5.4 Discussion.....	122
5.4.1 p50 Nuclear localization sequence is not essential for nuclear transport.....	122
5.4.2 Interaction with HDAC1 is vital to p50's ability to repress NF- $\kappa$ B target genes.....	122
<b>Chapter 6 General Discussion and Conclusion .....</b>	<b>126</b>
6.1 The complexities of NF- $\kappa$ B dimerization: control of the p50 homodimer .....	126
6.2 The p50 Nuclear localization sequence as a dynamic scaffold for the control of gene induction and suppression. ....	127
6.3 Interaction with HDAC1 is critical to the active gene repression of p50 homodimers.....	129

6.4 Conclusion .....	129
6.5 Future Work .....	130
6.6 Summary.....	132
<b>Chapter 7 Appendices.....</b>	<b>133</b>
<b>References .....</b>	<b>138</b>
<b>Chapter 8 Publications.....</b>	<b>138</b>

## Lists of Tables and Figures

---

<b>Figure 1.1 The NF-<math>\kappa</math>B Family.....</b>	<b>9</b>
<b>Figure 1.2 The NF-<math>\kappa</math>B Activation Pathway. ....</b>	<b>12</b>
<b>Figure 1.3 Post-translational Modifications of the NF-<math>\kappa</math>B Family. ....</b>	<b>16</b>
<b>Figure 1.4 The p50:p50 Homodimer. ....</b>	<b>19</b>
<b>Figure 1.5 Structure of the p105/p50 gene.....</b>	<b>21</b>
<b>Figure 1.6 Overview of the HDAC1 Molecule .....</b>	<b>29</b>
<b>Figure 3.1 Crystal Structure of a p50 Homodimer.....</b>	<b>50</b>
<b>Figure 3.2 Phylogenetic Tree of Species Used in Evolutionary Multiple Sequence Alignments. ....</b>	<b>52</b>
<b>Figure 3.3 Evolutionary Multiple Sequence Alignment of Serine Residues near Serine 340 (Human S343). ....</b>	<b>53</b>
<b>Figure 3.4 Serine Residues near S340 (Mouse) and their Relative Accessibility....</b>	<b>54</b>
<b>Figure 3.5 Western Blot Analysis of p50 S340A (Mouse) Expression.....</b>	<b>57</b>
<b>Figure 3.6 Molecular Dynamics Simulation of p50:p50S340A Homodimer .....</b>	<b>59</b>
<b>Figure 3.7 Relative Atomic Flux of a p50:p50S340A Molecular Dynamic Simulation .....</b>	<b>61</b>
<b>Figure 3.8 Evolutionary Analysis of all NF-<math>\kappa</math>B Subunits relative to their Respective Crystal Structures.....</b>	<b>63</b>
<b>Figure 3.9 Evolutionary Comparison of p50 and all other subunits and p50 against p65 .....</b>	<b>64</b>
<b>Figure 3.10 Dimerization Residues which differ between p50 and p65 through evolution .....</b>	<b>66</b>
<b>Figure 3.11 Metrics for a Wild Type p50 homodimer Molecular Dynamics Simulation.....</b>	<b>67</b>
<b>Figure 3.12 Metrics for a wild type p50:p65 Heterodimer Molecular Dynamics Simulation.....</b>	<b>68</b>
<b>Figure 3.13 Metrics for a p50;p50p65 Mutant Heterodimer Molecular Dynamics Simulation.....</b>	<b>69</b>

<b>Figure 3.14 Comparison of wild type p50 homodimers and p65 heterodimers against a mutant p50 homodimer which contains a p65 interface in one chain. ....</b>	<b>71</b>
<b>Figure 4.1 Immunofluorescent Microscopy of Endogenous p50/p105.....</b>	<b>79</b>
<b>Figure 4.2 Optimization of p50 Immunoprecipitation Assays.....</b>	<b>80</b>
<b>Figure 4.3 p50 Interacts with HDAC1 under Resting Conditions.....</b>	<b>82</b>
<b>Figure 4.4 Investigation of Tertiary Members of the p50:HDAC1 Complex .....</b>	<b>83</b>
<b>Figure 4.5 Direct binding prediction of the p50:HDAC1 interaction by the GRAMMX Server for Protein-Protein -Interactions.....</b>	<b>85</b>
<b>Figure 4.6 Coomassie Blue Stain of Purified TEV Protease.....</b>	<b>87</b>
<b>Figure 4.7 Generation of Expression Constructs of p50, p65 and HDAC1: Purification of recombinant p50.....</b>	<b>88</b>
<b>Figure 4.8 Recombinant Protein Expression Assay for Full and Fragment Length HDAC1 .....</b>	<b>90</b>
<b>Figure 4.9 Recombinant Protein Expression Assay of p65.....</b>	<b>91</b>
<b>Figure 4.10 Mapping the p50 Interaction on HDAC1 .....</b>	<b>93</b>
<b>Figure 4.11 Comparison of Predicted p50-HDAC1 Binding and Peptide Array Data .....</b>	<b>94</b>
<b>Figure 4.12 Mapping the HDAC1 interaction on p50 .....</b>	<b>95</b>
<b>Figure 4.13 Refinement of Residues Responsible for the p50:HDAC1 Interaction.</b>	<b>97</b>
<b>Figure 4.14 Mutation of Key Residues in the NLS of p50 Ablates the p50:HDAC1 Interaction.....</b>	<b>98</b>
<b>Figure 4.15 p50<sup>Mu</sup> disrupts endogenous p50:HDAC1 Interaction in Multiple Cell Types.....</b>	<b>101</b>
<b>Figure 5.1 Analysis of various cell types for expression of key complex components.....</b>	<b>108</b>
<b>Figure 5.2 p50<sup>Mu</sup> does not affect its ability to interact with p65 or IκBα .....</b>	<b>109</b>
<b>Figure 5.3 p50<sup>Mu</sup> does not affect nuclear localization.....</b>	<b>111</b>
<b>Figure 5.4 p50<sup>Mu</sup> does not alter DNA binding .....</b>	<b>113</b>
<b>Figure 5.5 p50<sup>Mu</sup> does not affect p50's ability to bind known target promoters .....</b>	<b>114</b>
<b>Figure 5.6 Cells reconstituted with p50<sup>Mu</sup> possess significantly more acetylation at promoters of known p50 target genes. ....</b>	<b>115</b>

<b>Figure 5.7 TNF<math>\alpha</math> time course in nfkb1<sup>-/-</sup> cells .....</b>	<b>117</b>
<b>Figure 5.8 Cells reconstituted with p50<sup>Mu</sup> display a more proinflammatory phenotype in comparison to wild type. ....</b>	<b>118</b>
<b>Figure 5.9 Cells reconstituted with p50Mu secrete more IL-6 than wild type. ....</b>	<b>119</b>
<b>Figure 5.10 p50Mu promotes significantly more neutrophil chemotaxis .....</b>	<b>121</b>
<b>Figure 5.11 Summary of a proposed mechanism for p50 homodimer and BCL3/HDAC1 mediated NF-<math>\kappa</math>B transcription repression. ....</b>	<b>125</b>
<b>Figure 6.1 Crystal structure of p65 homodimer bound to I<math>\kappa</math>B<math>\beta</math> .....</b>	<b>128</b>
<b>Appendix 7.1 petM30 Vector Map .....</b>	<b>133</b>
<b>Appendix 7.2 pcDNA3 Vector Map .....</b>	<b>134</b>

# Chapter 1 Introduction

---

## 1.1 p50: A Canonical Member of the NF- $\kappa$ B Family

### 1.1.1 The NF- $\kappa$ B Family

Nuclear Factor  $\kappa$  Light Chain Enhancer of B Cells or NF- $\kappa$ B in short, refers to a family of proteins, the first of which was discovered in the search for transcription factors that regulate the expression of the immunoglobulin  $\kappa$  light chain in B lymphocytes [1]. Today it is known that, in mammals, the NF- $\kappa$ B family consists of five distinct proteins, namely p65 (sometimes referred to as RelA), RelB, c-Rel, p105/p50 and p100/p52 [2]. As transcription factors, proteins which bind DNA and regulate the transcription of genes, they act to control a host of gene expression primarily involved in but not limited to cell proliferation and immune regulation [3]. The ability of these five proteins to regulate a wide variety of genes is believed to be accomplished by dimerization in various combinations. To some, historically NF- $\kappa$ B refers to heterodimers of p65 and p50 proteins, however, family members may combine in almost any homodimeric or heterodimeric configuration to drive or repress the transcription of a gene with one notable exception. In particular, the best studied case where a dimer does not form is that deconstructed by Vu *et. al.* [4]. They note that RelB is unable to form homodimers and is apparently only able to form heterodimers with p52 and p50 due to its unique structural evolution. RelB notwithstanding, each family member as well as its binding partner inform its affinity for particular DNA sequences greatly increasing its specificity and the numbers of potential binding sites. As a result, this family of transcription factors has become understood to be one of the most vital and responsible for the transcription of thousands of genes in multiple cell types and tissues.

Seen in **Figure 1.1** all five members contain an N-terminal region termed the Rel Homology Domain (RHD), which is an area of high sequence conservation and

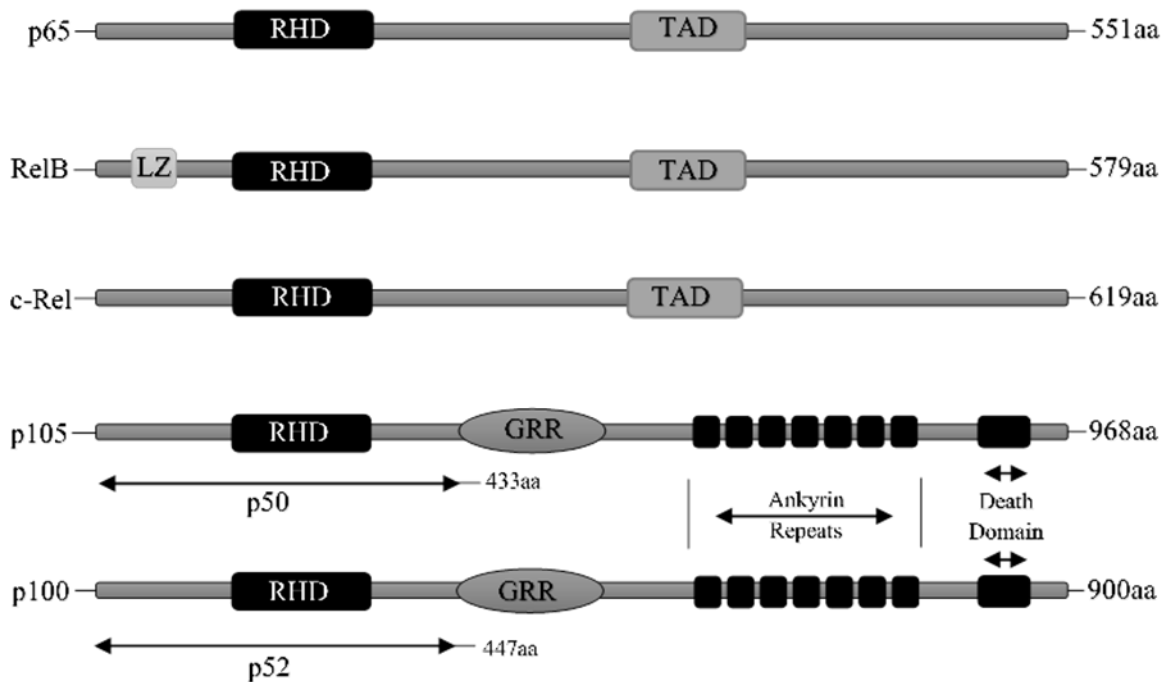


**Figure 1.1 The NF-κB Family.**

*The five members of the NF-κB family noting their unique structural similarities and differences including an evolutionarily conserved Rel Homology Domain (RHD). Other important elements include a Leucine Zipper-like (LZ) region unique to RelB and a Transcription Activation Domain (TAD) shared by class 1 family members. Class two members are presented in their unprocessed forms noting the presence of a Glycine Rich Region (GRR), used as the partial processing stop signal as well as seven Ankyrin repeats and a Death Domain involved in their function as an inhibitor of κB (IKB).*

contains both the region that allows dimerization (Dimerization Domain [DD]) and DNA Binding Domain (DBD) [5]. The five proteins are further divided into two classes based on the presence of a Transcription Activation Domain (TAD) which is required to drive transcription; only present in p65, RelB and c-Rel (Class II). Though some of their individual functions will be discussed later, it has been shown that independent of dimer partner, the family has a propensity to bind enhancer regions of DNA with the conserved sequence 5'-GGRNNYYCC-3' (where N is any base and Y is any pyrimidine) which has been termed the kappa-B consensus sequence [5]. Knowing that each subunit has its own effects and slightly different preferential DNA binding sequence and that its effects can be modulated based on its choice of binding partner all begin to describe some of the complexity relating to NF- $\kappa$ B function. To add to this, another layer of complexity can be found in how NF- $\kappa$ B itself is activated and regulated within the cell.

### **1.1.2 NF- $\kappa$ B Activation**

Prior to regulating gene transcription, NF- $\kappa$ B family members must themselves first be transcribed. Unlike some cases where the gene must be transcribed as a result of an external signal and then carry out its effect, it has been shown that NF- $\kappa$ B activation is a cytoplasmic process. This is due largely to the fact that NF- $\kappa$ B proteins are maintained in an inactive state in the cytoplasm by a class of inhibitory molecules known as the Inhibitors of  $\kappa$ B (I $\kappa$ B). Thought to include I $\kappa$ B $\alpha$ , I $\kappa$ B $\beta$ , I $\kappa$ B $\epsilon$ , I $\kappa$ B $\gamma$  and BCL-3 along with p105 and p100, they inactivate NF- $\kappa$ B by binding and masking the nuclear localization signal of the subunits preventing nuclear translocation [2]. Additionally, I $\kappa$ B's contain nuclear export signals ensuring they are kept mainly in the cytoplasm. It is noted that p105 and p100 are capable of inhibiting themselves and is a token of their unique origins. Unlike those in class two, these class one NF- $\kappa$ B subunits can be transcribed in larger forms than their active transcription regulation size. They must be cleaved into their p50 and p52 subunits before they are transcriptionally active and it is in these longer regions which are cleaved off that one can find the distinctive ankryin repeats shared by

the I $\kappa$ B family [6]. Recently, Kravtsova-Ivantsiv *et al.* found that KIP1 ubiquitination-promoting complex (KPC1), a ubiquitin ligase, was integral in the process of p105 degradation into p50 [7]. In 2006, Moorthy *et al.* found that p50 can be generated from p105 by the 20s proteasome in a ubiquitin independent manner and that the glycine rich region on p105 was the stop signal used by the proteasome in the processing of p105 to p50 [8]. They also noted, however, that p105 pools seemed to be protected from complete conversion to p50 which agrees with evidence found by Lin *et al.* who saw that p105 is not the only source of cellular p50 [9]. They found that p50 can be co-transcribed along with p105 and does not necessarily require partial processing of p105 for its creation. Nevertheless, p105 and p100 do serve as cytoplasmic inhibitors of not only p50 and p52 but other subunits as well as in the cytoplasmic high molecular weight complexes described by Savinova, Hoffmann and Ghosh [6].

While these different I $\kappa$ B's are responsible for sequestering cytoplasmic NF- $\kappa$ B, I $\kappa$ B Kinases (IKKs) are responsible for the release of NF- $\kappa$ B subunits to be taken into the nucleus to drive transcription. Made up of three subunits, namely IKK $\alpha$ , IKK $\beta$  and IKK $\gamma$  (also known as NF- $\kappa$ B essential modulator - NEMO), the IKK complex is responsible for the release of NF- $\kappa$ B from I $\kappa$ B by phosphorylation-directed polyubiquitination and proteasomeal degradation leading to nuclear localization of now free NF- $\kappa$ B subunits [10]. Recall though that there are several different I $\kappa$ B proteins and that NF- $\kappa$ B subunits can form many different dimer combinations, so one major area of poor understanding in the current literature is how specific pairs are formed and whether their co-localization partner in the cytoplasm remains unchanged or how and if they are able to switch their partner once transported to the nucleus. While it is known that different subunits have different affinities for different I $\kappa$ B's, the global picture is far from complete. Nevertheless, there is some understanding on the matter described in the three overall pathways of activation.

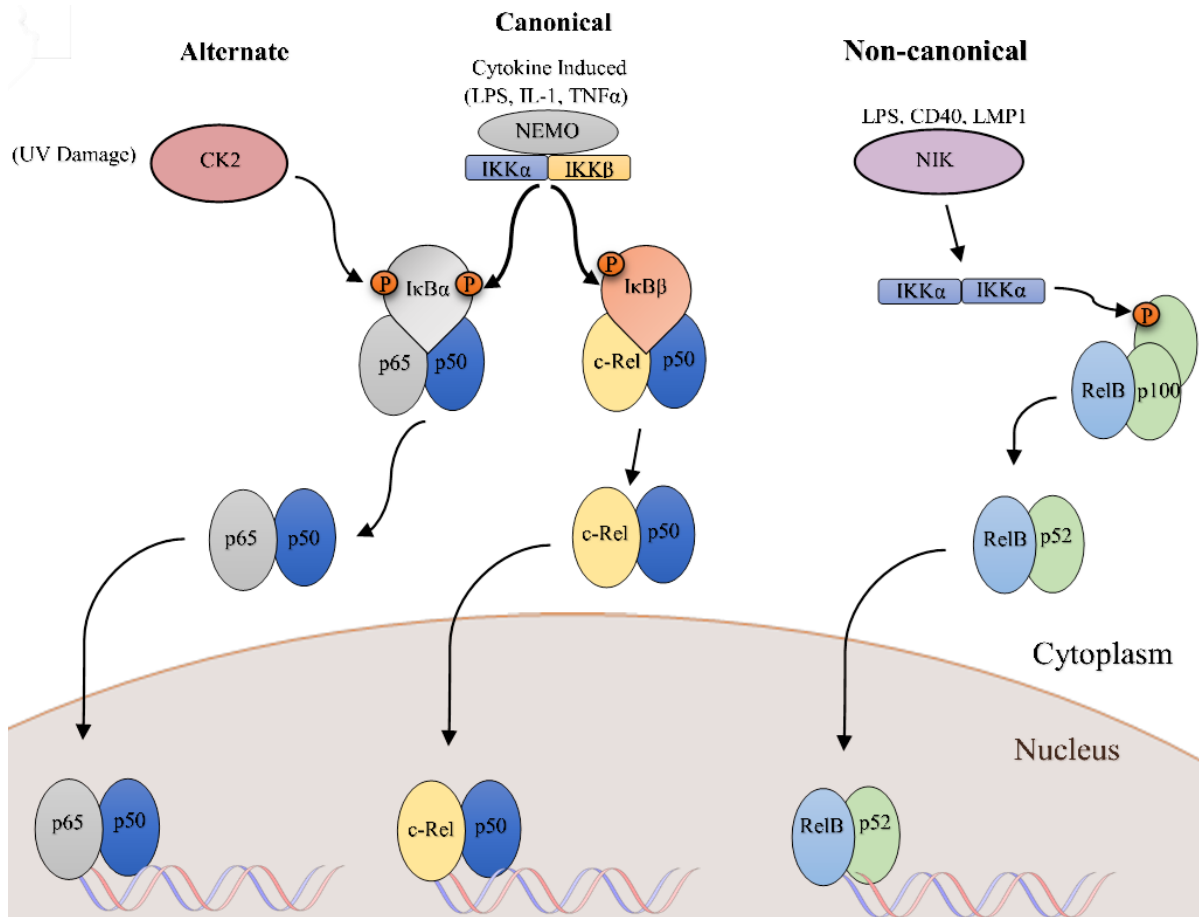


**Figure 1.2 The NF-κB Activation Pathway.**

Three major pathways of NF-κB activation including canonical, non-canonical and alternate pathway. In the canonical pathway, inflammatory ligands including TNFα and LPS activate the IKK complex consisting of IKKα, IKKβ and NEMO which phosphorylates IκB targeting it for ubiquitination and degradation and releasing active NF-κB dimers which can then go on to drive gene transcription in the nucleus. In the non-canonical pathway stimuli such as CD40 ligand activate NIK which phosphorylates an IKKα homodimer which may go on to phosphorylate p100 to facilitate its conversion to p52 by partial proteasomeal processing. RelB:p52 is then free to enter the nucleus and drive its own subset of genes. The alternate pathway is the most poorly described however it is usually initiated by stressors such as UV damage which activates kinases such as CK2 that can directly phosphorylate IκBs and similarly lead to active transcription factor release.

In the canonical pathway p65:p50 or c-Rel:p50 heterodimers are depicted as being sequestered by I $\kappa$ B $\alpha$  or I $\kappa$ B $\beta$  respectively and through signal transduction mediated by inflammatory cytokines such as TNF $\alpha$ , the IKK complex is able to phosphorylate I $\kappa$ B $\alpha$  on Serine 32 and 36. This signals I $\kappa$ B $\alpha$  for polyubiquitination and subsequent proteasomal degradation leading to the release and nuclear transport of p65:p50 [3]. In the non-canonical pathway, stress caused by viral means or binding of CD40 ligand to its receptor among others causes the activation of NF- $\kappa$ B Inducing Kinase (NIK) which activates IKK $\alpha$  which can phosphorylate p100, in a cytoplasmic RelB:p100 heterodimer, signaling its processing into p52, also mediated by a ubiquitination dependent mechanism [11]. Finally, another pathway described by Kato *et al.*, describes an IKK-independent activation in which Casein kinase 2 (CK2), in response to Ultra Violet DNA damage, can phosphorylate I $\kappa$ B $\alpha$  and, similar to the canonical pathway, lead to p65:p50 heterodimer release [12]. These pathways, summarized in **Figure 1.2**, make no mention of, and provide no explanations as to the mechanism of other types of dimer formations, especially homodimers and therefore do not tell the whole story but provide a basic framework from which to understand the complexity of NF- $\kappa$ B activation.

### 1.1.3 Deactivation of NF- $\kappa$ B Signaling

While work has uncovered nuances in the various pathways of NF- $\kappa$ B activation, less is known about how activation is resolved into a resting state. Analysis of genes transcribed by NF- $\kappa$ B subunits reveals that I $\kappa$ Bs themselves are transcribed [13]. Since the main defined role of these proteins is to sequester subunits and retain them in an inactive form in the cytoplasm, this has historically been thought of a major potential mechanism of post activation repression of signaling. This view has proven controversial however as there has been little evidence of the I $\kappa$ Bs' ability to enter the nucleus and export active subunits [14]. While others have shown evidence of active dimer shuttling between the nucleus and cytoplasm of stimulated cells, the involvement of I $\kappa$ Bs and terminators of signaling by active nuclear export remains unclear [15]. Nevertheless as a part of

their normal function, newly synthesized I $\kappa$ Bs can once again sequester subunits leading to loss of signal transduction.

In addition to eventual loss of signal through I $\kappa$ B re-synthesis, the ubiquitin system has been implicated as another major mechanism by which NF- $\kappa$ B signals can be terminated [16]. RelA has been shown previously to be a target of ubiquitin mediated proteasomal degradation. Additionally, BCL3 (a previously mentioned I $\kappa$ B) has been shown to bind nuclear p50 and block its ubiquitin mediated degradation [17]. To do this, unlike other I $\kappa$ Bs, BCL3 is a predominantly nuclear protein [18]. For p50 to require this protection along with evidence of p65 degradation suggests ubiquitin mediated ablation of NF- $\kappa$ B signaling and degradation of active subunits as a typical deactivation pathway. The extent to which ubiquitin mediated nuclear subunit degradation and I $\kappa$ B mediated cytoplasmic sequestration work in concert is not well established. These could represent two distinct deactivation pathways that are utilized in a stimuli or even subunit specific manner so that the correct subset of genes are modulated in an appropriately.

### **1.1.4 NF- $\kappa$ B Interactions and Modifications**

#### **1.1.4.1 RelA/p65**

In addition to the family's various pathways of activation, NF- $\kappa$ B activity is also under the control of numerous post-translational modifications and protein interactions. Among the subunits, p65 is without question the most well studied to date and therefore unsurprisingly it also has the most known post translational modifications, many of which have been understood reasonably well. It is well known that p65 is a critical subunit with knockout mice displaying embryonic lethality due to hepatocyte apoptosis [19]. Additionally, it has been shown to play critical roles in immunity by transcribing Fas (an apoptosis related factor) and TRAF1 (Tumor Necrosis Factor receptor-associated factor 1) [20]. Often p65 is studied in the form of p65:p50 heterodimers but p65 has been attributed many functions independent of p50. Of note is its role in the transcription of c-fos (another

transcription factor associated with cell proliferation and differentiation) and TNF $\alpha$  mediated transcription of I-CAM1 (intracellular adhesion molecule 1) [16,17]. Besides these direct transcription targets, work has shown that p65 also forms many direct protein-protein interactions. Fazal *et. al.* found that p65's interaction with cytoskeletal actin formed a basis for a pathway leading to its nuclear translocation with the assistance of thrombin [21]. Evidence by Akiyama *et. al.* showed that TNF $\alpha$  mediated activation of human telomerase reverse transcriptase (hTERT) involved direct interaction with p65 and Deng *et. al.* showed that  $\beta$ -catenin can interact with and inhibit p65 transcriptional activation [20,22]. Chen *et. al.* note that acetylation of p65 on lysine residues 218, 221 and 310 have marked impacts on its DNA binding affinity and transcriptional activity but also its association with I $\kappa$ B $\alpha$  [23]. Furthermore, they discovered that acetylation was caused by its association with p300, which was enhanced by its phosphorylation at serine 276 and 536 and that these modifications enhanced p65 activity. Kiernan *et. al.* also found an important role for acetylation in the inactivation of p65 [24]. They propose that acetylation at lysine 122 and 123 performed by p300 and PCAF plays a part in its removal from DNA and thus subsequent nuclear exportation by association with I $\kappa$ B $\alpha$ . Also, Moles *et. al.* were able to reduce NF- $\kappa$ B driven fibrosis by inhibiting serine 536 phosphorylation, believed to be another p65 activation modification [25]. As seen in **Figure 1.3** these descriptions are not exhaustive, however, they highlight the great deal of work that has been done on p65. Unfortunately, the same cannot be said for the other subunits, in particular, less is known about c-Rel.

#### **1.1.4.2 c-Rel**

Discovered as a proto-oncogene, c-Rel has most extensively been studied in the field of immunology since it was found that c-Rel was critical in the ability of T-cells to produce interleukin 2 (IL-2) [26]. Much of the work around c-Rel has involved the use of knockouts to highlight its role in various pathways, diseases and in one interesting case, head and neck cancer [27]. To date a role for c-Rel has been elucidated in rheumatoid arthritis, heart disease and in mice loss of c-Rel was shown to be protective against inflammatory bowel disease (IBD) [25–27].

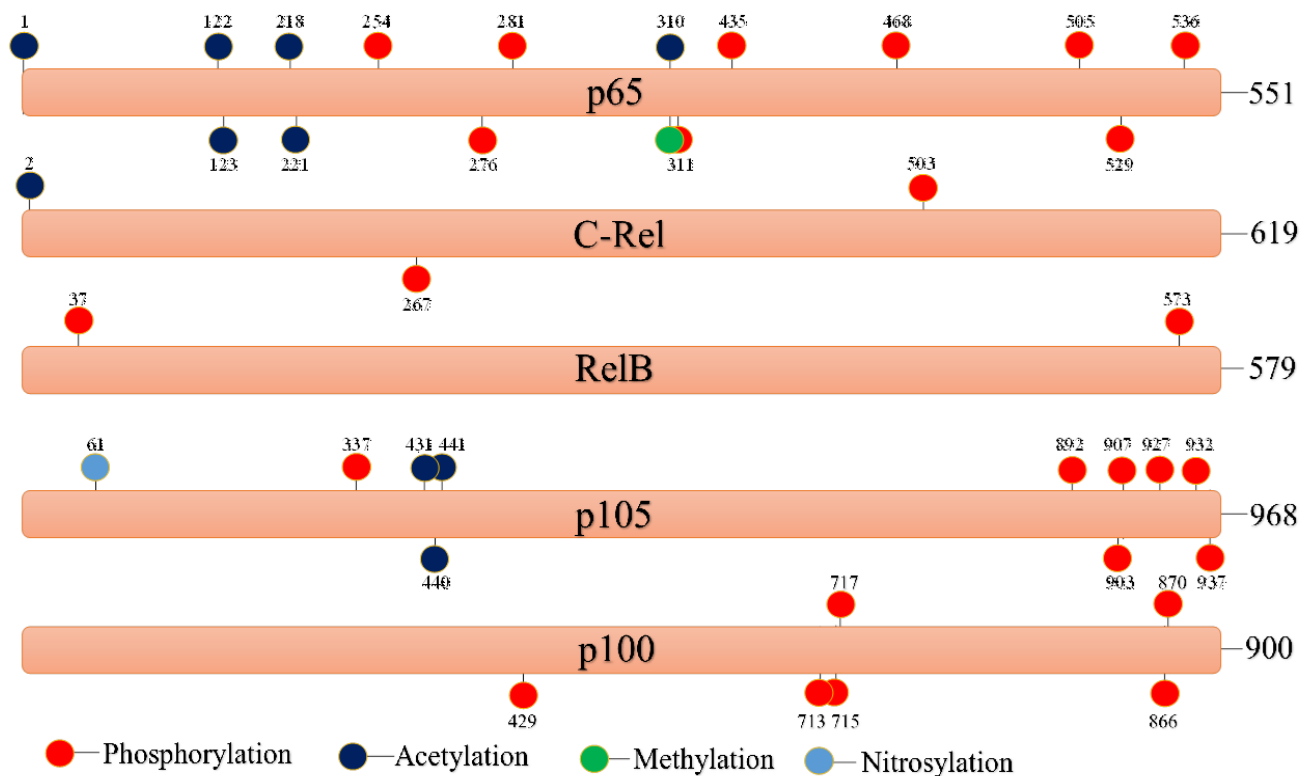


**Figure 1.3 Post-translational Modifications of the NF-κB Family.**

*Current known post-translational modifications within the five subunits of the NF-κB family. Designations refer to positions in the human protein. Only residues which been experimentally verified have been included.*

Bunting *et. al.* have also shown that c-Rel can regulate transcription of itself in addition its many other targets, a trait shared by most proteins in the NF- $\kappa$ B family [28]. As it relates to post-translational modifications, knowledge about c-Rel is limited to work by Martin and Fresno citing the most convincing case related to phosphorylation at serine 503 being required for TNF $\alpha$  activation [28]. While Huang *et. al.* have solved the crystal structure of c-Rel and Clark *et. al.* have shown c-Rel is inhibited by I $\kappa$ B $\epsilon$  in addition to I $\kappa$ B $\beta$ , very little else had been published in relation to the structural complexities of this subunit [29,30]. Like p65, however, c-Rel has been implicated in many protein-protein interactions (including CREB binding protein and MAPK8) which are too numerous to reasonably list here but serve to enforce its known importance in immune regulation [31,32].

#### **1.1.4.3 RelB:p52**

Often described together with p52 due to their close association and its inability to homodimerize, RelB along with p52 are possibly by far the least well understood subunits. Evidence for RelB modification is limited to a study by Dephore *et. al.* in 2008 which provided evidence for phosphorylation at serine 37 and 573 [33]. Many more sites of modification are noted in p100/p52 but these are almost all related to signals involving p100 degradation into p52 [34]. Mutagenesis in the same studies found that residues 247-249 were critical in p65:p52 heterodimerization. Finally, RelB has been described by Vogel *et. al.* and Jacque *et. al.* as crucial in hydrocarbon receptor mediated transcription and an inhibitor of tumor growth, respectively [35,36]. While by no means capturing all of the great deal of work since their discovery this brief overview has hopefully highlighted some of the many intricacies of the NF- $\kappa$ B family. One subunit has yet to be discussed however, and is emerging as perhaps one of the most critical in the control of and balance of the inflammatory process.

### 1.1.5 NFKB1 - The p105/p50 Subunit

Described previously as a class one member of the NF- $\kappa$ B family as well as an I $\kappa$ B in its own right, p105/p50 arguably plays a critical role in both gene activation and repression. As a canonical heterodimer with p65 it is able to upregulate genes critical to the inflammatory response such as many of the interleukins, interferon  $\beta$ , TNF $\alpha$  as well as CXCR7, CD40, Complement components, MHC class I and tapasin [37]. Conversely Cao *et. al.* found that unlike other subunits, p50 in a homodimer configuration, along with CREB Binding protein, can upregulate the expression of anti-inflammatory cytokine IL-10 [38]. This anti-inflammatory role has made p50 an exciting new prospect for therapy since such targeted control of inflammation is sure to produce less side effects than the broad inhibition of upstream pathway kinases as attempted previously [39]. To gain a better understanding of its function *nfk1*, the gene that codes p105/p50 found on the q arm of chromosome 4, was knocked out in mice. From this several different studies describe that though the knockout is not lethal as in p65, mice suffer from neural degeneration, sleep irregularities, immune response defects, apparent resistance to certain forms of arthritis as well as altered response to various models of injury [40–44]. These observations in knock outs however neither describe the complete role of p50 nor separates it from p105, which is known to have distinct functions. For example, p105 has been shown to bind G protein-coupled receptor kinase 5 and Prostaglandin E receptor type 4-associated protein and alters the biology of macrophages [45,46]. Also, it has been shown to bind the Tax protein when cells are infected by human T cell leukemia virus type 1 and these interactions are all in addition to its regulatory role as an I $\kappa$ B protein [47]. Perhaps most importantly, Beinke *et. al.* have shown that p105 is a direct negative regulator of TPL-2 (MAP3K8), an important kinase in a variety of cellular pathways [48]. While p105/p50 may have a diverse role in cells much can be learnt from the studies that have been done that relate to its structure and interactions.

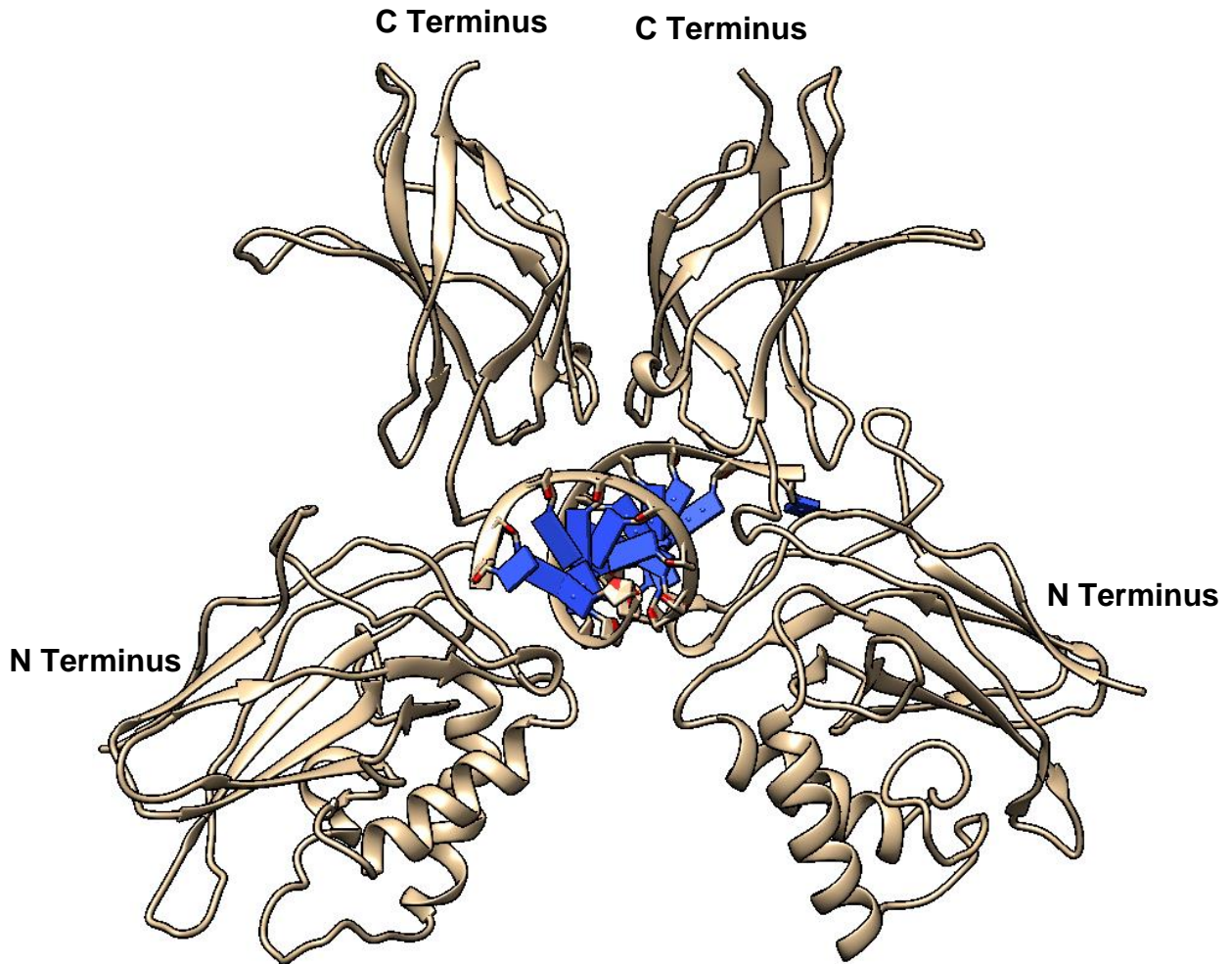


**Figure 1.4 The p50:p50 Homodimer.**

*The original crystal structure of a p50:p50 homodimer bound to DNA. (PDB ID: 1NFK)  
Rendered in UCSF Chimera with rounded ribbons. Blue indicates base pairs of DNA with  
red phosphate sugar backbones.*

Shown in **Figure 1.4** and determined by Ghosh *et. al.* (mouse) and Müller *et. al.* (human), the crystal structure of a p50 homo-dimer bound to DNA gave the first insights into the process of homo-dimerization and how p50 interacts with DNA [49,50]. Classically described as resembling “a butterfly with protein domains as wings connected to a cylindrical body of DNA”, the structure includes defined amino acids 39 to 350 (mouse). Although a few loops of the structure were poorly defined in the electron density maps, each p50 molecule appeared to have two domains connected by a single linking chain of amino acids. Also noted by the authors was that the DNA binding regions of the protein is almost exclusively made up of loops and not the  $\alpha$ -helices that are customarily associated with transcription factors. The proteins are arranged in a side by side confirmation and mirrored along the z-axis. Additionally, binding does not seem to greatly affect the coiling of DNA and does not apply significant strain to the double helix [49].

## **1.1.6 Interactions and Modifications of p50**

### **1.1.6.1 Posttranslational Modifications**

In addition to the crystal structure, information about p50's post-translational modification is more abundant than in some of the other subunits but, like p52, much of it is centered on its processing from its precursor. These known modifications as well as an overview of all the *nfkb1* gene products can be found in **Figure 1.5**. Phosphorylation events at serine 903, 907, 927 and 932 have all been well documented and all relate to priming p105 for ubiquitination and partial degradation [51–53]. Demarchi *et. al.* in 2003 describe a working model where p105 phosphorylation by Glycogen synthase kinase-3 (GSK-3 $\beta$ ) in the first instance can stabilize p105 but subsequent phosphorylation by IKKs then triggers its ubiquitination and degradation [54]. Protein Kinase B (Akt) which is upstream of IKK and activates it via the TNF $\alpha$  pathway, has also been shown to deactivate GSK-3 and so it is important to remember that cross-talk between upstream kinases is commonplace and that activation of p50 does not happen in isolation. Besides phosphorylation of sites on p105 that lead to its degradation, other PTMs

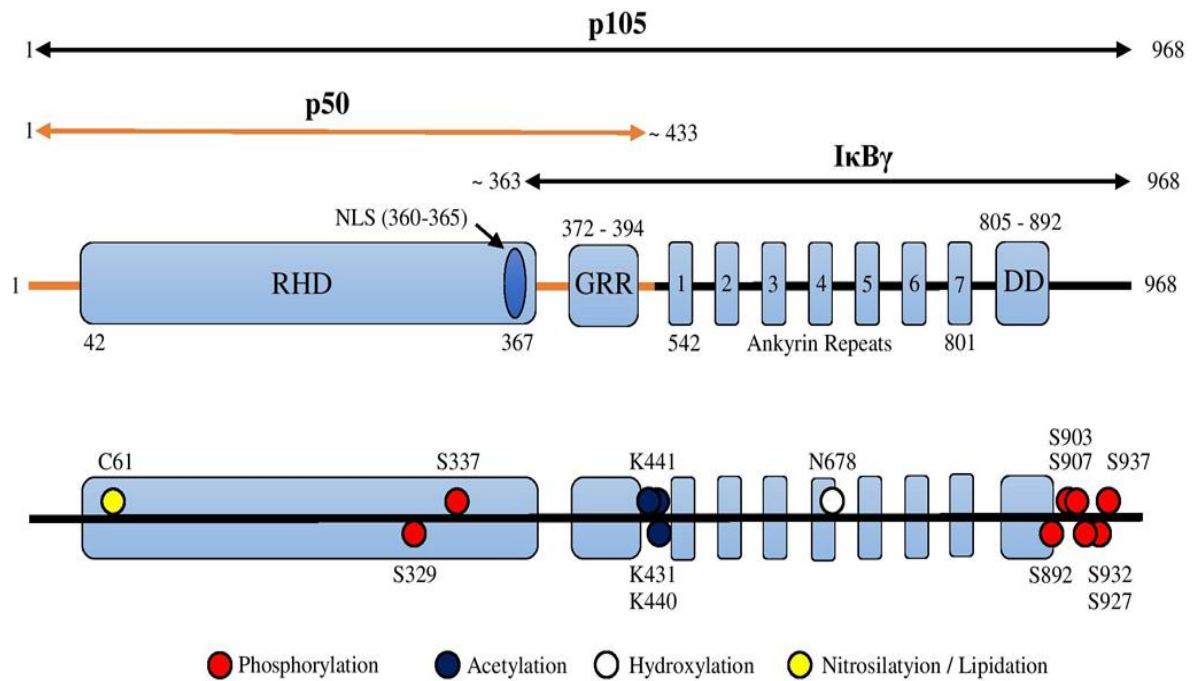


**Figure 1.5 Structure of the p105/p50 gene.**

A schematic of the gene products of the *nfkb1* gene including known sites of post-translational modification and boundaries of the p50 and IκBγ proteins. RHD - Rel Homology Domain. NLS - Nuclear Localization Sequence. GRR - Glycine Rich Region. DD - Death Domain. (Reproduced from Cartwright et. al. 2016 [37]). Amino acid positions refer to locations in the human gene.

have been found directly on p50. Marshall and Stamler in 2001 found that cysteine 61 on p50 could be nitrosylated, which inhibited transcription of p50 targets without interfering with other interactions with I $\kappa$ B [55]. Furia *et. al.* described acetylation at lysine 431, 440 and 441 by p300 and cAMP-responsive element-binding protein-binding protein (CBP) [56]. They suggest that acetylation here may aid in p50 release from I $\kappa$ B. Hou *et. al.* found that serine 337 phosphorylation was able to significantly increase its ability to bind DNA and that mutations at this serine as well as 65 and 342 (340 in mice) was able to disrupt homo-dimerization [57]. Though this effect could be rescued by threonine substitution at 65 and 337, mutation at serine 342 to threonine was unable to rescue this loss of homo-dimerization. Wilson *et. al.* confirmed and exploited this mutation (though to alanine) in a study that implicated p50 homo-dimers as a key repressor of chronic inflammation leading to hepatocellular carcinoma (HCC) [58]. In addition to the reduction in DNA and homodimer affinity caused by phosphorylation at serine 337, p50 has also been shown to be phosphorylated at nearby serine 329 [59]. Crawley *et. al.* found that S329 phosphorylation leads to a distinct shift in  $\kappa$ B site recognition where sites containing a -1 cytosine have a lower binding affinity for p50 than their -1 adenosine counterparts [60]. They go on to suggest that S329 phosphorylation primes cells for DNA damage induced cell death due to this altering of binding affinity and maintaining genome stability.

#### **1.1.6.2 Mutations**

In addition to its structure and post-translational modifications, multiple mutations in p50 have been found in patients with numerous forms of cancer. A search through the COSMIC (Catalogue of Somatic Mutations in Cancer) database reveals 124 mutations [61]. While it is unknown if these are functional or play a key role in the progression of the associated cancer, some of them will no doubt play a part in future specific cancer work. Studies also have found that mutations in the promoter of p50 also increased the risk of HCC [62]. All of this evidence points to a critical protein that is complexly regulated and serves a diverse role as both a promoter and suppressor of inflammation. Nevertheless, it is important to

remember that, as seen with other members of the family, p50 does not impart its effects in isolation.

### **1.1.6.3 Protein-protein Interactions**

Since proteins that directly interact with p105 have been mentioned previously, here, suspected interactions of proteins with p50 will be elaborated upon. Most often, protein-protein interactions are difficult to tease apart when considering transcription factors that dimerize in the manner of NF- $\kappa$ B since it is difficult to be sure of the nature of the interaction. For example, Lee *et. al.*, found that SMRT (Silencing Mediator of Retinoic acid and Thyroid hormone receptors) interacts with p50, however it also appears to interact with p65 [63]. Though they go on to show it is a case of interaction with both subunits, without careful analysis it can be easy to attribute a binding partner to the wrong subunit. Nevertheless, there are many p50 protein-protein interaction that have been uncovered.

Recall, p50 homo-dimers were able to upregulate transcription of IL-10 in macrophages by binding CREB [38]. He *et. al.*, has gone on to show that this interaction is mediated by protein kinase g (PKG) [64]. Rudders *et. al.* was able to show that through binding of ESE-1 ( a member of the E26 transformation-specific transcription factor family) EST, p50 was able to regulate nitric oxide synthase, important in intracellular signaling [65]. Also Drew *et. al.* found that Interferon regulatory factor-2 could interact with p50 and inhibit its transcription of MHC class I and the  $\beta$ 2-microglobulin genes [66]. In a paper that determined STAT3's interaction with p65, it was also found that p50, independent of p65, interacts with STAT5b to modulate haptoglobin expression [67]. Others have shown that p50 interacts with STAT3 to inhibit nitric oxide synthase and with STAT6 to synergistically induce IL-4 mediated transcription [68]. In addition to this interaction with the STAT family of transcription factors, p50 has been shown to interact with and control other transcription factors and as such indirectly control those subsets of genes as well. Wang *et. al.* showed that p50 was the subunit responsible for the induction of C/EBP $\alpha$  transcription which allows it to stimulate neutrophil production

in response to inflammation [69]. C/EBP has also been shown to remove HDAC1 (a chromatin modulating enzyme that will be discussed later) from p50 homodimers to induce pro-inflammatory gene expression [70].

This list continues and is quite extensive and points ever more to this anti-inflammatory and repressive role of p50. Indeed, Oakely *et. al.* have shown that p50 is important in limiting the inflammatory response especially in the context of chronic injury [71]. These anti-inflammatory properties are perhaps highlighted best by its known interaction with Bcl-3. Wessells *et. al.* showed that LPS induced TNF $\alpha$  expression could be inhibited by Bcl-3 through its association with p50 in macrophages and Collins *et. al.* in 2014 have shown that Bcl-3 gene repression in general requires this association with p50 homo-dimers in particular [17,72]. Since this discovery, Collins *et. al.* have gone on to find that the Bcl-3:p50 interaction occurs along the Ankyrin repeat 1, 6 and 7 of Bcl-3 and have made a mimetic peptide that can bind p50 in a similar manner [73]. They have also shown this peptide to have anti-inflammatory properties and explain that it is due to the protection of p50 from degradation via ubiquitination, a property believed to be held by Bcl-3. These 'protected' p50 homo-dimers are then free to compete with the transcriptionally active p50:p65 heterodimers for gene promoters and can severely dampen the activation of such genes.

With these established interactions, it is not hard to imagine p50 as an important regulatory molecule in the NF- $\kappa$ B family serving to attenuate the function of p50:p65 heterodimers through multiple protein-protein interactions. In addition to this passive or competitive based approach to gene inhibition, others believe that p50 can also actively down-regulate gene transcription by its association with another protein, Histone Deacetylase 1 (HDAC1).

## **1.2 HDAC1 and p50: Repressors of Inflammation**

### **1.2.1 Nuclear Genetic Organization**

Transcription factors, like p50, bind genes in promotor regions which contain the specific site within the DNA sequence recognized by each protein. More diversity of regulation than simple gene promotor affinity exists however, and our understanding of the epigenetic control of genes is revealing its complexity as the field continues to grow. Generally, in all cells genes are organized into areas of active transcription (euchromatin) and regions of condensed 'inactive' DNA referred to as heterochromatin [74]. DNA strands are wrapped onto nucleosomes which are looped by the molecules CTCF and cohesin into either active or inactive regions referred to as topological associated domains [75]. These are regions where DNA sequences are associated in three-dimensional space but not necessarily sequence. It is believed that whether a region is available for transcription is tightly regulated by post-translational modification of both the DNA sequence itself and also the previously mentioned nucleosomes around which it is wrapped [74].

A major method by which transcription can be repressed through DNA modification is through DNA methylation. DNA methylation is thought to block some transcription factors from binding their intended sequences due to base modifications but also allows the recruitment of methyl-CpG-binding domain proteins (MBDs) which can in turn recruit more transcriptional repression machinery to the locus of genes intended to be switched off [76]. The target of such machinery is often the C-terminal tails of proteins which make up nucleosomes, broadly termed histones.

Nucleosomes are octamers which consist of dimers of the tetramer histones H2A:H2B:H3:H4. Together, these eight proteins make up the smallest unit of DNA organization in the nucleus of cells and each of which are subject to a number of post-translational modification which have a profound effect on the transcription of nearby genes [74].

### **1.2.2 Epigenetic Modification of Histones**

Histone methylation can serve to both repress and enhance gene transcription in a gene specific as well as histone specific manner. For example, histone 3 (H3) K9 di or tri-methylation is a well-known silencing mark and is found on inactive copies of the X chromosome in females. Conversely, H3 K4 methylation is a well described mark of transcriptional activation. Methylation of histone tails is not the only post-translational modification that affects gene transcription [77]. Histones can also be phosphorylated at numerous sites on all four major histone variants which can have differing effects. A canonical marker of DNA damage is the phosphorylation of histone variant H2AX. With regard to gene transcription, phosphorylation at H3 S10, T11 and S28 along with H2B S32 have all been shown to have an impact on the control of highly proliferative genes [78]. These phosphorylation events are, in the literature, correlated with another important post-translational modification; acetylation. Histone acetylation occurs at many residues along histone tails and some of the most well studied sites include K4, K9 and K27, all of which can also be tri-methylated [79]. Acetylation, phosphorylation and methylation together form a complex code on the tails of each histone molecule that together determine the overall accessibility of nearby genes and the numerous enhancers and co-factors that may bind DNA. Acetylation, however also plays a physical role in the organization of DNA. Acetylated histones carry positive charges which tightly bind negatively charged DNA. Deacetylation neutralizes this positive charge and decreases the affinity of histones for DNA and allows for a looser conformation which exposes more of the DNA to any potential binding proteins [79].

<b>Modified Residue</b>	<b>Modification</b>	<b>Function</b>
K4	Acetylation	Activation of Transcription [80]
K9	Acetylation	Activation of Transcription [81]
K14	Acetylation	Activation of Transcription, Histone Deposition & DNA Repair [82]
K18	Acetylation	Activation of Transcription, DNA Replication [83]
K23	Acetylation	Histone Deposition, DNA Repair & Transcriptional Activation [83]
K27	Acetylation	Activation of Transcription [83]
K4	Methylation	Activation of Transcription [80]
R8	Methylation	Repression of Transcription [84]
K9	Methylation	Repression of Transcription & Gene Silencing [81]
R17	Methylation	Activation of Transcription [85]
K27	Methylation	Repression of Transcription [86]
K36	Methylation	Activation of Transcription [87]
K79	Methylation	Activation of Transcription [88]
T3	Phosphorylation	Mitosis [89]
S10	Phosphorylation	Mitosis & Activation of Transcription [89]
T11	Phosphorylation	Mitosis [89]
S28	Phosphorylation	Mitosis [89]

**Table 1.1.1 Relevant Epigenetic Modifications of Histone H3**

*A table of well characterized posttranslational modifications of histone H3 which impart various outcomes on the three dimension arrangement of chromatin.*

### 1.2.3 HDAC1: A Class 1 Histone Deacetylase

Histone Deacetylase 1, one of 18 in its protein family, is responsible for the maintenance of the three-dimensional structure of chromatin by the removal of acetyl groups from histones that bind DNA. Once de-acetylated, histones are able to more tightly bind DNA, leading to gene repression in that region by denying access to transcription factors [90]. Due to this potent role as major ubiquitous modifier of 3-dimensional chromatin structure and gene expression, it is not surprising that loss of HDAC1 is embryonic lethal [90]. Oh *et. al.* found that a mutation of histidine to alanine at amino acid 141 completely destroys its deacetylase activity and thus it is known that this forms the active catalytic site of the protein [91]. It contains a few important sites of PTM in serine 421 and 423 which are phosphorylated and enhance deacetylase activity and is acetylated on lysine 74 and 220 (**Figure 1.6**) [92,93]. Additionally, it has been found that HDAC1 can deacetylate p65 on lysine 310, which promotes apoptosis [94].

Unlike some other members of its family, HDAC1 is an exclusively nuclear protein and forms the catalytic core of several nuclear remodeling complexes. Found along with HDAC2, HDAC1 is a known component of the Sin3A, CoREST and NuRD complexes [95]. Within these complexes, HDAC1 and HDAC2 act as the catalytic core while other components of the complex supporting this function. For example, it is known that Sin3A is recruited and tethered to DNA by MAD:MAX heterodimers [96]. The NuRD complex works in a similar way and shares a few of its components with the Sin3A complex [97]. Work on co-REST has found that HDAC1 is also a component of this complex which plays a role in the downregulation of neural genes in non-neural cells and has been shown to be important in Huntington disease and neuroblastomas [98]. Together, the presence of HDAC1 as the catalytic core responsible for the modulation of genes in numerous systems implicates it as a definitive protein required for epigenetic gene repression through deacetylation.

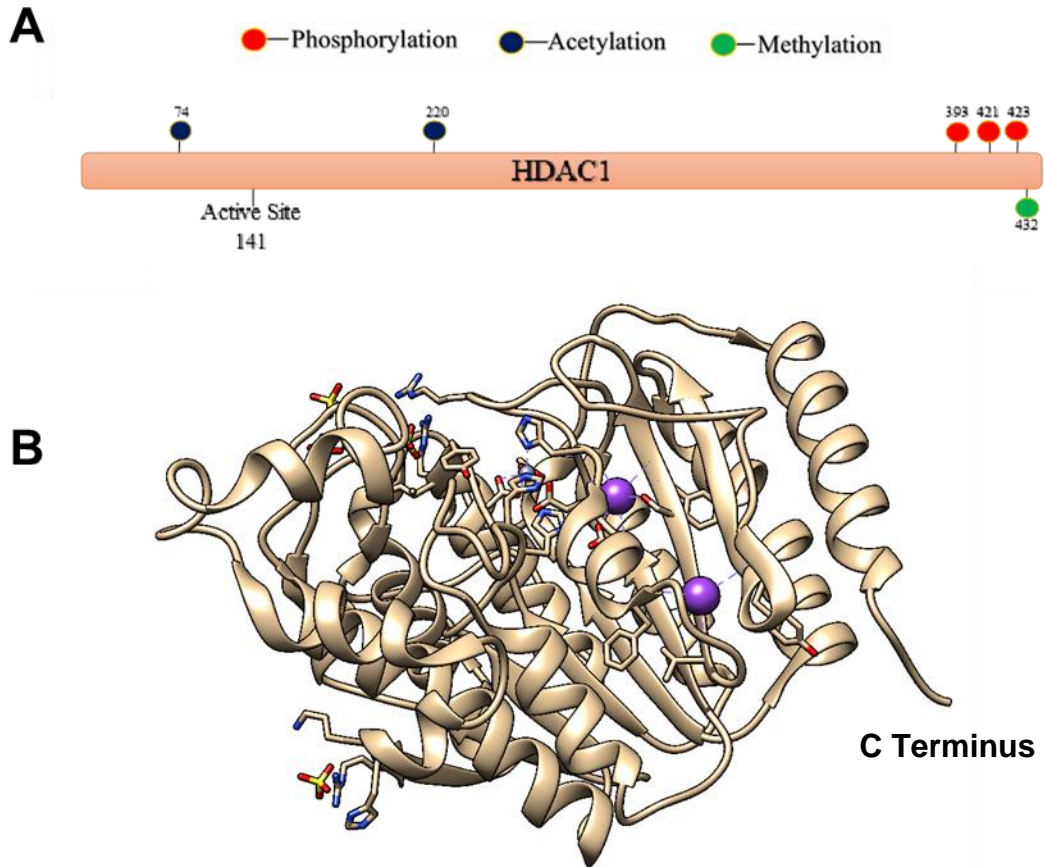


**Figure 1.6 Overview of the HDAC1 Molecule**

**A.** Known post-translational modifications in HDAC1. **B** Crystal structure of the catalytic core of HDAC1 (PDB ID 4BKX). Rendered in UCSF Chimera with rounded ribbons. Purple indicates potassium ions included in the resolved structure. Residues which participate in the catalytic core of the enzyme and are critical for enzyme function have been displayed in stick representation. The N-terminus is obscured behind the core of the protein.

### 1.2.4 Repression of Active NF- $\kappa$ B

As mentioned previously NF- $\kappa$ B has been well established as a critical and potent transcription factor family in terms of the transcription and initiation of both acute and chronic inflammation [99]. Therefore, such a system would require an equally effective regulator to initiate and maintain the resolution of any inflammatory event. While it is known that I $\kappa$ B's serve as initial cytoplasmic inhibitors, very little evidence outlines the fate of NF- $\kappa$ B dimers in the nucleus post-stimulation. Work which goes against this widely supported dogma of constant cytoplasmic sequestration is the growing number of studies that show that dimers are not static and that even under resting conditions they are trafficked in and out of the nucleus [15]. Nelson *et. al.* found that the number and amplitude of these cycles of phosphorylation, dephosphorylation and degradation had a significant impact on genes transcribed [15]. With this in mind a theory could emerge that once activated, and gene transcription commences, inhibitors may be transcribed which may then enter the nucleus and sequester active dimers to the cytosol once more in a negative feedback loop. This is the argument proposed by Arenzana-Seisdedos *et. al.* who showed that nuclear I $\kappa$ B $\alpha$  could bind active p65:p50 and export it to the cytosol however this has not been widely accepted as the major mechanism for inhibition post activation for a number of reasons [100].

I $\kappa$ B $\alpha$ , like other I $\kappa$ B's, bind active dimers using several of its Ankyrin repeat domains and masks the otherwise accessible nuclear localization signals on all NF- $\kappa$ B subunits. In addition to this, I $\kappa$ B $\alpha$  can disrupt the DNA binding domain of dimers such that they are no longer able to bind DNA. Finally, I $\kappa$ B $\alpha$  itself is not usually present in the nucleus of cells and other studies which have found small amounts of nuclear I $\kappa$ B $\alpha$  were unable to confirm its ability to bind DNA bound active dimers [101]. To affect the ablation of response, newly synthesized I $\kappa$ B $\alpha$  would have to be first imported, bind active dimers and then exported. While there is some evidence in support of this, other mechanisms have been discovered which are becoming

more widely accepted as pathways to resolve inflammation including p50:p50 homodimers [14].

### **1.2.5 Evidence for the p50:p50:HDAC1 Interaction**

Recall, p50 homodimers are thought of as resting state repressors of gene activation and through the binding of other co-factors such as CBP and Bcl3 they can upregulate anti-inflammatory genes or deny pro-inflammatory gene producing dimers access to target promoters [102]. In addition to this passive dimer blockade and active anti-inflammatory gene transcription, it is believed that p50 may recruit another co-factor to augment the structure of gene promoters and switch off transcription in a more permanent active manner through the recruitment of HDAC1. Zhong *et. al.* were the first to show that HDAC1 could bind both p50 and p65 and that phosphorylation of the subunit determined its preferred co-factor [103]. Since then, Elsharkawy *et. al.* also found a major role for the p50:p50:HDAC1 complex in the repression of many traditional pro-inflammatory genes [104]. In particular, they found that inhibition of HDAC1's deacetylase activity mimicked the pro-inflammatory phenotype observed in *Nfkb1<sup>-/-</sup>* cells. Moreover, Paz-Priel *et. al.* found that C/EBP $\alpha$  was able to displace HDAC1 from p50 homo-dimers that were actively repressing anti-apoptotic genes and the removal of this gene repression was key in acute myeloid lymphoma [70]. These two cases highlight an important role in cancer and immunity and are both continually supported by new evidence. In 2015, Wilson *et. al.* have shown that p50 homo-dimers are critical in neutrophil driven hepatocellular carcinoma and also attribute this to their association with HDAC1. Their work shows that, in the absence of p50, HDAC1 does not associate with the potent neutrophil chemotaxis genes *cxc1* and *cxc2*.

Though this and other evidence makes a strong case for this p50:HDAC1 interaction, very little structural evidence has been provided thus far. If this interaction is as important as the evidence so far suggests, it may be key in developing better ways to selectively repress inflammation and may ultimately lead to better anti-cancer and anti-inflammatory therapeutics.

### 1.3 Aims

Though some preliminary studies on the interaction between p50 and HDAC1 have been reported, little detail about how these two proteins physically interact as well as the contribution to homo-dimerization makes has not been studied. As such the aims of this project were as follows:

- Understand the role of p50 homo-dimerization in the context as scaffold for gene repression.
- To determine the exact region of p50:HDAC1 interaction and gain insights into its possible mode of regulation.
- To understand the relative importance of active p50:HDAC1 repression of NF- $\kappa$ B driven inflammation.

## Chapter 2 Materials and Methods

---

### 2.1 Cell Culture

Cos-7, U2OS, HeLa, LX-2 and *Nfkb1*<sup>-/-</sup>, WT and *Nfkb1*<sup>S340A</sup> Murine Embryonic Fibroblasts (MEFs) from a C57Bl/6 background were maintained in Dulbecco's Modified Eagle Medium (DMEM) (GIBCO) supplemented with 100 U/ml penicillin, 100µg/ml streptomycin, 2mM L-glutamine and 10% fetal bovine serum at 37°C at an atmosphere of 5% CO<sub>2</sub>. THP1 cells were maintained in RPMI 1640 (GIBCO) supplemented with 100 U/ml penicillin, 100µg/ml streptomycin, 2mM L glutamine and 10% fetal bovine serum at 37°C at an atmosphere of 5% CO<sub>2</sub>.

### 2.2 Cell Harvest and Protein Lysate Preparation

Cells were washed in PBS and then scraped into PBS and harvested by centrifugation. Cell pellets were then resuspended in RIPA lysis buffer (150mM NaCl, 50mM Tris-HCl pH 7.5, 0.1% SDS, 1% Triton, 0.5% Deoxycholic acid with phosphatase and protease inhibitors) on ice at for 20 minutes followed by storage at -80°C.

### 2.3 Western Blot

Protein lysate concentration was determined by Bio-Rad Protein Assay Kit as per manufacturer's instructions along with photo spectrometry at a wavelength of 450nm. 30µg or 50µg of protein was denatured at 95°C for 5 minutes. Total protein or immunoprecipitated samples were fractionated by 7–12% SDS-PAGE and transferred to nitrocellulose membrane. Blots were blocked with TBS-Tween (0.1% TBS-T) containing 5% milk protein before overnight incubation with primary antibodies (1 hour at room temperature for HRP conjugates) in either 5% milk TBS-T or 5% Bovine Serum Albumin (SIGMA). Primary antibodies against (1:1000) p65 (sc372 Santa Cruz), (1:2000) GAPDH (ab22555 Abcam), (1:1000) p105/p50-HRP conjugate (ab195854 Abcam), (1:1000) p105/p50 (Abcam, ab7971), (1:1000 ) Sin3A (ab3479 Abcam), (1:2000) c-Rel (sc71 Santa Cruz) or (1:1000) HDAC1-HRP conjugate (ab193096 Abcam). Next, membranes were washed in TBS-T and

further incubated with (1:1000) HRP-conjugated mouse anti-rabbit IgG (7074S CST) for one hour at room temperature. After a final wash antigens were detected by chemiluminescence (Amersham Biosciences).

## **2.4 Proteasome Inhibition**

*Nfkb1*<sup>-/-</sup>, WT and *Nfkb1*<sup>S340A</sup> MEFs were serum starved overnight and then treated overnight with 10uM MG132 Proteasome Inhibitor (SIGMA) or left untreated and lysed in 50µl RIPA lysis buffer for 20 minutes followed by sonication for 5 minutes. Protein was then analyzed by western blot.

## **2.5 Transient Transfection**

Mammalian expression constructs were transfected into Cos-7, U2OS, HeLa and *Nfkb1*<sup>-/-</sup> and WT MEF cell lines for an assay dependent time period using Effectene Transfection reagent (301427, Qiagen) following manufacturer's instructions. Briefly, cells were seeded to 40-60% confluency and DNA for transfection incubated in EC Buffer with Enhancer (1:8) and Effectene reagent (1:10) for 5 and 10 minutes respectively. This mixture was further diluted in DMEM and added dropwise to cells under normal culture conditions for the indicated time period. Following incubation, cells were then treated or harvested.

## **2.6 Luciferase Assay**

Luciferase assays were performed using a Dual Luciferase Assay Reporter System (E1910, Promega) following manufacturer's instructions. pGL2 reporter plasmids containing a 3X κB promotor, IL-6 promotor or IκBα promotor were transfected at 0.5µg/well in 6 well plates for 24 hours along with either WT p50-Flag, or p50Mu-Flag at 0.5µg/well as well as a Renillia luciferase reporter construct at 0.05µg/well. Relative luminescence was normalized to co-transfected Renilla luciferase, control luciferase reporter as well as total protein.

## **2.7 Molecular Dynamics Simulations**

Molecular dynamics simulations were carried out on various dimer pairs. In short, PDB ID 1NFK (WT p50:p50 homodimer) and 1LE5 (WT p50:p65 heterodimer)

along with 1NFK p50S340A chain A and 1LE5 p50:p65p50 were massaged for molecular dynamics and topology and coordinate start files generated in both dry and TIP3PBOX explicit water, Na<sup>+</sup> charge balanced configurations. Using Amber force field ff99SB unrestrained molecular dynamics simulation were run to a total of 100 ns using the grand canonical ensemble after 100ps of equilibration to 300°K. Simulations were carried out on the Polaris SGI High Performance Computing Cluster at Leeds University. Data analysis was then carried out with Amber ptraj, UCSF Chimera or in R with trajectory visualization in VMD and UCSC Chimera [105].

## **2.8 Multiple Sequence Alignment and Evolutionary Analysis**

Amino acid sequence data was gathered from the Ensembl Database by using human gene orthologues across all available species and from the Uniprot Database by gene ID. Greater than 60 sequences representing evolutionarily separated organisms from *Homo sapiens* to *Ciona intestinalis* was aligned and viewed in JalView using MAFFT with defaults or Clustal W with defaults. Alignments were then visualized on 3D crystal structures of the various NF-κB subunits using UCSF Chimera and PDB files stored in the Protein Data Bank (PDB). Crystal structures used were as follows, 1NFK – p50 Homo-dimer bound to a kappaB site [49], 1LE5 – p50:p65 Heterodimer bound to interferon β kappa B site [106], 3DO7 – p52:RelB heterodimer bound to kappaB site [107] and 1GJI- c-Rel homo-dimer bound to *IL-2* response element [29].

## **2.9 Immunofluorescence Microscopy**

### **2.9.1 Endogenous Immunofluorescence**

U2OS cells were seeded at 40-50% confluency in 4 well chamber slides. Cells were then washed with PBS and fixed in 4% formaldehyde followed by permeabilization with 1% (v/v) Triton-X and blocked for 1 hour in 5% (w/v) Bovine Serum Albumin (BSA). Cells were then incubated over night at 4°C with anti-p105/p50 (Santa Cruz, SC114-X) in 5% BSA. Cells were then washed in PBS and incubated for one hour with anti-rabbit-IgG-Rhodamine (SAB3700846, Sigma). Cells were then washed in

PBS and mounted with ProLong Gold Antifade Mountant with DAPI (P36935, Thermo-Fisher) and imaged on a Nikon Inverted Confocal Microscope at 20x.

### **2.9.2 Nuclear Localization Immunofluorescence Microscopy**

U2OS cells were seeded at 40-50% confluency in 4 well chamber slides and transfected with 0.5µg of either WT p50-FLAG, p50Mu-FLAG or vehicle only and incubated for 24 hours. Cells were then washed with PBS and fixed in 4% formaldehyde followed by permeabilization with 1% Triton-X and blocked for 1 hour in 5% Bovine Serum Albumin (BSA). Cells were then incubated over night at 4° with anti-FLAG-FITC antibody (F4049, Sigma) in 5% BSA. Cells were then washed in PBS and mounted with ProLong Gold Antifade Mountant with DAPI (P36935, Thermo-Fisher) and imaged on a Nikon Inverted Confocal Microscope at 20x.

### **2.10 Flag, Endogenous and Co-Immunoprecipitation**

Tissue or cells were washed in PBS and lysed for 20 minutes in Co-IP lysis buffer (50mM Tris-HCL pH 7.4, 150mM NaCl, 1mM EDTA and 1% (v/v) Triton-X) with fresh protease inhibitors (118735801, Roche). 25µg of lysate was kept as input and 500µg of lysate was incubated with 2µg of anti-p105/p50 (D7H5M CST), nuclear localization specific anti-p50/p105 (sc-114x Santa Cruz), anti-p105/p50 (H119 Santa Cruz), anti-p65 (sc 372 Santa Cruz), anti-IkBα (L35AS CST), Sin3A (ab3479 Abcam), anti-Gal 4 (SC 510, Santa Cruz) normal IgG (ab46540-1 Abcam) or anti-FLAG beads (A2220 Sigma) for 1 hour at 4°C diluted to a total volume of 500µl in Wash Buffer (50mM Tris-HCL pH 7.4 and 150mM NaCl). Apart from samples with FLAG beads, a 1:1 mix of Protein A and Protein G agarose beads (P6649 and P3296 Sigma) were then added to samples and incubated a further hour at 4°C. All samples were then washed in Wash Buffer three times and bound complexes eluted by boiling with 1X SDS-Loading Dye (0.5% (v/v) SDS, 0.5% (v/v) Glycerol, 65mM Tris HCl pH 8.1, 2.5% β-mercaptoethanol and trace Bromophenol Blue) at 95°C or by incubation with Wash Buffer (50mM Tris-HCL pH 7.4 and 150mM NaCl) containing excess FLAG peptide (100ug/ml) in the case of FLAG IPs. Samples along with inputs were then assessed by Western Blot.

## **2.11 GRAMM-X Protein Interaction Prediction and Visualization**

p50 HDAC1 interaction predictions were performed by the GRAMM-X software for rigid body protein-protein interactions [108]. Chain A and B of the available crystal structure of the p50 homodimer (PDB:1NFK [49]) were used as a receptor molecule for its ligand, chain B of the HDAC1 crystal structure (PDB:4BKX [95]). Potential interacting intermolecular hydrogen bonds were calculated using the HBond function in UCSC Chimera with relaxed bond constraints of 7Å and 20% bond angle flexibility. Structural modelling and images were generated in UCSF Chimera [105].

## **2.12 Solvent Accessibility Calculations**

Solvent accessibility for residues were calculated by the POPS algorithm [109] for solvent accessible surface areas using crystal structures of each of the NF-κB subunits as follows. 1NFK – p50 homo-dimer bound to a κB site [49], 1LE5 – p50:p65 heterodimer bound to interferon β κB site [106], 3DO7 – p52:RelB heterodimer bound to κB site [107] and 1GJI- c-Rel homo-dimer bound to *IL-2* response element [29]

## **2.13 PCR, Hi-Fidelity PCR and DNA Gel Purification**

Standard PCR was carried out using ThermoScientific Dream Taq DNA polymerase Master Mix along with 1µl of cDNA and assorted primers at various melting temperatures. High fidelity PCR was carried out using ThermoScientific Phusion High Fidelity DNA polymerase at 0.02U/µl along with X1 HF Buffer, 200µM Nucleotide Mix, or Q5 High Fidelity Polymerase (New England Biolabs) and 0.5µM of each forward and reverse primer and 1µl of cDNA. This was made up to 20µl in nuclease free water and denatured at 98°C for 30 seconds followed by 35-40 cycles of 10 seconds denaturation (98°C), 10 seconds annealing (primer specific temperature), 30seconds/Kb extension (72°C). This was followed by a final extension at 72°C for 10 minutes. Results were then visualized by either Ethidium Bromide Gel Electrophoresis or Gel Green Nucleic Acid Stain (Biotium) on 1-2% (w/v) agarose gel and imaged under UV light or by Dark Reader Transilluminator

(Clare Chemical Research). Utilizing a sterile scalpel, bands of interest were excised and DNA purified by QIAquick Gel Extraction Kit (Quiagen). Purified samples were quantified by Nanodrop (Thermo). Primers lists can be found in **Figure 2.1 and 2.2**.

## 2.14 RNA Isolation, Quantitative Real Time PCR and General PCR

### Conditions

Total RNA was isolated from cells using an RNeasy Mini Kit (74104, Qiagen) and treated with DNase. Briefly, cells were washed with PBS and lysed directly in appropriate amounts of Buffer RLT. This was then mixed with 1 volume of 70% ethanol and RNA isolated on an RNeasy Mini spin column after washes with buffer RPE. RNA was eluted in RNase-free water and treated with DNase (Promega) to remove any contaminating DNA. This RNA was then used as a template for the synthesis of complementary DNA using random primers (Promega). SYBR Green quantitative RT-PCR was performed using primers listed in **Appendix 7.3** and the PCR scheme detailed below in **Table 2.1**.

	30-45 cycles				
Initial Denaturation	Denaturation	Annealing	Elongation	Final Elongation	Hold
95° 1 minute	95°C 30sec	Variable	72°C 30sec	72°C 10 minutes	4°C

**Table 2.1.1 General PCR Cycling conditions used to perform PCR and RT-PCR unless otherwise indicated**

## 2.15 Generation of Mutant p50-FLAG Constructs

Mutant constructs were all generated from a parent p50-FLAG pcDNA3.1 backbone kindly provided by N. D. Perkins (Newcastle University) **Appendix 7.2**. Mutations were generated using a Q5 Site Directed Mutagenesis Kit (E0554S, New England Biolabs). Briefly, template p50-FLAG pcDNA3.1 was incubated at 95°C followed by 3 minute cycles at the appropriate annealing temperature with a final incubation at 72°C for 10 minutes. This linear mutant DNA was then circularized

using the KDL enzyme mix at room temperature for 15 minutes and products transformed into DH5 $\alpha$  competent *E. Coli* (C2987H, New England Biolabs) and colonies selected by antibiotic resistance. Plasmids were then purified using an Endotoxin Free Plasmid Maxi Kit (12163, Qiagen). All mutants were confirmed by Sanger sequencing (GATC Bio-tech). Primers used in mutagenesis can be found in **Appendix 7.3**.

### **2.16 Generation of Chemically-competent DH5 $\alpha$ *E.coli***

Competent *E. coli* were generated using the Inoue method as described by A. Untergasser with minor amendments [110]. Competent DH5 $\alpha$  *E. Coli* (Invitrogen) were grown in an overnight culture of 10ml Luria-Bertani medium (LB) and 5 mls used to inoculate two flasks each with 250mls LB. Cell were allowed to grow at 37°C to an optical density of 0.6 before being placed on ice for 10 minutes. Bacteria were then pelleted at 2500g for 10 minutes at 4°C. Pelleted cells were then re-suspended in 80ml ice cold Inoue Solution (55mM MnCl<sub>2</sub>, 15mM CaCl<sub>2</sub>, 250mM KCl and 0.01M piperazine-N,N'-bis(2-ethanesulfonic acid) (PIPES) [Sigma]) then re-pelleted at 2500G for 10 minutes at 4°C. Pelleted cells were then re-suspended in a final volume of 20mls of Inoue buffer and 1.5 ml DMSO added. 500 $\mu$ l aliquots were placed in 1.5ml Eppendorf tubes and flash frozen in liquid nitrogen and stored at -80°C for future use.

### **2.17 Generation of petM30 protein expression constructs**

Using a petM30 backbone (**Appendix 7.1**, Gift from Will Stanley NICR Newcastle University), various bacterial expression constructs were created to express recombinant human p50, p65 and HDAC1 with n-terminal 6xHIS-GST-TEV tags. Constructs were created using the Gibson assembly method using the NEB HiFi DNA Assembly kit. Briefly, petM30 was linearized using NcoI and HindII and ligated to PCR products (primers and annealing conditions found in **Appendix 7.4**) containing full length or fragments of genes of interest along with a 20-25 bp overlap of backbone sequence at restriction sites. The cloning regime is covered below in **Table 2**.

Insert	Amino Acids	5' Restriction Site	3'Restriction Site
HDAC1 Full Length	483aa	NcoI	HindIII
HDAC1 Fragment	8-378aa	NcoI	HindIII
p50 Full Length	435aa	NcoI	HindIII
p50 Fragment Length	40-353aa	NcoI	HindIII
p65 Fragment Length	20-291aa	NcoI	HindIII

**Table 2.2. Cloning Regime for bacterial expression vectors for recombinant protein expression.**

## 2.18 DNA Ligation, Bacterial Transformation and Protein Expression

Ligation reactions were set up with gel purified DNA in a 1:3 vector to insert ratio with no more than 100ng of total DNA with X1 T4 DNA Ligase Buffer and 20U/μl T4 DNA Ligase (New England Biolabs) either overnight or for 2 hours at 16°C. Additional ligation reactions for Gibson Assembly Inserts were performed using the NEBuilder HiFi DNA Assembly Cloning Kit (NEB) as per the manufacturer's instructions into petM30 expression vectors containing both GST and 6x His tags. Transformation of competent cells was carried out using either NEB Ultra Competent DH5α cells, Rosetta 2(DE3) pLysS Singles Competent Cells (Novagen), BL21 DE3 (New England Biolabs), Limo21 (New England Biolabs), Tunner (Novagen), Arctic Express (Agilent) or those made as described previously (Details in **Appendix 7.5**). Briefly, 50μl cells were thawed and mixed with 1-100ng DNA and incubated on ice for 30 minutes. Cells were then heat shocked at 42°C for 45 seconds and placed on ice for 2 minutes. 250μl of SOC (New England Biolabs) was used to outgrow cells for 1 hour with shaking at 37°C and 200μl of outgrowth spread onto LB plates treated with appropriate antibiotics (100μg/ml Ampicillin, 100 μg/ml Carbenicillin, 34 μg/ml Chloramphenicol or 30-50μg/ml Kanamycin [Sigma]). Finally, cells were incubated at 37°C overnight and examined for colony formation the next morning. Expression was carried out in LB buffered to pH 7.4 with 50mM Tris.Cl and 1% glucose, Auto Induction Media (Formedium) or TB Media (Formedium). Cells were induced for 16 hours at 25°C with IPTG at a final concentration of 1mM (LB and TB only) once cells reached an OD of 0.5. Cells

harvested by centrifugation at 25000g were lysozyme treated for 20 minutes and sonicated for 5 minutes to liberate protein and analyzed by SDS-PAGE and Coomassie Blue Stain.

## **2.19 Bacterial DNA MiniPrep, MaxiPrep and Restriction Enzyme**

### **Digestion**

Bacterial colonies of interest were picked from overnight plate growth and outgrown in 10mls LB media. Plasmid DNA was isolated by QIAprep® Spin Miniprep or MaxiPrep Kit (Qiagen) following manufacturer's instructions. Purified DNA was quantified using ThermoScientific NanoDrop™ and used for further analysis. Restriction DNA digestions were performed using 5ng of DNA and 10U/μl of appropriate Enzyme and buffer (New England Biolabs and Promega) in a total volume of 20μl of nuclease free water. Reactions were resolved on a 2% agarose gel with ethidium bromide and visualized via UV trans-illumination.

## **2.20 Protein Purification**

Protein lysates from various bacterial strains were passed through columns loaded with HisTrap nickel charged affinity gel (GE) to bind expressed 6X His -tagged proteins. Proteins were then eluted in fractions with buffers (50mM NaPO<sub>4</sub>, 150mM NaCl, 10% Glycerol with varying imidazole) containing increasing imidazole concentration. Fractions collected were analyzed by SDS-PAGE and Coomassie stain to identify expressed proteins. Fractions with high yield were then further purified by GST-affinity column chromatography (GE). GST-His6X tags were then cleaved from recombinant proteins using in-house purified TEV protease at 4°C overnight. After cleavage proteins were again purified via HisTrap affinity and pure recombinant protein flow through collected. Purified proteins were then buffer exchanged against PBS using dialysis tubing (D9652, Sigma) and stored at -80°C for future use.

## 2.21 Coomassie Blue and Silver Stains

Coomassie Blue stains were performed using SimplyBlue SafeStain (Thermo). Proteins fractionated on 9-12% SDS-PAGE Gels were washed with distilled water and incubated with SimplyBlue SafeStain for 1 hour at room temperature followed by a wash with distilled water until background was sufficiently reduced to visualize targets. For silver stains, proteins fractionated on 9-12% SDS-PAGE Gels were fixed for 1 hour at room temperature (40% ethanol, 10% acetic acid, 50% H<sub>2</sub>O). Gels were then washed for 30 minutes at room temperature and then sensitized in 0.02% sodium thiosulphate for 1 minute again washed with water and then incubated with 0.1% silver nitrate at 4°C for 20 minutes. Gels were then washed and developed in 3% sodium carbonate solution until bands were observed. The reaction was quenched with 5% acetic acid and analyzed.

## 2.22 Peptide Arrays

HDAC1, p50 and alanine substitution peptide arrays were kindly provided by the Kiely Lab (University of Limerick) and were generated as previously described [111]. Membranes were blocked in 5% Milk TBS-T for one hour followed by incubation with anti (1:5000) 6x-His Tag Monoclonal Antibody HRP (R931-25, Invitrogen) or anti-p105/p50-HRP conjugate (ab195854 Abcam) for 2 hours at room temperature and developed by chemiluminescence (Amersham Biosciences) to assess peptide antibody cross reactivity. 6xHis tagged recombinant HDAC1 (14-838, Millipore) at 5µg/ml in 1% milk TBS-T was then added to p50 arrays and generated recombinant p50 to HDAC1 arrays overnight at 4°C followed by TBS-T wash and incubation again with the appropriate antibody and detection as described (Anti 6x His-HRP or anti p105/p50-HRP). This procedure was also performed on the p50 alanine substitution array. Each array assay was performed in duplicate.

## 2.23 Nuclear and Cytoplasmic Extracts

U2OS or *Nfkb1*<sup>-/-</sup> MEF cells transfected with WT, p50Mu (mutant p50) or vehicle were washed with PBS and pellets lysed in cytoplasmic lysis buffer (50mM Tris-

HCL pH 7.4, 50mM NaCl, 1mM EDTA, protease inhibitors and 0.1% Triton-X) and homogenized using a 27G needle. Supernatant was kept as cytoplasmic extract and pelleted nuclei were washed in cytoplasmic lysis buffer and resuspended in RIPA lysis buffer (150mM NaCl, 50mM Tris-HCl pH 7.5, 0.1% SDS, 1% Triton, 0.5% Deoxycholic acid with phosphatase and protease inhibitors). Samples were then analyzed by western blot.

## **2.24 Chromatin Immunoprecipitation (ChIP)**

Briefly, *Nfkb1*<sup>-/-</sup> MEFs transfected for 48 hours with WT p50, p50Mu (mutant p50) or vehicle only were cross-linked by addition of formalin at 1% final concentration for 5 minutes at RT, then quenched with glycine buffer at final concentration of 125 mM. The cells were rinsed in cold PBS, and harvested into PBS with protease inhibitors and centrifuged for 5 min, 4°C, 1,000g. The pellet was resuspended in ChIP lysis buffer (1% SDS, 10mM EDTA, 50mM Tris-HCl pH8.1) and incubated for 20 min on ice. Lysate was sonicated to generate average size fragments of 200-700bp; cell debris was pelleted by centrifugation for 10 min, 4°C, 8,000 x g. 25 µg of chromatin per IP was diluted 1:10 with dilution buffer (1.1% Triton, 1.2mM EDTA, 16.7mM TRIS-HCl pH8.1, 167mM NaCl, with protease inhibitors) and precleared by incubating with 25 µl blocked Staph A membranes (Sigma, P7155) for 15 minutes. Pre-cleared chromatin was then incubated with 5 µg anti-acetyl H3 (ab47915, Abcam), anti-p50/p105 (ab7971, Abcam) or irrelevant IgG (ab171870, Abcam) overnight at 4°C. Immunoprecipitated chromatin was collected with blocked Staph A membranes, which were then sequentially washed with cold buffers; Low Salt Wash Buffer (0.1% SDS, 1% Triton X-100, 2 mM EDTA, 20 mM Tris-HCl pH 8.0, 150 mM NaCl), High Salt Wash Buffer (0.1% SDS, 1% Triton X-100, 2 mM EDTA, 20 mM Tris-HCl pH 8.0, 500 mM NaCl), LiCl Wash Buffer (0.25 M LiCl, 1% NP-40, 1% Sodium Deoxycholate, 1 mM EDTA, 10 mM Tris-HCl pH 8.0) and two washes in TE Buffer (10 mM Tris pH 8.0, 1 mM EDTA). The immunoprecipitated chromatin was eluted in 500 µl Elution buffer (1% SDS, 100mM NaHCO<sub>3</sub>), cross-links reversed and DNA obtained by phenol:chloroform extraction and gel purification.

The level of *cxcl1* and *cxcl2* gene promoter association with acetylated H3 were quantitatively measured by real-time PCR using primers listed in **Appendix 7.3**.

## **2.25 TNF $\alpha$ Treatment**

Cells were treated with recombinant TNF $\alpha$  (300-01A, Peprotech) for 1, 3 or 6 hours at a final concentration of 10ng/ml in specified cell culture media.

## **2.26 Enzyme Linked Immunosorbent Assay**

Enzyme Linked Immunosorbent Assay Mouse IL-6 DuoSet (DY406, R&D Systems) was used to quantify total mouse IL-6 in supernatant of *Nfkb1*<sup>-/-</sup> MEFs transfected with vehicle, WT or p50Mu for 18 hours followed by treatment with or without TNF $\alpha$  (10ng/ml) for 6 hours. This sandwich ELISA was performed as per manufactures instruction. Briefly, diluted capture antibody was used to coat a 96-well microplate at room temperature overnight. After three washes (PBS) plates were blocked in reagent diluent (provided) for one hour at room temperature. After three PBS washes 100ul of sample or standards were added to appropriate wells and incubated at room temperature for 2 hours. After three PBS washes diluted detection antibody was added for 2 hours at room temperature. After washes 100ul streptavidin-HRP working solution was added to wells for 20 minutes followed by a final wash and the addition of 100ul substrate solution in the dark for 20 minutes. 50ul of stop solution was then added and plates read and 450nM and well as 570nM for optical correction and analyzed against standards.

## **2.27 Neutrophil Isolation and Chemotaxis Assay**

Bone marrow derived neutrophils were isolated from the femur and tibia of C57BL/6 WT mice by flushing HBSS (Hanks' Balanced Salt Solution, Sigma) supplemented with 20mM HEPES and 0.5% (v/v) fetal calf serum. Red blood cells were lysed with BD PharmLyse buffer (BD Biosciences; Ref: 555899) and cellular debris removed using a 40 $\mu$ m filter. Neutrophils were isolated by negative depletion of non-target cells through magnetic-labelling and column separation (Neutrophil Isolation Kit - Mouse, Miltenyi Biotec; Ref: 130-097-658). Isolated neutrophils were then added

to 3µm inserts in complete DMEM which were inserted into wells containing media from *Nfkb1*<sup>-/-</sup> MEFs reconstituted with WT p50, p50Mu, vehicle controls or unconditioned media only with or without TNFα. After 2 hours neutrophils that migrated into the lower chamber were stained with trypan blue and counted by haemocytometer. Chemotaxis was performed in triplicate with n=3 conditioned media.

## **2.28 Statistical Analysis**

Data are expressed as mean ± standard error. Microsoft Excel was used to perform unpaired Students T-test and one-way ANOVA and \*p<0.05, \*\*p<0.01 or \*\*\*p<0.001 was considered significant.

## Chapter 3 p50 Dimerization: Residues Critical to p50 Stability and Partner Selection

---

### 3.1 Introduction

It is well established that NF- $\kappa$ B subunits carry out their role as activators and repressors of transcription in the form of dimers which differentially regulate gene expression in a partner dependent manner [99]. As mentioned previously, however, the stage at which dimer partner selection occurs remains unclear. Current dogma assumes that cytoplasmic inhibited pre-formed dimers are released based on specific inhibitor degradation by the appropriate stimuli and these free dimers are then able to undergo nuclear import with the assistance of molecules such as importin [112]. This would imply that all possible dimer combinations exist in resting cells but shed no light on the ability of dimers to swap partners upon activation. This lack of understanding is also compounded by the fact that the degree of compensation between dimer combinations is poorly characterized. In particular, the differential binding of p65:p50 heterodimers and p65 homodimers has been technically difficult to elucidate. Work by Sengchanthalangsy *et. al.* showed that differences in the dimerization domains of p50 and p65 seemed to account for some of the observed affinity differences between p50 and p65 homo and heterodimers. Their work suggested that mutation in these distinct residues were partially responsible for dimer affinity though they note a major drawback of their study was that it was performed in the presence of the mutation in both partners of the dimers tested [113]. Moreover, several studies have shown that mutations outside of the dimerization domain can have major implications on dimer formation [4,58,114].

Ganchi *et al.* found that mutations of C216 to alanine caused a disruption of p65's ability to form homodimers [115]. Moreover, non-interface residues are responsible for the unique binding nature of RelB dimerization as discussed previously [115]. It has also been discovered that p50 homo-dimerization is greatly

influenced by mutation at serine 343 (human). Wilson *et al.* report that p50 S340A (mouse) mutants are completely unable to form homodimers, though heterodimers are unaffected [58]. Notwithstanding these alternative methods for dimer control, previous studies have identified a hierarchy of affinities for NF- $\kappa$ B dimers where p50:p65 > p50:p50 > p65:p65 [116]. While this hierarchy relates to dimer formation affinities other studies have shown that p50 homodimers in some instances bind target DNA more strongly than its p50:p65 heterodimer counterpart [117]. This was generally dependent on the consensus site being observed but raised the question of whether or not the key regulatory mechanism for the deactivation of NF- $\kappa$ B signaling is through some form of dimer swapping or replacement regime [118].

Current theories surrounding post stimulation switch off of NF- $\kappa$ B signaling are in general poorly understood when compared with NF- $\kappa$ B activation. As mentioned previously, one method through which signaling may terminate is through the ubiquitin mediated proteasomal degradation of subunits. Subunits which are active for prolonged period will, without protection, become subject to poly-ubiquitination and are degraded, removing them from the pool of active NF- $\kappa$ B. Much of the specifics of this mechanism is poorly characterized but Collins *et al.* have documented a case for BCL-3 acting as a guard against p50 homodimer poly ubiquitination. In light of these finding, understanding factors which contribute to the internal and environment mediated stability of subunits becomes vital in understanding their ability to associate with their selected partners. Additionally, it is thought that a combination of post-translational modifications to active dimers as well as the negative feedback loop generated by the transcription of I $\kappa$ B eventually switch off the signal but finer details are elusive. Nevertheless, as it relates to p50 homodimers, one could hypothesize that, in the context of binding sites for which it has higher affinity, p50 homodimers may both blockade active p50:p65 heterodimers or assist in the termination of signal by displacement of p50:p65 from promoters. To in anyway validate this theory, a much better understanding of how homodimers are formed and controlled is needed. In turn, understanding the

formation and potential for displacement of 'active' signaling subunits will further elucidate the functions of a potential p50:HDAC1 co-repressor.

### **3.2 Aims**

Given the poor understanding of p50 and p65 dimerization affinities in the context of residue specific contribution the aims of this chapter are as follows:

- To determine the mechanism by which p50 S343 mutation disrupts p50 homodimerization.
- To investigate all possible unique residues that could lead to preferential dimerization in the context of evolutionary conservation in p50 and p65.
- To determine the contribution of conserved structural differences between p50 and p65 and their effects on p50 homodimer formation.

## 3.3 Results

### 3.3.1 Phosphorylation of p50 S343 as a master regulator of p50 homodimerization

Few studies in the literature have addressed the unknowns surrounding dimer selection in the NF- $\kappa$ B field. However, it has been shown that dimerization of p50 homodimers, but not p50:p65 heterodimers is affected by a serine to alanine mutation at serine 343 (340 in mouse). Due to the nature of this site, an accessible serine residue, it is quite possible that a phosphorylation event here could be a master regulator of p50 dimerization. Whatever the mechanism of its homodimer prevention, Wilson *et. al.* showed that loss of p50 homodimers as a result of p50 S343A mutation recapitulated the pro-inflammatory phenotype observed in p50 knock out mice [58]. Therefore, whether it is through dynamic control of p50 dimers through phosphorylation or some other mechanism, this site warranted further investigation. As such I set out to investigate the role of S343 in the control of p50 homodimers, specifically, its role in dimer stabilization.

As seen in **Figure 3.1**, serine 340 (the mouse equivalent of human serine 343) occupies a region at the far C-terminal of p50 and is on the opposite side of the dimerization domain of the rel homology region of p50. This positioning grants solvent access to the residue and due to the flexible nature of p50 (two globular domains tethered by a single unstructured linker), it is therefore not hard to imagine that this residue is a candidate for phosphorylation. As a result attempts were made to detect phosphorylation at this site in both endogenous p50 as well as generated recombinant protein (see chapter 4). Antibodies raised against phosphorylated p50 S340 were used to probe cell and tissue lysates from mouse and human sources, however, a clear signal that provided confidence was not obtained by western blot. Additionally, samples from immuno-precipitated endogenous p50 as well as recombinant generated p50 (discussed in Chapter 4) did not yield convincing evidence for p50 S340 phosphorylation by mass spectrometry. Issues with these mass spectrometry experiments arose from the detection of p50 peptides and it

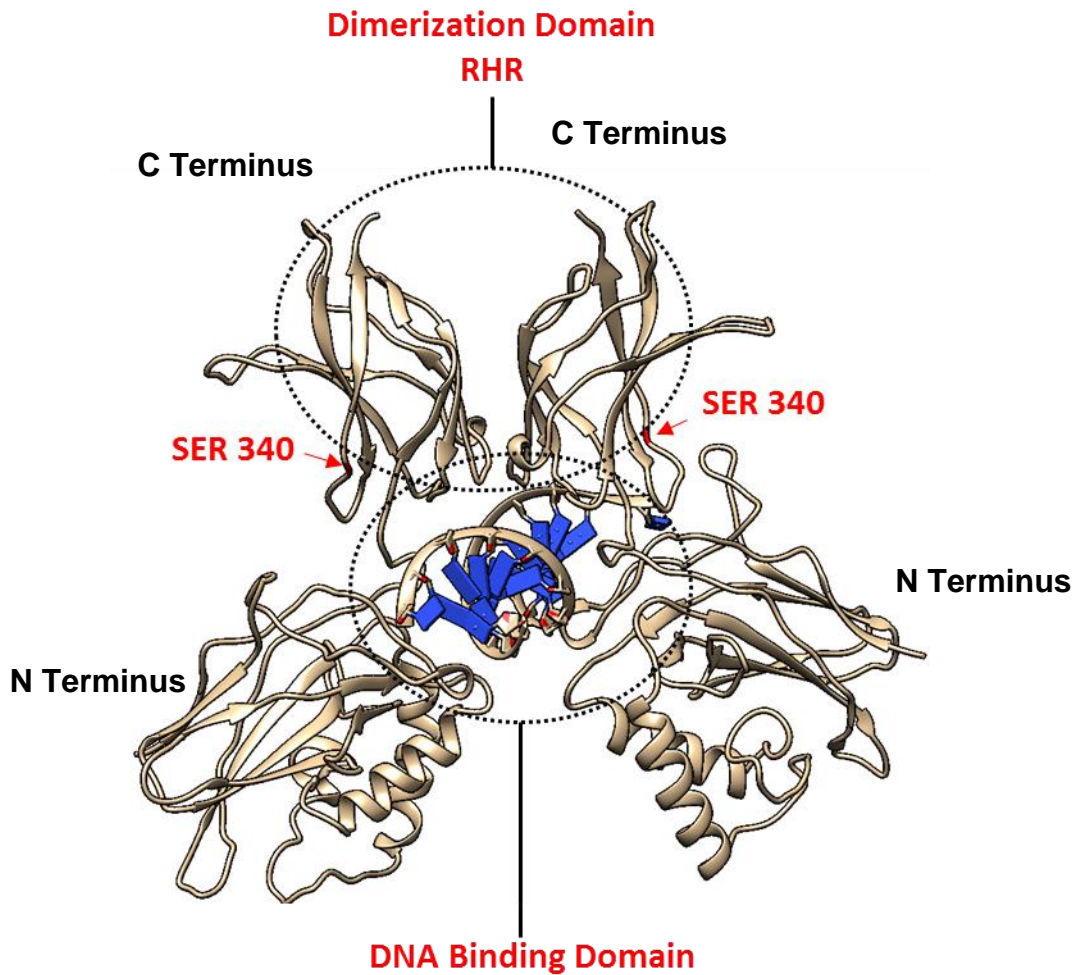


**Figure 3.1 Crystal Structure of a p50 Homodimer.**

*Structural model of a mouse p50 homodimer bound to  $\kappa$ B site highlighting the location of Serine 340 on an external loop of the Dimerization Domain of the rel homology region (RHR). Residues which facilitate DNA binding are also highlighted in the DNA binding domain. Rendered in UCSF Chimera with rounded ribbons. Blue indicates base pairs of DNA with red phosphate sugar backbones.*

did not rule out or support a phosphorylation event at this residue on p50. Further evidence for a potential phosphorylation event at p50 S340 is supported by previous data from our lab and others which show that serine 381, the equivalent residue on p65, is indeed phosphorylated.

Having a known homologous phosphorylation site on p65, all possible phospho-residues in this region of p50 were compared to all other NF- $\kappa$ B subunits. Additionally, as it would be useful in clarifying the complexity involved in dimer selection at the structural level in relation to p50, in depth sequence analysis through evolution on the five subunits of the NF- $\kappa$ B family was performed. Sequences were derived from the reference genomes of 56 organisms spanning the evolutionary spectrum from drosophila to humans. The longest protein coding transcript was used per species and full list can be found in **Figure 3.2**. Multiple sequence alignments were carried out within each of the five-member subunits on 56 species including the known orthologues of the genes if a direct gene comparison was not possible. These multiple sequence alignments were then analyzed for sites of conservation between species and between subunits at key residues. Seen in **Figure 3.3**, alignment of consensus sequences of p65 and p50 with other subunits showed a high degree of conservation between all subunits and through evolution at serine 340 (p50)/ 281(p65). Another site of interest that arose from this analysis is S276 in p65 which is conserved in p50 (S355) and a known phosphorylation site in both proteins [23]. **Figure 3.4A** also highlights that that both of these residues (p65 281 and 276) exist at similar point in three-dimensional space of the crystal structure of p65 and match well with the positions of the equivalent p50 residues on the p50 crystal structure. **Figure 3.4B** also shows that residue conservation at S276 is high in p65 and its equivalent residues in p50 and c-Rel. Moreover, conservation at p65 S281 and equivalent residues is even higher and suggests an important conserved role for this residue in NF- $\kappa$ B function. Nevertheless, solvent accessibility analysis of the available crystal structures does

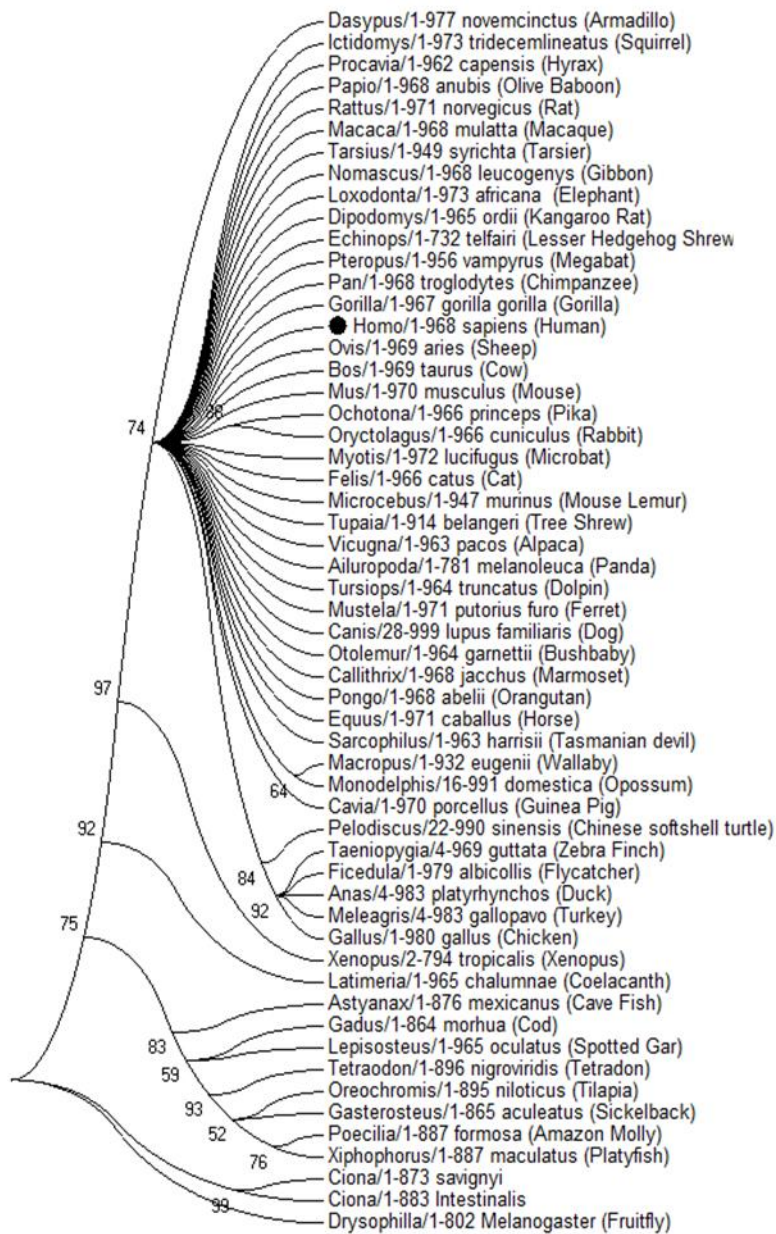


**Figure 3.2 Phylogenetic Tree of Species Used in Evolutionary Multiple Sequence Alignments.**

Phylogenetic tree of all organisms used in the evolutionary multiple sequence alignment analysis of all five NF- $\kappa$ B subunits. Organisms are presented in the format: Genus/#Nucleotides in the p50 orthologue Species (Common Name)



**Figure 3.3 Evolutionary Multiple Sequence Alignment of Serine Residues near Serine 340 (Human S343).**

Multiple sequence alignment of residues on the external surface of the dimerization domain of all subunits. Residues with previously determined phosphorylation events in at least one residue or nearby residues which may be phosphorylated are highlighted. Consensus sequences are labeled based on the positions in mouse p65.

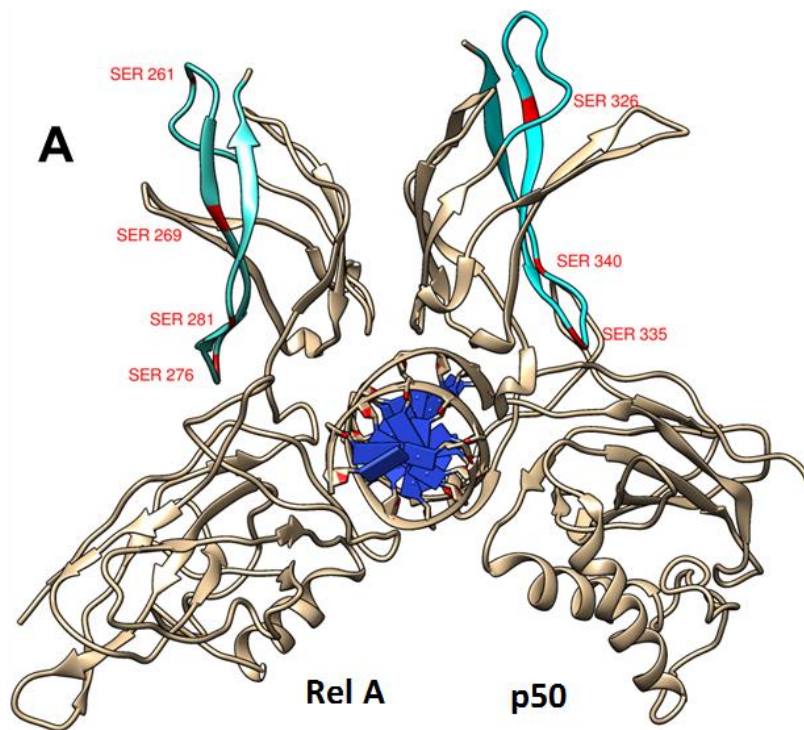
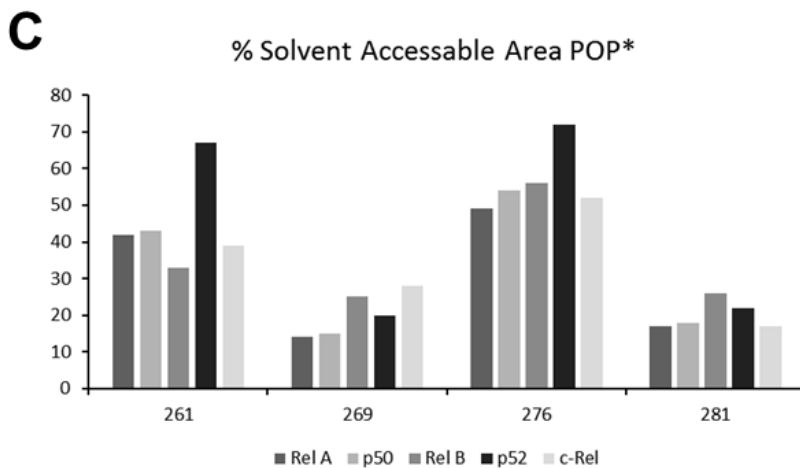
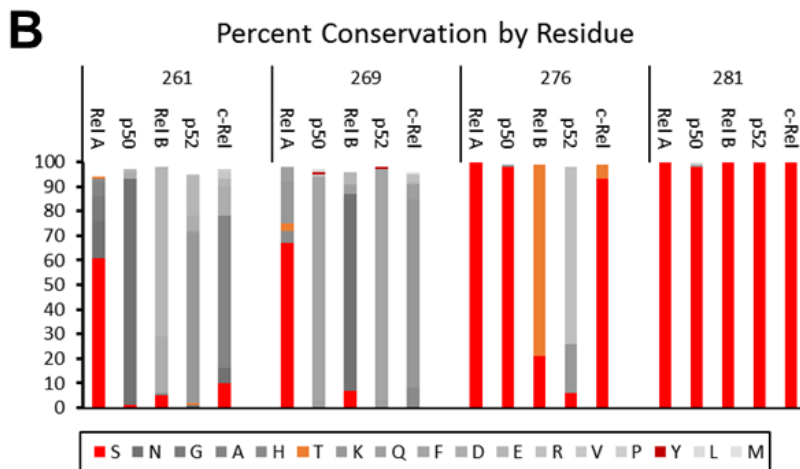


**Figure 3.4 Serine Residues near S340 (Mouse) and their Relative Accessibility**

**A.** Crystal structure of p50:p65 heterodimer highlighting the positions of potential phosphoserines on both proteins. **B.** Analysis of residues by percent conservation through evolution by plotting the percentage occupancy for a particular residue at a given location on a given subunit. **C.** Predicted solvent accessibility based on the POPS algorithm for solvent accessibility of residues investigated [109].



indicate that S281 is less accessible than S276, though as mentioned previously these residues are located in highly flexible regions of the protein (**Figure 3.4C**).

While direct evidence of a phosphorylation event at p50 S343 could not be determined by mass spectrometry or western blot with antibodies raised against phospho-S343 peptides, circumstantial evidence presented here and in previously published work which describe the deleterious effects of p50 S343A mutations strongly suggest that p50 is indeed phosphorylated at this residue [58]. Additionally, this phosphorylation event could have major impacts on the function of p50 and could be the main regulatory site which determines the switch between p50 homodimer repressors and active p65:p50 heterodimers. Regardless, more evidence is required to confirm these assertions and warrants an in depth investigation in its own right.

### **3.3.2 Serine 343 of p50 is critical for protein stability**

During the course of experiments used to confirm loss of homodimerization of p50 as well as expression in transgenic mice which express p50 S343A, it was observed that there was reduced expression of this mutant p50 compared to wild type. Indeed, as compared to wild type murine embryonic fibroblasts (MEFs), p50 S343A MEF's showed a huge reduction in p50 expression (**Figure 3.5A**). However, it was unclear whether there was suppression of p50 expression or if p50 was somehow being degraded in an aberrant way that lead to loss of protein observed in resting cells. Previous work in the lab has shown that p50 transcripts in p50 S340A mice appear at levels comparable to wild type p50 (data not shown). As such this leads one to believe that p50 S340A was leading to some form of premature, constant p50 degradation. To test this p50 wild type and knock out MEFs were transformed with equal amounts either wild type or p50 S340A expressing adenovirus. **Figure 3.5B** shows, however, that overexpressed p50 S340A was observed at lower levels of expression compared to its wild type counterpart.

This observed difference in p50 expression within the same constructs lead us to believe that p50 S340A was having a profound effect on the stability of the protein in resting conditions leading to degradation. Initially it was thought that this ineffective p50 was simply being recycled since it was unable to form homodimers in resting cells. To show this p50 S340A, wild type and p50 knock out MEFs were left untreated or treated with proteasome inhibitor mg132 for 6 hours. The rationale for this experiment being that unstable p50 S340A would accumulate to levels comparable to wild type showing a proteasome mediated degradation of p50 which was unable to carry out its normal function. Surprisingly, p50 S340A still showed reduced levels of protein compared to wild type p50 even after proteasome inhibition (**Figure 3.5C**). This finding was a bit perplexing as it meant that either our initial assumption that p50 S340A did not affect protein production (RNA transcript generation and translation) was incorrect or p50 S340A degradation was occurring independent of the proteasome.

To try and tease apart these different theories *in silico* analysis of the crystal structure of p50 was used to create a better understanding of the contribution of p50 S340A both locally and to the structure of p50 as a whole. To do this I collaborated with Dr. Sarah Harris in The Astbury Centre for Structural Molecular Biology at Leeds University. Together, we were able to perform molecular dynamics simulations on available crystal structures to ascertain the overall contribution made to the stability of p50 by the serine 340 residue. All calculations were performed on Polaris, the high performance computer cluster operated by the N8 HPC collaboration. Using the amber package for molecular dynamics simulations and the available crystal structure of a p50 homodimer (PDB ID: 1NFK), I performed unrestrained molecular dynamics simulations on a wild type p50 homodimer, a p50 homodimer in which one molecule of p50 carried the p50 S340A mutant and a p50:p65 heterodimer (PDB ID: 1LE5). Residues in the crystal structures were first converted to amber format and disulphide bridges conserved.

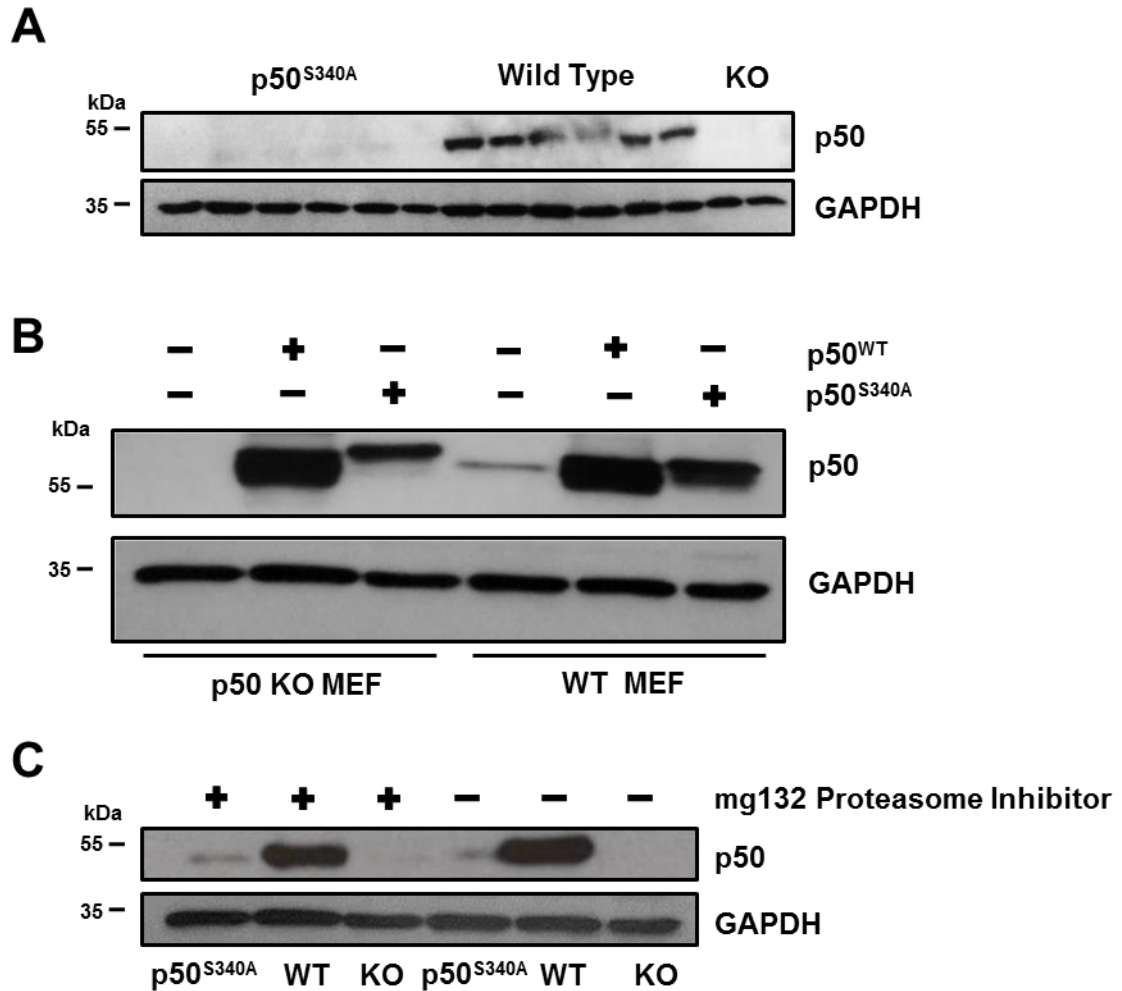


**Figure 3.5 Western Blot Analysis of p50 S340A (Mouse) Expression**

**A.**

Western blot analysis of p50<sup>S340A</sup>, WT and *nfk1<sup>-/-</sup>* (KO) MEF extracts to determine basal expression levels of p50 protein in the various cells. Wild type MEFs contained nominal levels of p50 while in KO cells p50 levels were undetectable as expected. p50<sup>S340A</sup> MEFs however showed a severe reduction in p50 expression. **B.** Western blot analysis of WT and *nfk1<sup>-/-</sup>* MEFs reconstituted with either WT or p50<sup>S340A</sup> through adenoviral delivery. After over expression with an adenoviral expression vector p50<sup>S340A</sup> was present in lower levels compared to the WT protein in the same expression vector. **C.** Western blot analysis of p50<sup>S340A</sup>, WT and *nfk1<sup>-/-</sup>* (KO) MEFs treated for 6 hours with proteasome inhibitor mg132. p50 levels remain exceedingly low in cells which have had their proteasome inhibited. GAPDH was probed in all blots as loading control to ensure comparable levels of protein.

Molecules were then charge balanced with sodium chloride and hydrated with explicit water molecules (**Figure 3.6A and B**). This process was performed for all three structures mentioned previously and then slowly raised to a temperature of 300 degrees Kelvin and allowed to proceed through an unrestrained simulation up to 100ns in length. **Figure 3.6C** shows the representative metrics of a p50wt:p50S340A homodimer throughout the first 25ns of its full simulation including the protein's total Root Mean Square Deviation (RMSD) of atoms of the entire molecule. Interestingly, when observed at the residue level, alanine 340 (of the p50 S340A mutant structure) had almost twice the average RMSD of the wild type serine residue in the same crystal structure dimer (A340=4 Å vs. S340=2 Å). This finding suggests that the S340A mutation on p50 is having a profound effect on the local structural flexibility and potentially stability of this region of the protein.

In an attempt to determine if this local effect in any way translated to the protein as a whole, complete 100ns simulations of a wild type p50 homodimer, wild type p65:p50 heterodimer and the mutant S340A p50 wild type p50 homodimer were all compared per residue by average RMSD over the full length simulation; termed atomic flux. As shown in **Figure 3.7**, wild type p50:p65 heterodimers show the highest degree of divergence from the p50 homodimer simulations which is unsurprising given that half of the residues in the simulation are p65 in origin. When wild type p50 homodimers are compared to their single chain mutant counterparts however, several insightful observations can be made. First, the amino acids in the wild type chain (amino acids 1-311) of the p50:p50S340A homodimer appear to roughly follow the atomic deviation found in the wild type p50 homodimer, especially near residues 135- 200. This region corresponds to the N-terminus of p50 which does not participate in dimer formation. Residues corresponding to the mutant chain of p50:p50S340A (312-622) however, show much greater divergence from the wild chain of the wild type p50 homodimer. With the exception of a few points along the protein, p50 S340A mutant chain show substantially

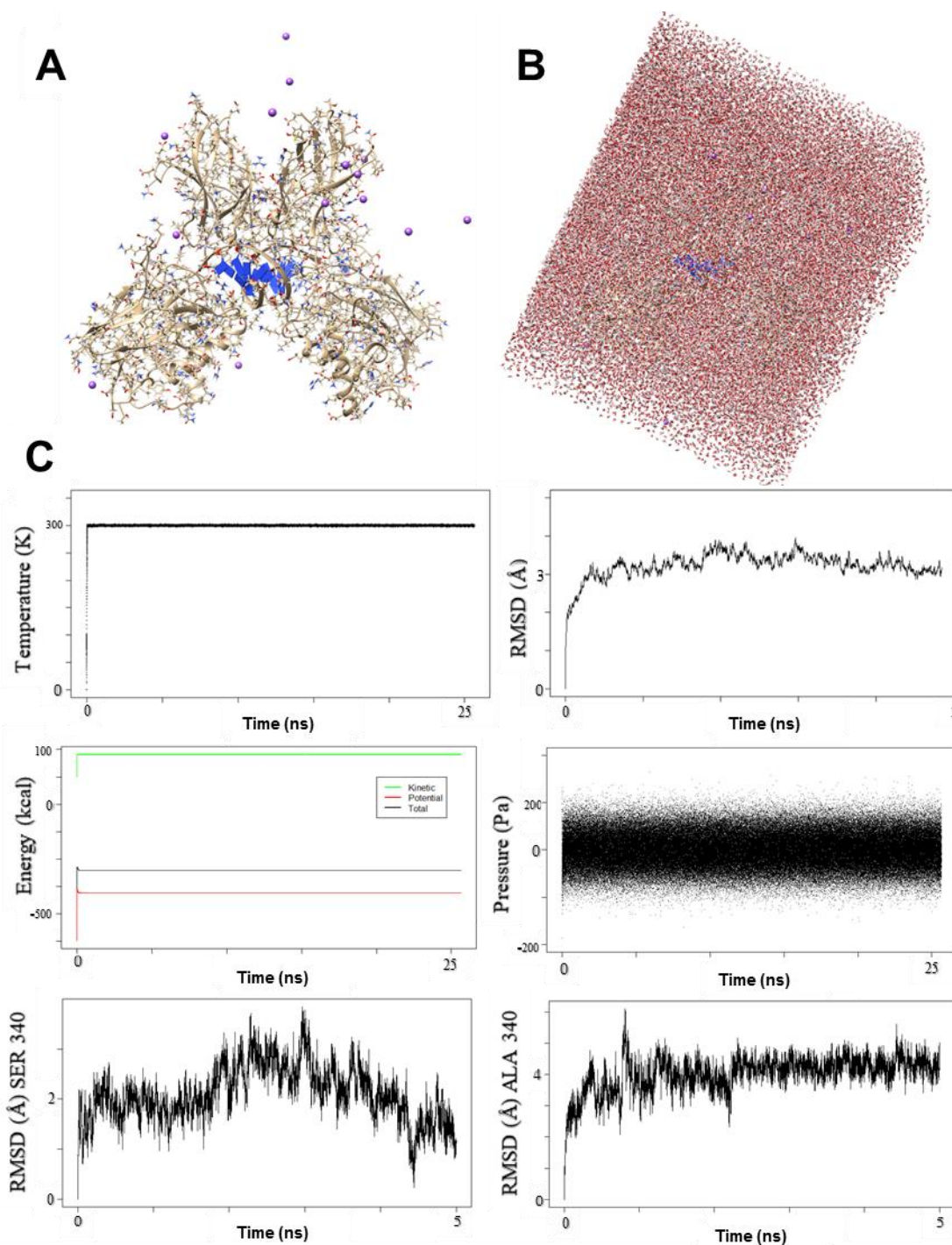


**Figure 3.6 Molecular Dynamics Simulation of p50:p50S340A Homodimer**

**A.** Initial atomic positions of a p50 WT: p50<sup>S340A</sup> heterodimer bound to DNA and charge balanced by chloride ions (purple). **B.** Implicit water box surrounding the complex in which molecular dynamics simulations were performed. **C.** Quality control graphs indicating the integrity of the simulation as well as analysis of the Root Mean Squared Deviation (RMSD) of both Serine 340 and Alanine 340 in their respective chains to determine their positional stability during the simulation.

higher atomic fluctuations than its wild type counterpart and in general the dimers diverge overall.

While on its own this study has a few drawbacks, most evidently the fact that crystal structures are not complete, it provides more evidence for the destabilization of the p50 homodimer by S340A mutation. Moreover, the direct comparison between dimers with the only difference being this change in one residue highlight the potential regulatory importance of the residue and warrants further study.

## NF- $\kappa$ B Dimer Atomic Flux

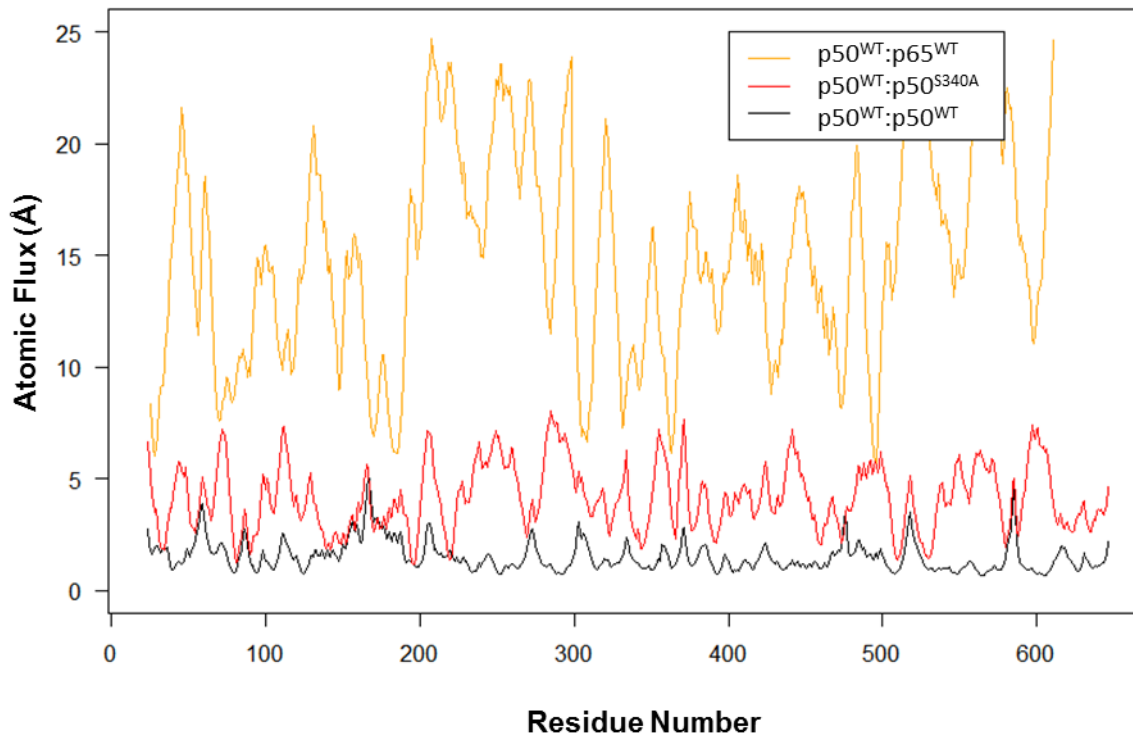


**Figure 3.7 Relative Atomic Flux of a p50:p50S340A Molecular Dynamic Simulation**

Comparison of atomic flux of three separate molecular dynamics simulations by residue number showing greater flux (less stability) in mutated p50 homodimer (p50:p50<sup>S340A</sup>) compared to WT (p50:p50).

### 3.3.3 p50 Dimerization: Evolutionary Insights into Dimer Selection

In addition to the stability of subunit dimers imparted by phosphorylation, little has been uncovered regarding the structural basis of NF- $\kappa$ B dimerization. Having generated a library of sequence alignments (see **Section 3.3.1**) for all subunits across species and evolution it was decided to investigate whether this library could highlight residues in the dimer interface that could be critical in dimerization and therefore conserved. To better visualize these results, multiple sequence alignments for each subunit through evolution was mapped onto the respective crystal structures available for each subunit and each residue colored by percentage conservation. **Figure 3.8** confirms the well-known conservation in the NF- $\kappa$ B family, especially as it relates to p65 which displays <90% conservation of many residues present in the crystal structure; particularly those responsible for dimerization and DNA contacts [99]. p50, as well as the other subunits, also show a high degree of conservation in the core rel homology region. With this high degree of conservation within the subunits I decided to also look at conservation between subunits to gain insights into the differences between residues which confer subtle subunit specific changes. Of particular importance was the residues involved in dimerization and their contribution to dimer selection. As seen in **Figure 3.9**, a number of residues are conserved between p50 and all other subunits when the p50 evolutionary multiple sequence alignment is compared that of the aggregated evolutionary alignments of all other subunits. Of particular importance however is the comparison between the evolutionary alignments of p50 compared to that of p65 as differences in the dimerization domain here would be responsible for any observed differential binding. It would not be unreasonable to assume that different residues in regions that would make direct contacts between subunits in the p50 homodimer and p50:p65 heterodimer would have an effect on their binding affinity and may make a significant contribution to dimer selection upstream of activation.

Once the comparison between p50 and p65 was performed and visualized on the crystal structure of p50 it was noted that four residues in the dimerization

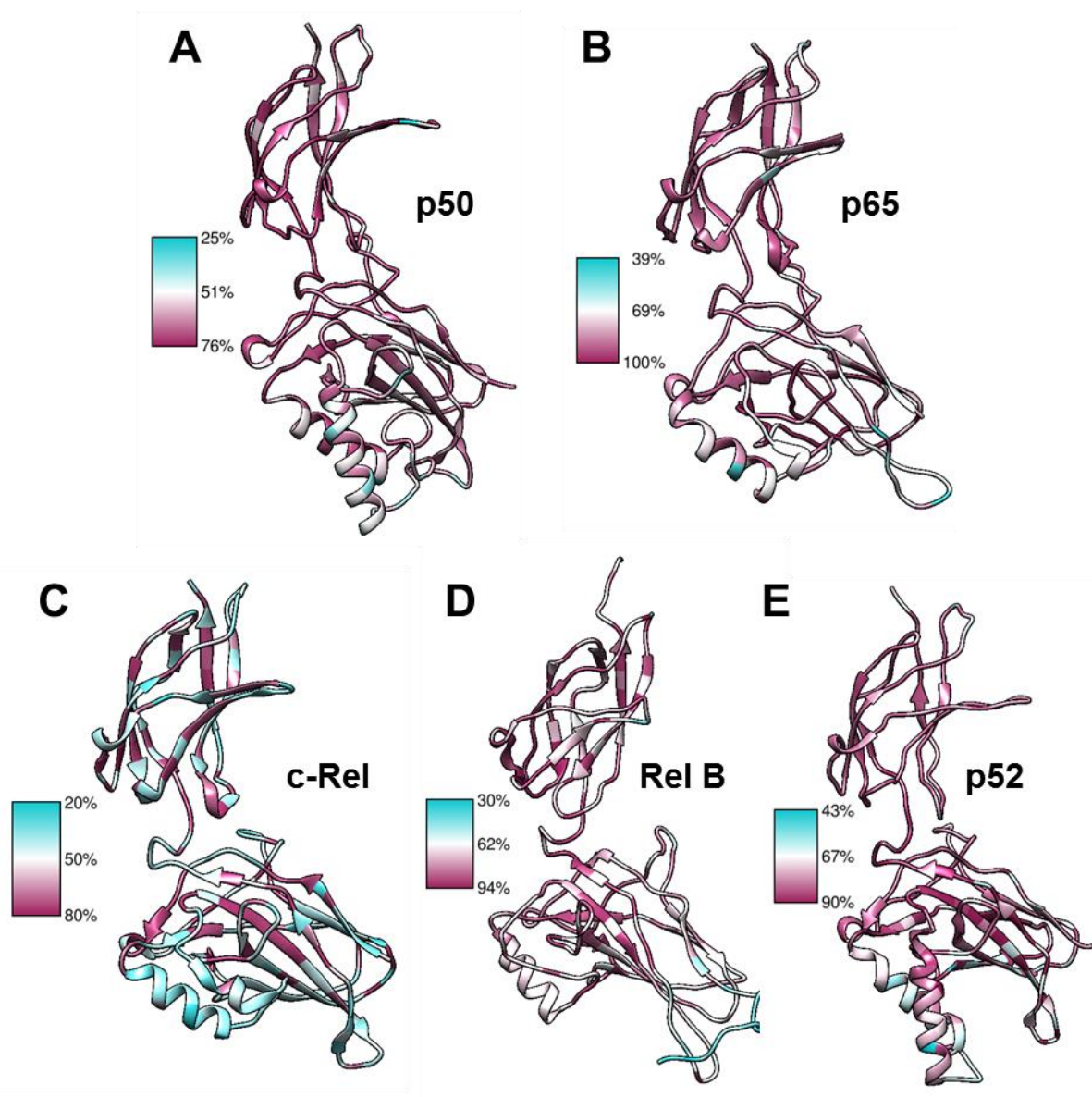


**Figure 3.8 Evolutionary Analysis of all NF-κB Subunits relative to their Respective Crystal Structures**

**A-E.** Percentage conservation of each subunit mapped onto the available crystal structure. Data derived from evolutionary alignments from species listed in Figure 3.2. Alignments visualized in UCSF Chimera.

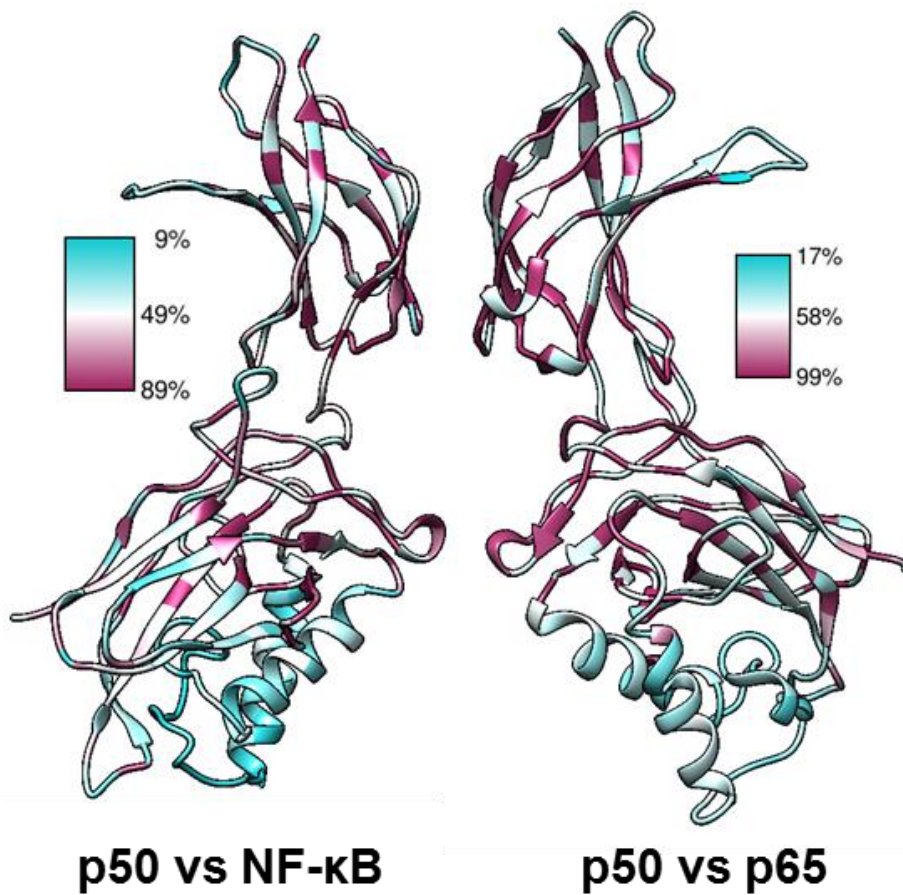


**Figure 3.9 Evolutionary Comparison of p50 and all other subunits and p50 against p65**

*Percentage conservation of residues in p50 compared with conserved residues in all other NF-κB subunits (left) or conserved residues in p65 (right). Alignments visualized in UCSF Chimera.*

domain differed between p50 and p65. With the exception of these four, all other residues that make contact between the two subunits were highly conserved. These four residues are highlighted in **Figure 3.10** and consist of methionine 253, asparagine 254, tyrosine 267 and phenylalanine 307 in mouse p50. These four residues appear to participate solely in subunit dimerization, however it was observed that P307 in p50 and its counterpart V248 in p65 have the potential to form hydrogen bonds with the nearby backbone of the DNA helix. Based on this better molecular understanding of subunit dimerization I decided to investigate whether these residue differences played a major role in the dimer selection process between p50 and p65. More specifically it was important to determine if these residues impart more or less dimer stability in the context of the full crystal structure. As such an experimental plan was made to use further molecular dynamics simulations to interrogate the contributions of these four residues collectively.

In order to fully appreciate the contributions of these residues collectively, three distinct simulations were performed under conditions previously described. As a basis of comparison, previously mentioned wild type p50 homodimers and wild type p50:p65 heterodimers were used. Additionally, a separate simulation was performed on a p50:p50 homodimer in which four residues in one of the p50 chains were mutated to those occurring in p65 at the same locations in the protein-protein interface. Atomistic data was compared for these three simulations over 100ns. Metrics for these experiments can be found In **Figure 3.11-13** which show that conditions of temperature and total energy per simulation were comparable throughout. Given that these simulations were carried out in the presence of DNA and that the wild type p50 homodimer and p50:p65 heterodimer were also examined, it was hypothesized that an interface change such that a p50 homodimer acquired a p65:p50 interface would lead to further protein-protein instability or stabilization. To measure these effects whole molecule RMSD was again employed.

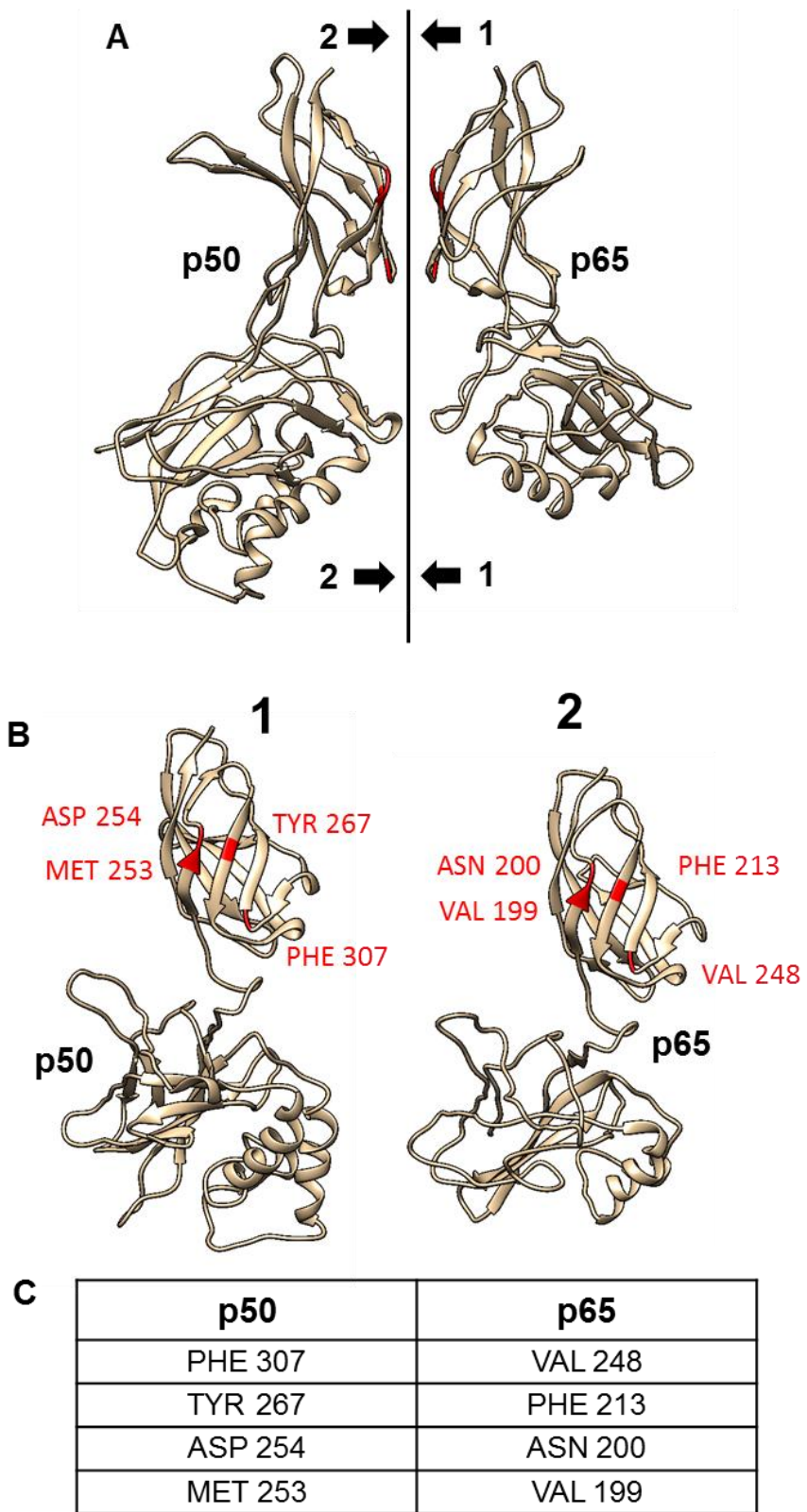


**Figure 3.10 Dimerization Residues which differ between p50 and p65 through evolution**

**A.** Crystal Structure of a p50:p65 heterodimer with evolutionary distinct interface residues highlighted (red).

**B.** Side on view of labeled distinct interface residues in p50 and p65.

**C.** Table of conserved residues and their counterparts in p50 or p65 structure.

## WT p50:p50 Homodimer

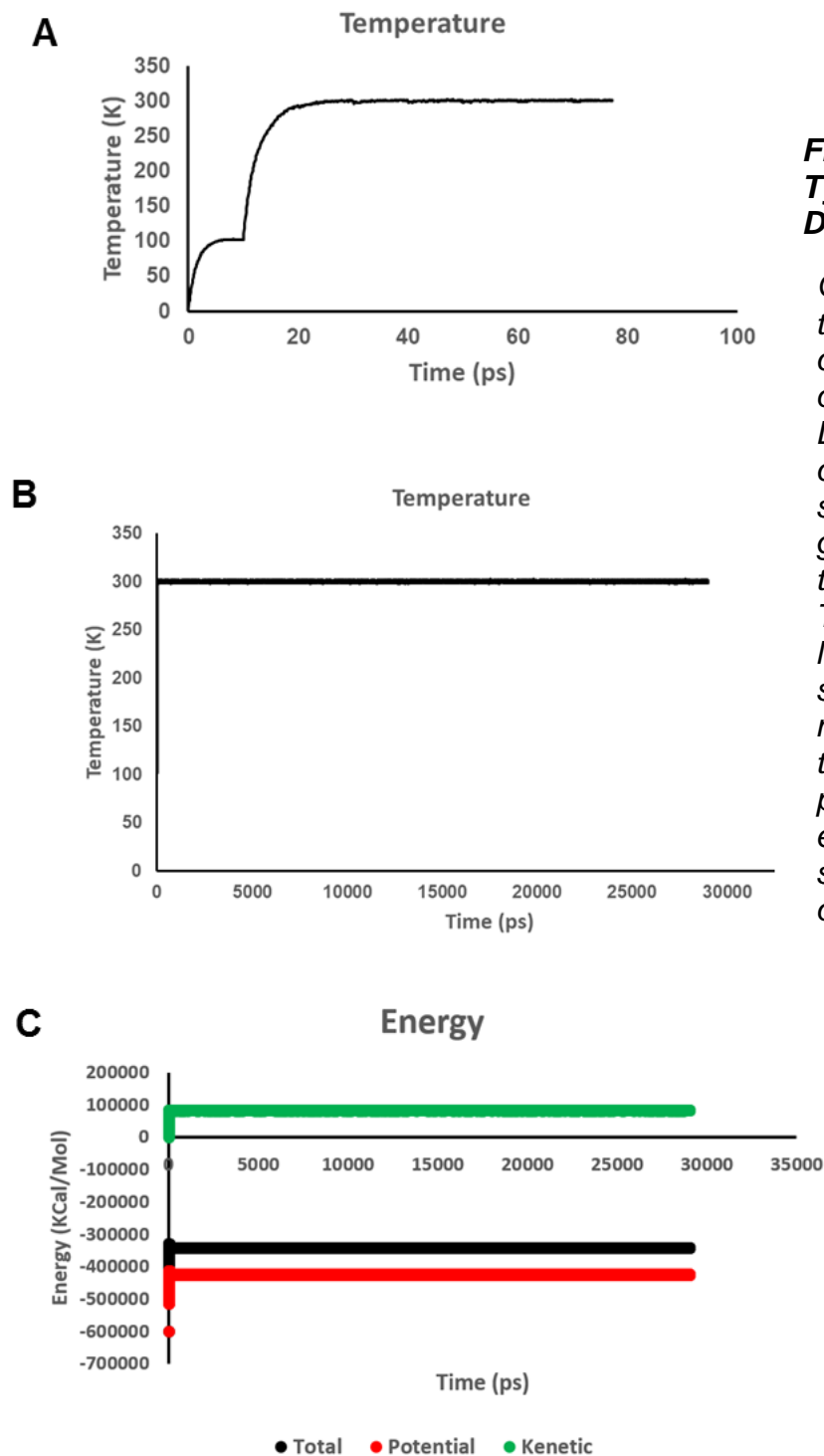


**Figure 3.11 Metrics for a Wild Type p50 homodimer Molecular Dynamics Simulation**

Quality control graphs indicating the integrity of a molecular dynamics simulation performed on a p50 homodimer bound to DNA. **A.** Increasing temperature during the initiation phase of the simulation graphed to show a gradual increase in two steps up to a run temperature of 300K. **B.** Temperature graphed over a longer period of time which shows a stable temperature is maintained for the duration of the simulation. **C.** Plot of potential, kinetic and total energy of the system ensuring system stability for the duration of the simulation.

## WT p50:p65 Heterodimer

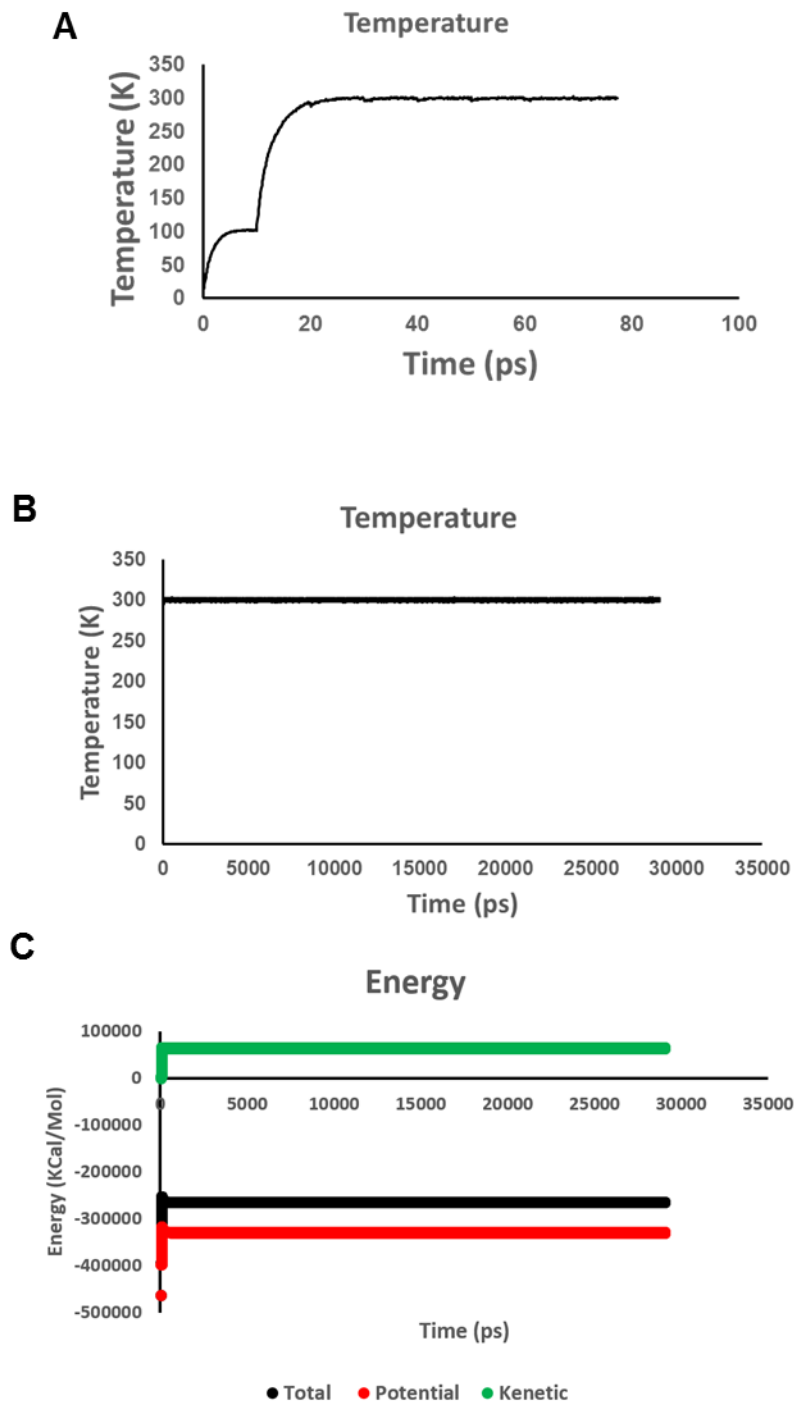
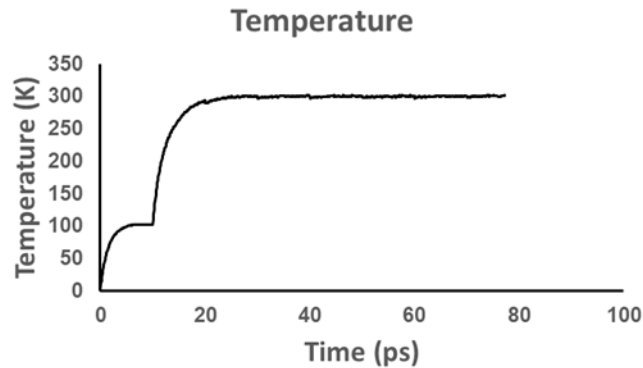


**Figure 3.12 Metrics for a wild type p50:p65 Heterodimer Molecular Dynamics Simulation**

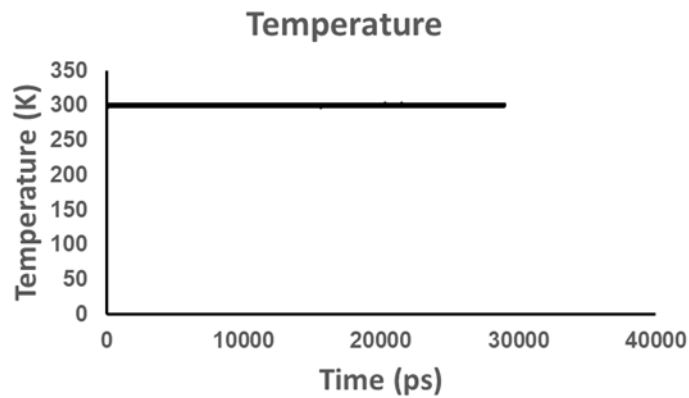
Quality control graphs indicating the integrity of a molecular dynamics simulation performed on a p50:p65 heterodimer bound to DNA. **A.** Increasing temperature during the initiation phase of the simulation graphed to show a gradual increase in two steps up to a run temperature of 300K. **B.** Temperature graphed over a longer period of time which shows a stable temperature is maintained for the duration of the simulation. **C.** Plot of potential, kinetic and total energy of the system ensuring system stability for the duration of the simulation.

## Mutant p50:p50<sup>p65</sup> Heterodimer

**A**



**B**



**C**

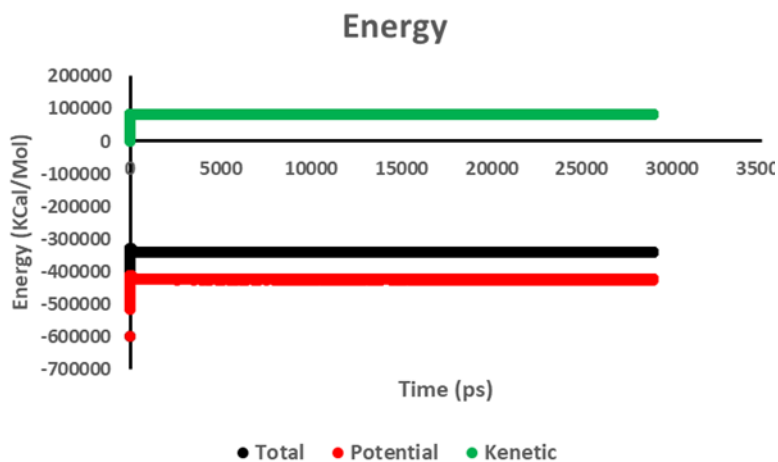


**Figure 3.13 Metrics for a p50;p50<sup>p65</sup> Mutant Heterodimer Molecular Dynamics Simulation**

Quality control graphs indicating the integrity of a molecular dynamics simulation performed on a homodimer of p50 in which one subunit of the dimer has been mutated to conform to p65 evolutionarily conserved interface. **A.** Increasing temperature during the initiation phase of the simulation graphed to show a gradual increase in two steps up to a run temperature of 300K. **B.** Temperature graphed over a longer period of time which shows a stable temperature is maintained for the duration of the simulation. **C.** Plot of potential, kinetic and total energy of the system ensuring system stability for the duration of the simulation.

Using wild type p50 homodimers as a base line it is seen that, overall, p50:p65 heterodimers form a less stable interaction. However, upon mutation of one of the p50 molecules in a p50 homodimer to an interface of p65 average RMSD of this mutant dimer falls to below that of a p50 homodimer. Shown in **Figure 3.14**, this analysis suggests that, in the presence of DNA, p50 homodimers exist in a more stable confirmation though this can be enhanced by changing dimerization critical residues to those that are p65 specific.

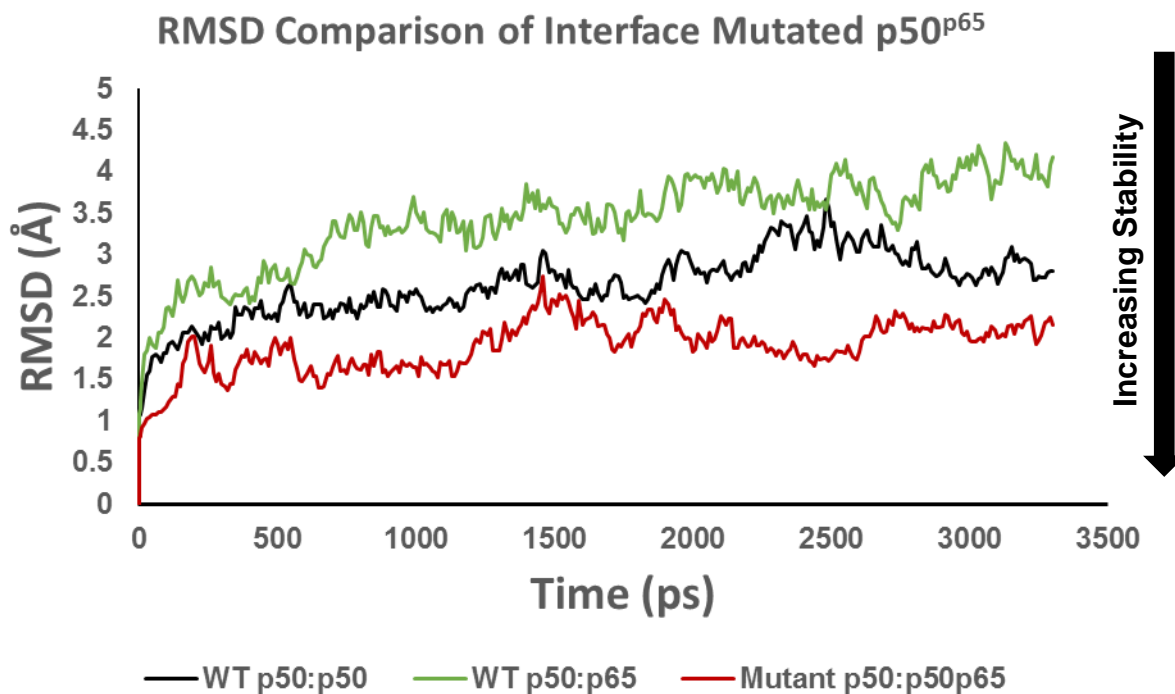


**Figure 3.14 Comparison of wild type p50 homodimers and p65 heterodimers against a mutant p50 homodimer which contains a p65 interface in one chain.**

RMSD comparison of three molecular dynamics simulations performed on a wild type p50 homodimer, wild type p50:p65 heterodimer and a dimer composing of wild type p50 and a molecule of p50 where residues have been mutated to those conserved in p65. (Amino acid changes include F307V, Y267F, D254N, M253V) All simulations were run under the same initial and maintenance conditions.

### **3.4 Discussion**

Dimer selection and rearrangement remains one of the least understood areas of wider NF- $\kappa$ B research. In particular, the rules governing the formation of repressive p50 homodimers versus canonical p50:p65 heterodimers which go on to activate gene transcription have been poorly characterized. Data presented here may be interpreted to support three different views on how this dimer selection/assembly may be carried out in cells. Firstly, dimer selection could be the result of post-translational changes carried out directly on subunits and determined by numerous signaling events in the cell. Second, evolutionary variation between subunits orchestrates a complex order of binding affinities which, over the course of a signaling event, lead to the appropriate proportions of active dimers which produce the desired result. The third and mostly likely scenario is some combination of the previous where numerous factors including modification events, specific subunit binding propensities as well as third party interactions all work in unison to achieve the desired outcome. While this would be the most elegant solution to understanding this issue of dimer selection, it makes interrogating the system a complex undertaking.

#### **3.4.1 Post-Translational Modification as a Mechanism for Dimer Selection**

Discussed previously, numerous sites of post-translational modification have been described on NF- $\kappa$ B subunits with wide ranging effects. As it related to dimerization, single amino acid modifications have been shown to augment correct dimerization. Jacques *et al.* found that phosphorylation on serine 276 of p65 encourages dimerization with RelB though it is unclear how it achieves this as it is not an interface residue [119]. One argument they propose is that an increased negative charge here may be having wide ranging effect on direct interface residues. A similar effect may be the cause of the observation that phosphorylation at serine 343 (human) may orchestrate a shift to repressive homodimers away from a more stable p50:p65 heterodimer. Evidence presented here however, suggests

that serine 343 of p50 is playing a larger role than dimer selection and is directly contributing to the overall stability of the protein in all observed dimer combinations. Given that percentage conservation at this site is near 100% in all subunits (**Figure 3.3B**), subsequent observations of the severe loss of protein expression/stability are not surprising. Moreover, the increase in flexibility described by a doubling of RMSD at the same residue with an S343A mutant (**Figure 3.5C**) and the overall sharp increase in the atomic flux of the subunit as a whole which contains an S343A mutant (**Figure 3.6**) all point to a residue critical to protein integrity. While these observations relating to stability are all performed *in silico*, they conform to the observed reduction in protein expression though cannot be used to claim with certainty that stability is the sole function of this residue. Further *in vitro* experiments are needed to more finely tune our understanding of this residue's role in dimer assembly and structural integrity.

### **3.4.2 Evolutionary Distinctiveness as the Major Control Mechanism of Dimer Assembly**

In addition to post-translational modification of subunits as a mechanism to account for dimer selection, observed evolutionary differences in interface residues must, in some part, contribute to dimer affinity. Indeed, Huxford and Ghosh discuss the known differences between p50 and p65, namely the Y269F and D256N substitutions [120]. They go on to explain that Y269 in p50 makes a significant contribution to the stability of the p50 homo and heterodimer and its substitution to phenylalanine in p65 accounts for the reduced binding affinity in p65 homodimers. Evolutionary analysis presented here, however, adds two other residues to the list of conserved differences noted in the dimerization interface p50 and p65 (**Figure 3.10**). While Huang *et al.* found that p50 heterodimers are more stable than their homodimer counterpart, it has been difficult to measure this difference accurately [116]. Presented here, molecular dynamics simulations on wild type and mutant versions of hetero and homodimers may help to resolve many of these dimer related assumptions. In **Figure 3.13** it can be seen that stability (measured by

proxy through RMSD) is greatest in a dimer composed of wild type p50 and mutant p50 where four interface residues are substituted for those found in p65 (p50<sup>p65</sup>). This simulation, performed in the context of bound DNA does however calculate the stability of a p50 homodimer to be greater than that of a p65:p50 heterodimer. As mentioned previously, however, dimer stability depends heavily on DNA interactions as well as interface differences which could account for this observation. Nevertheless, the fact that this combination of wild type and mutant p50<sup>p65</sup> dimers appear to be the most stable configuration and strongly suggests that dimer interface residues make up a major part of the decisions related to dimer assembly. The difficulty remains, however, in understanding to what degree these dimer interface residues contribute to dimer selection. Specifically, is there a pattern of mutation that could be achieved in which dimers of a specific type are always preferred? There is likely far more complexity as there is also the known contribution of co-factors to dimer choice.

### **3.4.3 Co-factors, Post-translational Modifications and Evolutionary Differences: The complexity of dimerization.**

Presented here are two methods by which dimerization may be regulated in the NF- $\kappa$ B family however the true complex signaling involved in dimerization and functional outputs of signaling cascades will depend on numerous factors. Aside from obvious tissue and cell specific differences, dimerization has also been shown by others to be, in part, regulated by the I $\kappa$ B's as well. Tsui *et al.* showed that I $\kappa$ B $\beta$  was able to encourage the formation of the lower affinity p65 homodimer [121]. This study suggests that regardless of innate affinity as determined by interface residues conserved through evolution, dimerization of a certain regime may be augmented by a tertiary binding partner. In support of this Ashkenazi *et al.* found that withaferin A, a small molecule inhibitor, was able to allosterically inhibit p65 dimerization [122]. These two cases reflect the complexity of control that may be at play when considering dimerization in any context. This area still needs far more investigation into both general control as well as in specific contexts such as under

resting and stimulated conditions as well as during resolution of a response. Findings presented in this chapter strongly suggest that when considering manipulation of NF- $\kappa$ B dimers several precautions are needed. Direct modifications of residues that disrupt a specific dimer may have catastrophic impact on the ability of that subunit to carry out other functions as well as maintain expression at appropriate levels. Additionally, while evolution has hardwired some general affinities into canonical dimers, their existence is highly context specific and requires a full understanding of co-factors and post-translational modifications that may be contributing to the final outcome of any particular signaling event.

## Chapter 4 Determining the Structural Basis of the p50:HDAC1 Interface

---

### 4.1 Introduction

Studies mentioned previously have suggested that p50 binds HDAC1 at least in the cell lines in which the original observation have been published. Since then, others have shown that the interaction between p50 and HDAC1 may in part be responsible for changes in gene transcription activity at certain NF- $\kappa$ B promoters [102]. However, this information has been observational and has lacked a deep structural understanding of how these proteins may be interacting as well as the mechanism for the formation of this complex in general. It has been originally reported by Zhong *et. al.* that phosphorylation plays a major role in whether or not p50:p65 heterodimers associate with the activating histone acetyl transferase p300 or HDAC1 [103]. This study however did not determine how p50 was interacting with HDAC1 specifically and whether this held true in the context of p50 homodimers on their own. In addition to work from Wilson *et. al.* which attributes much of the anti-inflammatory potential of p50 homodimer to its association with HDAC1 [58], Elsharkawy *et. al.* showed that HDAC1 activity was critical in the inhibition of pro-inflammatory genes by p50 [104]. While these reports all confirm the importance and presence of the complex, they do not elucidate its mechanism of formation or the precise nature of the interaction.

Recently, Bandyopadhaya *et. al.* found that p50 may be playing a major role in tolerance (the ability of cells to subdue their reactions to repeated introduction to the same stimuli) and their study has shed more light on the nature of the interaction. They show that cells tolerized with bacterial quorum sensing molecule 2-Aminoacetophenone leads to decreased HDAC1 mediated p65 acetylation and a reduction in p65:p300 binding. Moreover, this loss of p65 acetylation coincided with an increase in p50:HDAC1 binding and a decrease in p50:p65 binding [102]. These results confirm Zhong's original findings and provides further evidence that

HDAC1, through interaction with p50, is a major repressor of NF- $\kappa$ B driven pro-inflammatory gene expression.

#### **4.2 Aims**

Apart from these studies little has been done to more finely elucidate the structural interaction between p50 and HDAC1. As such this chapter aims to:

- Determine the conditions under which p50 associates with HDAC1.
- Determine the exact structural interaction between the p50 and HDAC1 molecules.
- Understand the effects and implications of the observed binding between the two proteins.

## 4.3 Results

### 4.3.1 p50 associates with HDAC1 in resting cells

Evidence for a direct association between p50 and HDAC1 in the literature is sparse, as eluded to earlier [123]. As such the assertions commonly made in the literature that p50 is present in the nucleus of resting cells and associates with HDAC1 needed to be re-examined. As HDAC1 is a well-established nuclear specific protein, the nuclear activity of p50 in unstimulated cells needed to be determined. Immunofluorescence for endogenous p50 was performed in U2OS cells under normal culture conditions with a variety of primary antibodies raised against p50. Under all conditions tested, many antibodies produced high, undesirable levels of background and were not conclusive, however, representative images shown in **Figure 4.1** do suggest both a nuclear and cytoplasmic pool of p50 when detected by SC 114-X (Santa Cruz) anti-p50/p105.

Given these technical issues with immunofluorescence, it was decided to attempt to confirm an interaction between p50 and HDAC1 in whole cell lysates using immunoprecipitation (IP). As such, a protocol was developed to facilitate p50 immunoprecipitation from cells and tissue using the commercially available antibody (Abcam ab7971), the details of which can be found in the relevant methods. After trying several conditions and systems, p50 was successfully immuno-precipitated from U2OS cells, shown in **Figure 4.2A**. To determine if p50 interacts with HDAC1, however, further optimization was required to preserve protein-protein interactions within the IP. Using the same p50 antibody mentioned previously as well as negative controls including non-specific rabbit IgG and mouse anti Gal4 antibody, IP experiments were performed using an anti-p65 antibody (Santa Cruz, SC-37) to see if the canonical association of p50 with p65 could be detected in a co-IP assay. Under optimized conditions used in **Figure 4.2B**, p50 is found associated with IP'ed p65 validating the conditions used. Unfortunately, during the course of these experiments, the originally optimized antibody became unavailable from the manufacturer and therefore, three alternatives had to be

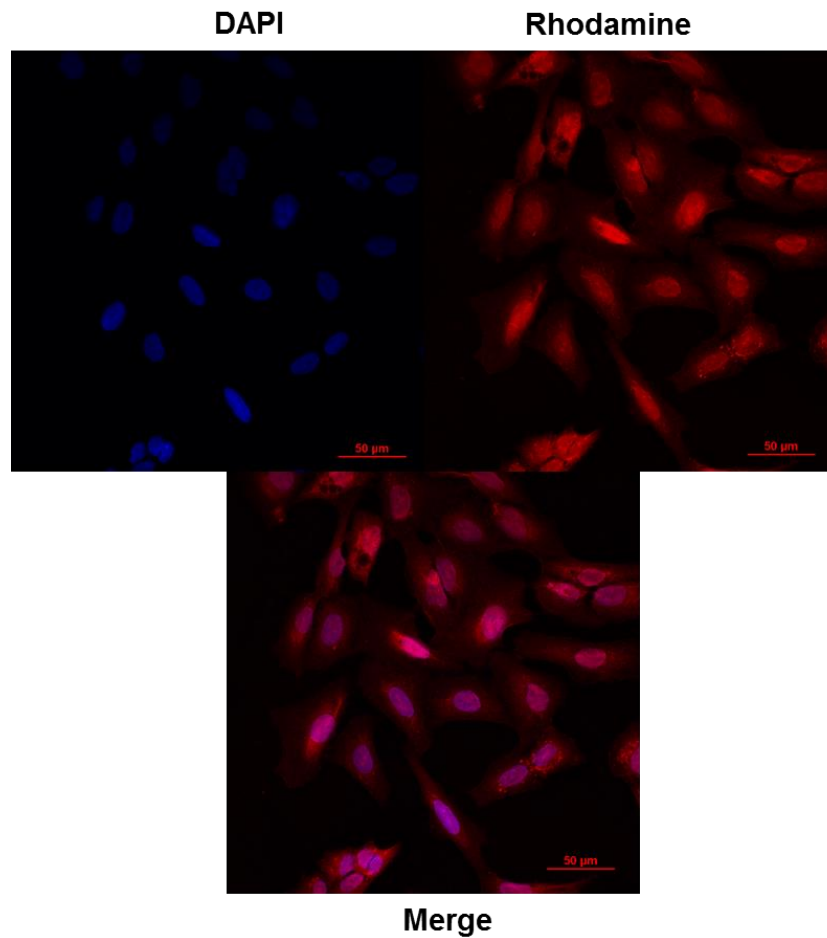


**Figure 4.1 Immunofluorescent Microscopy of Endogenous p50/p105**

*Confocal Immunofluorescent microscopy of U2OS cells with clear nuclear and cytoplasmic pools of wild type, endogenous p50 in resting cells. p50 shown in red (Rhodamine) with DNA shown in blue (DAPI) as well as a merged channel.*

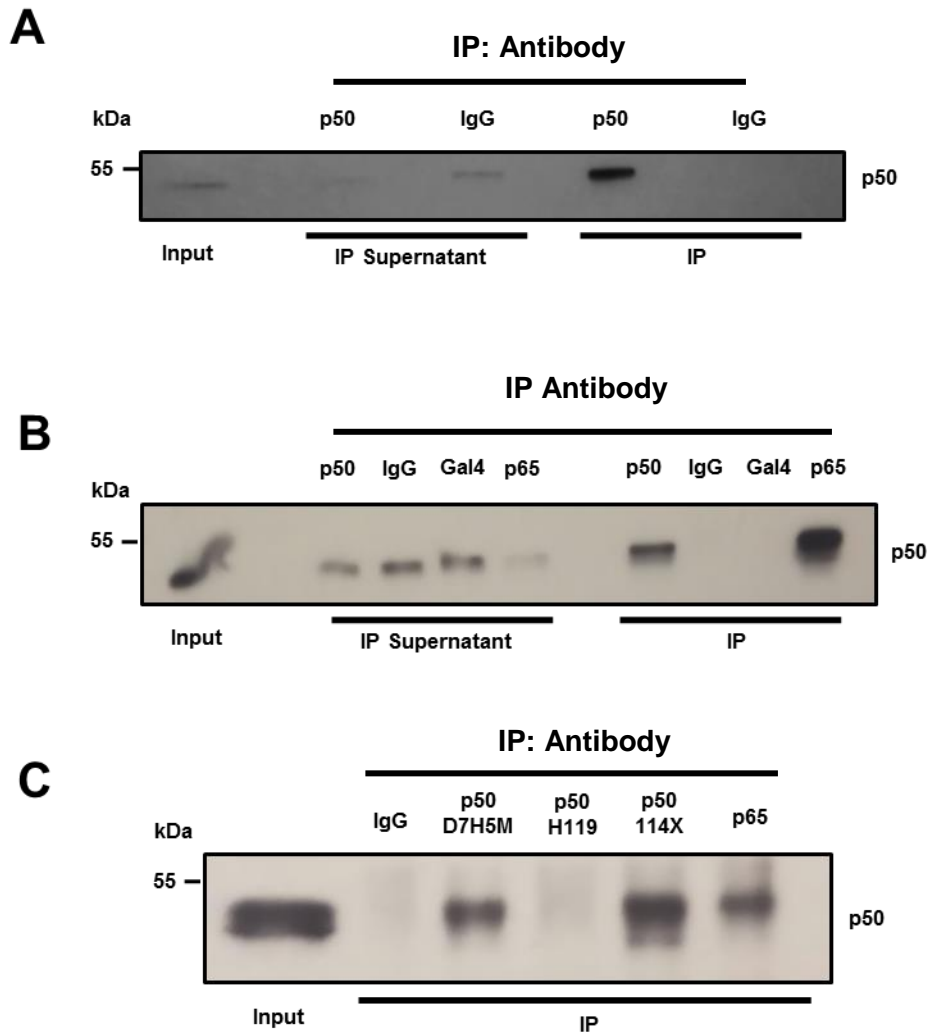


**Figure 4.2 Optimization of p50 Immunoprecipitation Assays**

**A.** Immunoprecipitation of p50 from U2OS cells showing a reduction of p50 in IP supernatant following incubation with anti p50/p105 antibody (Abcam) and subsequent enrichment in IP samples. **B.** Western blot for p50 showing optimization of co-immunoprecipitation assay in U2OS cells confirming co-precipitation of p50 along with p65. (Direct IP of p50 achieved using p50 antibody, IgG and Gal4 used as a negative controls and p65 to test co-ip of p50) **C.** Western blot of a Co-immunoprecipitation assay in wild type murine embryonic fibroblasts (MEF's) to determine which a commercially available antibodies were capable of precipitation of p50 for further experiments (IP antibodies used were IgG as a negative control, p50 D7H5M (CST), p50 H119 (Santa Cruz) and p50 114x (Santa Cruz) along with p65 to insure co-ip conditions were maintained).

screened under co-IP conditions to validate their effectiveness to IP p50. Shown in **Figure 4.2C**, two of the 4 antibodies tested successfully immuno-precipitated p50 under co-IP conditions and these were used for the remainder of the study.

Previous studies in cell lines have shown that p50 and p65 seem to associate with HDAC1 under resting conditions [103]. However, it was uncertain if this interaction could be observed *in vivo*. Therefore, wild type three-month-old whole liver was utilized from C57/B6 mice to perform endogenous co-IP assays for p50 and HDAC1. **Figure 4.3A** shows that, at least by co-IP, p50 and p65 both do associate with HDAC1 in primary tissue. As these experiments were performed on healthy untreated wild type tissues, this experiment provides further evidence for the p50:HDAC1 association under resting conditions. If this is indeed the case then it was hypothesized that bound HDAC1 would dissociate or at least have reduced binding to p50 under conditions of NF- $\kappa$ B stimulation. To test this, HeLa cells were left untreated or treated with 10 ng/ml TNF $\alpha$  for six hours followed by co-IP assay for HDAC1 bound to p50. As shown in **Figure 4.3B**, in untreated cells, p50 co-precipitated HDAC1 normally however upon TNF $\alpha$  stimulation this interaction appears to be severely attenuated. Together these experiments support the theory that p50, under resting conditions, recruits HDAC1 to the promotor of NF- $\kappa$ B target genes, however, it is unclear if other components exist in this complex.

As stated previously, HDAC1 is a nuclear protein and is often found in nuclear remodeling complexes such NuRD and Sin3A complex [96,98]. To see if the p50:HDAC1 interaction was mediated by one of these repressor complexes, co-IP assays were performed for Sin3A and p50 under resting conditions. While strong interaction was observed between HDAC1 and Sin3A and between p50 and HDAC1 (**Figure 4.4A**), only a small association between p50 and Sin3A was observed (**Figure 4.4B**). This suggests that the p50:HDAC1 interaction is occurring independently of the Sin3A nuclear remodeling complex and that either another

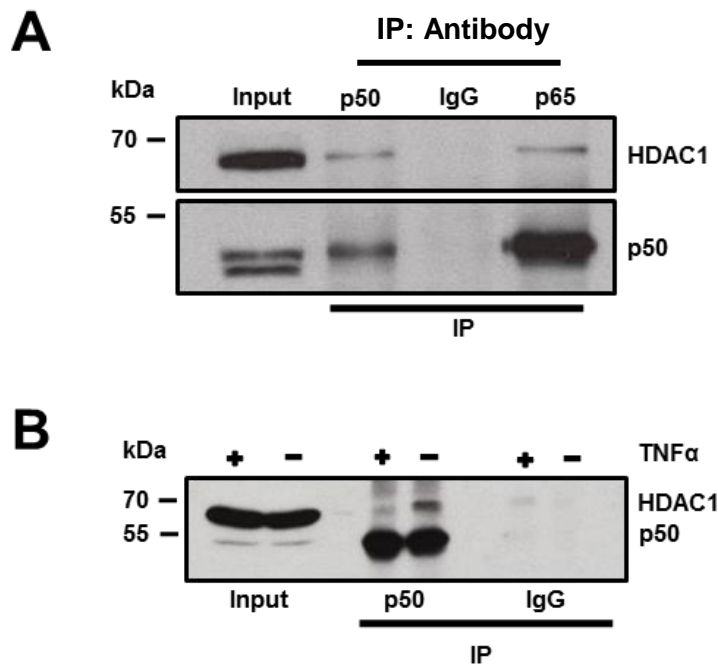


**Figure 4.3 p50 Interacts with HDAC1 under Resting Conditions.**

**A.** Western blot of an endogenous co-immunoprecipitation assay performed with indicated antibodies in whole liver extracts of wild type untreated mice showing that HDAC1 is bound to p50 as well as p65 under resting conditions. **B.** Western blot analysis of an endogenous co-immunoprecipitation (co-IP) assay performed in HeLa cells which were unstimulated or treated with 10ng/ml TNF $\alpha$ . In unstimulated cells more HDAC1 is detected bound to p50 than in cells stimulated with TNF $\alpha$ .

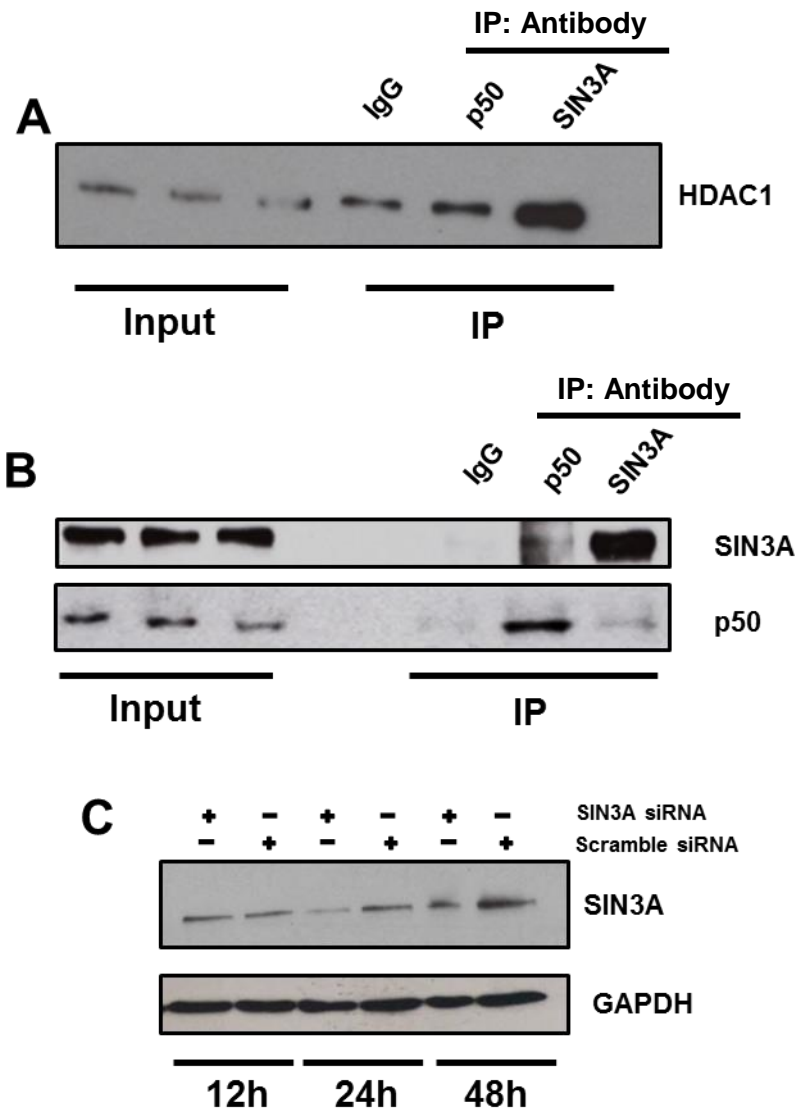


**Figure 4.4 Investigation of Tertiary Members of the p50:HDAC1 Complex**

**A.** Western blot analysis of a co-IP assay using antibodies against p50 or Sin3A verifying the presence of HDAC1 in complex with both p50 or Sin3A in U2OS cells. **B.** Western blot analysis of a co-IP assay to verify the pull down of p50 and Sin3A by their respective antibodies in U2OS cells. It should be noted that p50 signal is observed in the Sin3A IP. **C.** Western blot analysis of a Sin3A siRNA time course used to optimize a Sin3A knockdown in U2OS cells. Cells were incubated with siRNA for 12, 24 or 48 hours with partial knockdown observed at 24 hours compared to a scramble siRNA control.

complex, such as the NuRD complex, is mediating the interaction or p50 is forming direct contacts with HDAC1. Further studies using the partial Sin3A knockdown at 24 hours in **Figure 4.4C** failed to generate meaningful changes in p50:HDAC1 interaction by co-IP. Given this insecurity of whether p50 interacts with HDAC1 directly or through an associated complex, it was decided to identify the structural basis for this interaction at a residue level to provide some evidence for a direct interaction.

### **4.3.2 Predicting the p50:HDAC1 Interaction and Generation of Recombinant Proteins**

Given the available crystal structures of p50 and HDAC1 it was decided to see what information could be gained from *in silico* modelling of the two proteins. As such, the p50 homodimer crystal structure (PDB ID 1NFK) and the HDAC1 crystal structure (PDB ID 4BKX) were supplied to the rigid body docking algorithm GRAMM-X. Using conformations of residues observed in the crystal structure without DNA crystalized with p50 (**Figure 4.5A**), surface residues of HDAC1 were matched for the lowest free energy conformation configuration against p50 residues. This analysis returned a list of possible direct binding orientations assigned and ordered by a score determined primarily by free energy predictions. Of this list the top ten hits were visualized in the three-dimensional structure (**Figure 4.5B**). These top ten hits were further refined based on the symmetry of p50, near similar orientations as well as any obvious DNA clash (**Figure 4.5C**). This further refinement produced two potential sites of direct interaction that suggested HDAC1 would bind either in the cleft formed by the two globular domains of p50 or in the region of known interaction with other NF- $\kappa$ B interacting proteins previously established (I $\kappa$ B $\alpha$ , Importin  $\alpha$  and BCL3). This result suggested that HDAC1 may be binding p50 in a manner like that of other interacting proteins or at a novel site. With these two possible orientations in hand it was decided to test these possible interaction sites *in vitro* and attempt to co-crystalize the proteins to generate a bound crystal structure for the interaction.

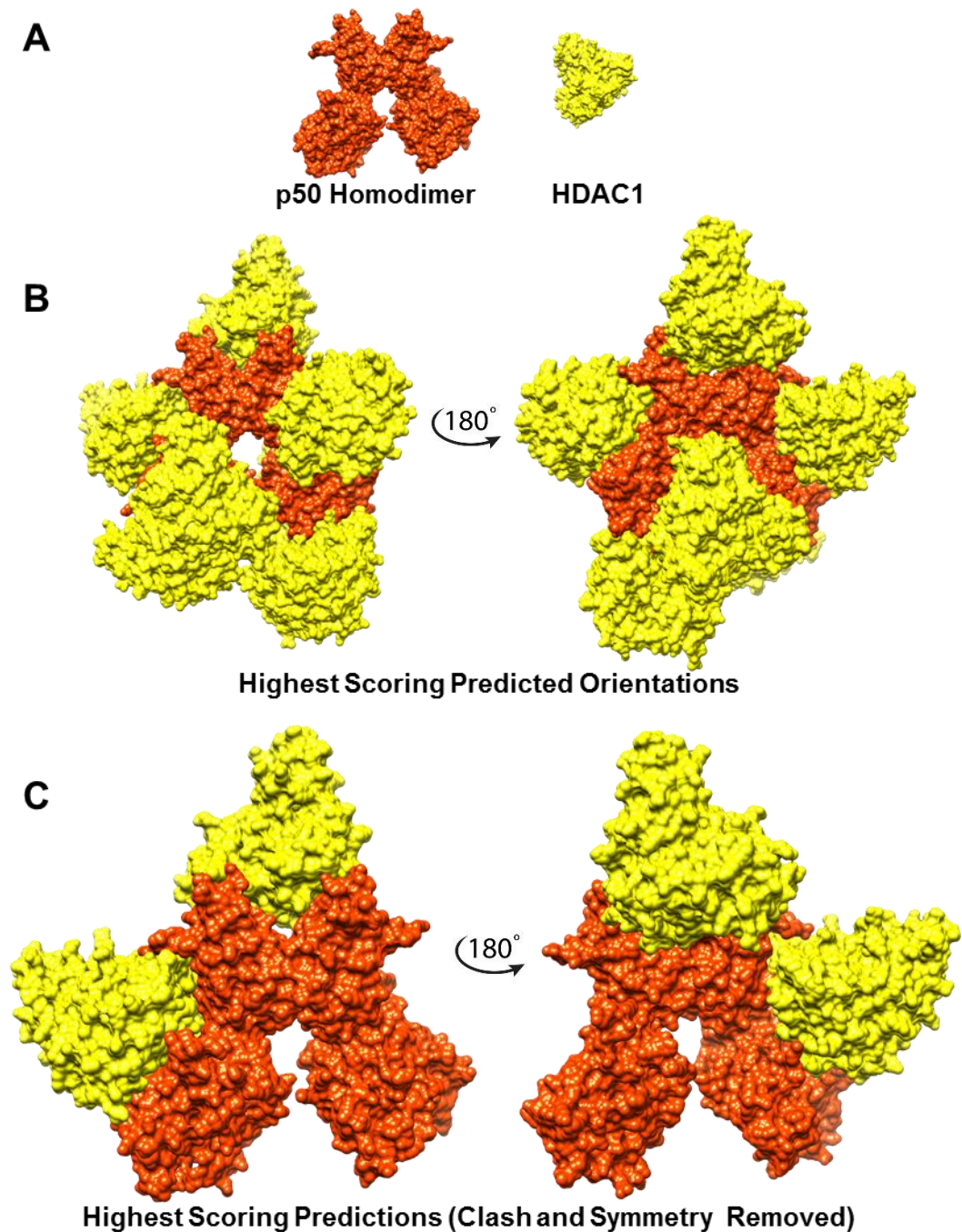


**Figure 4.5 Direct binding prediction of the p50:HDAC1 interaction by the GRAMMX Server for Protein-Protein -Interactions**

**A.** Crystal structure surface of a p50 (orange, PDB ID 1NFK) homodimer with DNA removed used as the receptor and HDAC1 (yellow, PDB ID 4BKX) as the ligand. **B.** Surface structure of p50 along with the highest scoring orientations of HDAC1 returned by the GRAMMX algorithm highlighting numerous possible binding orientations and contacts. **C.** Top two highest scoring HDAC1 binding orientations after replicates (caused by symmetry) and molecules which would clash with DNA were removed.

To achieve protein crystallization the petM30 vector system was used which generates HIS-GST fusion proteins with a linker which can be cleaved by TEV protease. As such TEV protease was recombinantly overexpressed in *E coli*. following usual recombinant protein generation and extraction techniques. Expressed TEV protease was purified by affinity chromatography on a nickel column and collected in fractions as seen in **Figure 4.6**. The three highest fractions of this generated HIS-TEV was then stored at -80°C to be used to remove tags from future generated fusion proteins. Given the previously established data in the crystal structures of p50 and HDAC1 and their associated papers, conditions for the purification of p50 from *E coli*. have been published, however, source material for the HDAC1 crystal structure was derived from protein expressed in human cells [95,106]. Using these published conditions for p50 as a starting point, full length as well as previously crystalized fragment length versions of both p50 and HDAC1 were cloned into petM30 vectors using Gibson assembly (**Figure 4.7A** shows PCR generated fragments before ligation into vector). As p50 is known to be expressed in bacterial systems, full length p50 was the first protein to be tested for expression in Rosetta 2 competent bacteria. Following lysis and nickel affinity purification, high percentile imidazole fractions were found to contain a full length p50-GST-HIS fusion protein at the expected molecular weight of near 77 kDa (**Figure 4.7B**). The top 4 fractions of this elution were pooled and further purified by GST affinity. This purified GST-p50 was then analyzed by serial dilution western blot to insure the purified fusion protein was p50. In **Figure 4.7C** serial dilution of pure p50 yielded a band detected by anti-p50 antibody at the same molecular weight observed by Coomassie blue stain. This verified pure p50 was then incubated with previously generated TEV protease followed by another round of HIS affinity purification with the flow though containing pure p50 which had its GST-HIS cleaved. This pure untagged form of p50 was then further purified by dialysis and stored at -80°C for future applications (**Figure 4.7D**).

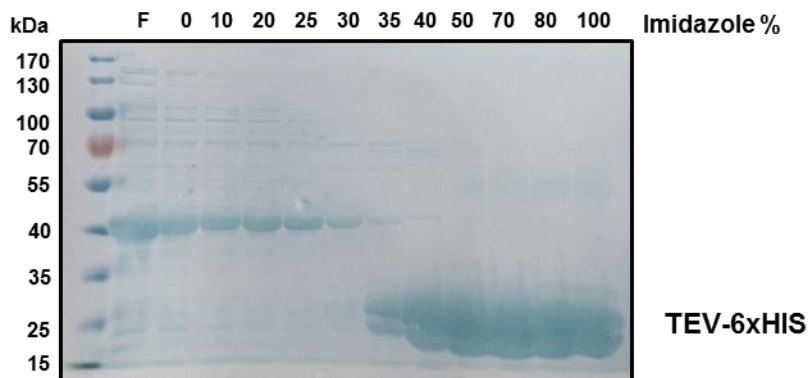


**Figure 4.6 Coomassie Blue Stain of Purified TEV Protease.**

*Coomassie stain of an Imidazole elution gradient used to purify recombinant TEV protease expressed in Rosetta (II) DH5 $\alpha$  E. coli to be used as a cleavage enzyme in the removal of purification tags from recombinant proteins.*

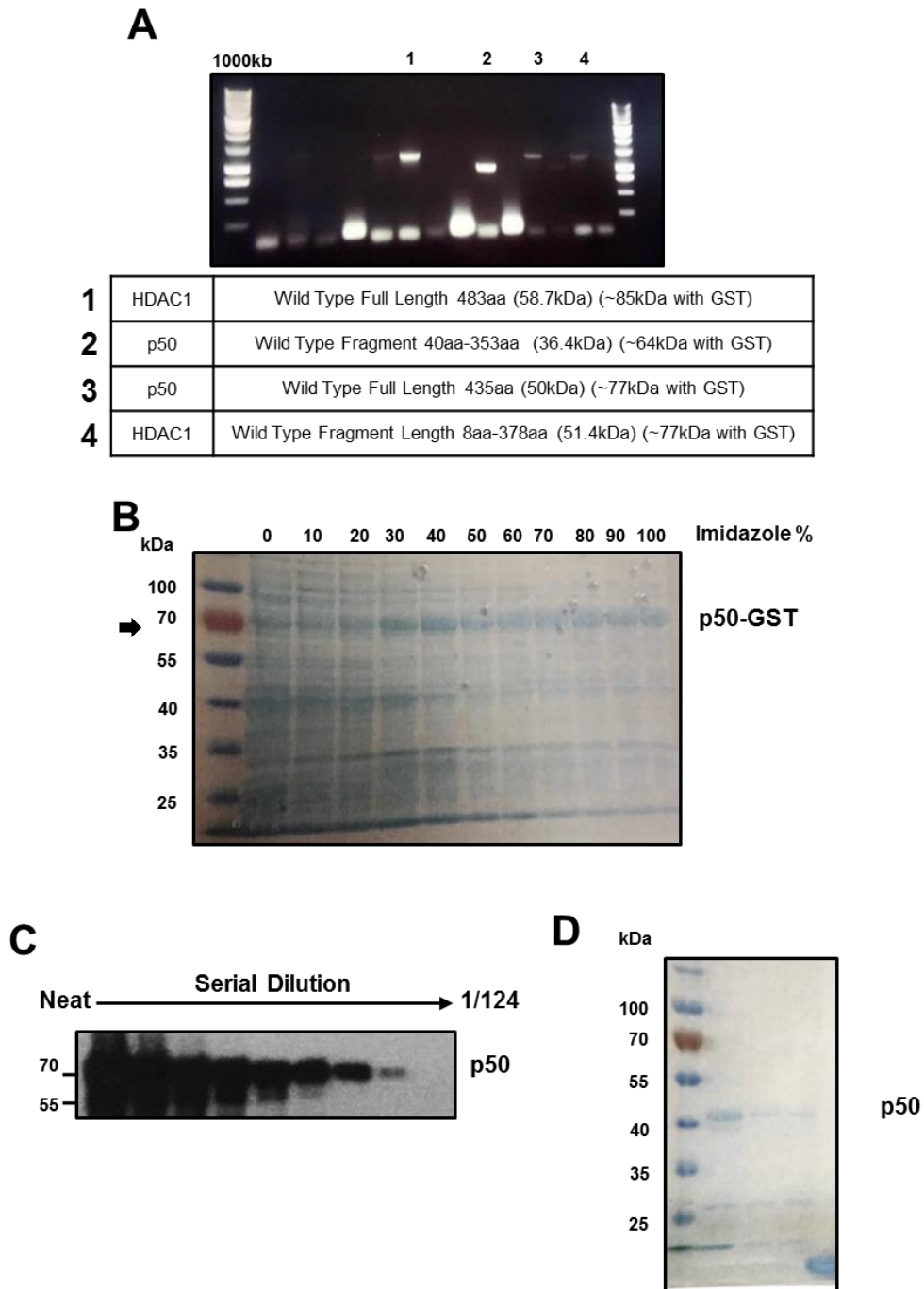


**Figure 4.7 Generation of Expression Constructs of p50, p65 and HDAC1: Purification of recombinant p50**

**A.** DNA electrophoresis PCR products including p50 and HDAC1 in full and indicated fragment lengths containing 5' and 3' regions complimentary to petM30 vector backbone.  
**B.** Coomassie stain showing an Imidazole gradient elution of full length p50-GST-His.  
**C.** Western blot analysis of a serial dilution of pure p50-GST-HIS to confirm its identity.  
**D.** Coomassie stain of pure full length recombinant p50 after GST-His cleavage and dialysis. Two lower molecular weight products are noted and assumed to be degradation products of p50.

Having successfully purified recombinant p50, this same protocol was applied to HDAC1. Unfortunately, no appreciable amount of protein was observed. Therefore an expression assay was performed. Full and fragment length HDAC1 along with fragment length wild type p65 were transformed into various expression strains of *E coli*. in three different types of culture media. After induction the whole cell lysate, soluble lysate fraction, GST purification flow through and GST purification eluate were analyzed by Coomassie Blue stain to determine if any protein was produced under any condition, and to determine its solubility. Seen in **Figure 4.8A**, full length HDAC1 was not observed under any condition of expression tested, however some expression of fragment length HDAC1 was observed in some cases (**Figure 4.8B**). Specifically, Arctic and Rossetta II cells in auto induction media seem to provide low levels of pure fragment HDAC1, however, the majority of this protein was observed in the whole lysate fraction. This suggested that HDAC1 could be produced in these cells but is highly insoluble. Subsequent attempts to increase solubility and yield of the protein were, however, unsuccessful. These same experiments were performed on the previously purified crystallographic length version of p65 as well and is shown in **Figure 4.9**. Pure p65 was observed under a number of conditions, however, Arctic cells in auto induction media provided a high yield, soluble, low contamination pool of p65 with little to no observable degradation products. Originally performed as a control experiment, this also provided optimized conditions for the expression of pure p65. Given the inability to produce high quantities of stable HDAC1, however, another method of determining the interacting residues between p50 and HDAC1 was required.

### **4.3.3 Peptide Arrays Identify the Nuclear Localization Signal of p50 as the Primary Motif of Interaction with HDAC1**

With trials to produce recombinant HDAC1 unsuccessful, peptide array technology was used to identify residues critical for the p50:HDAC1 interaction. Peptide arrays consisting of 18 amino acid fragments of p50 shifted by three amino

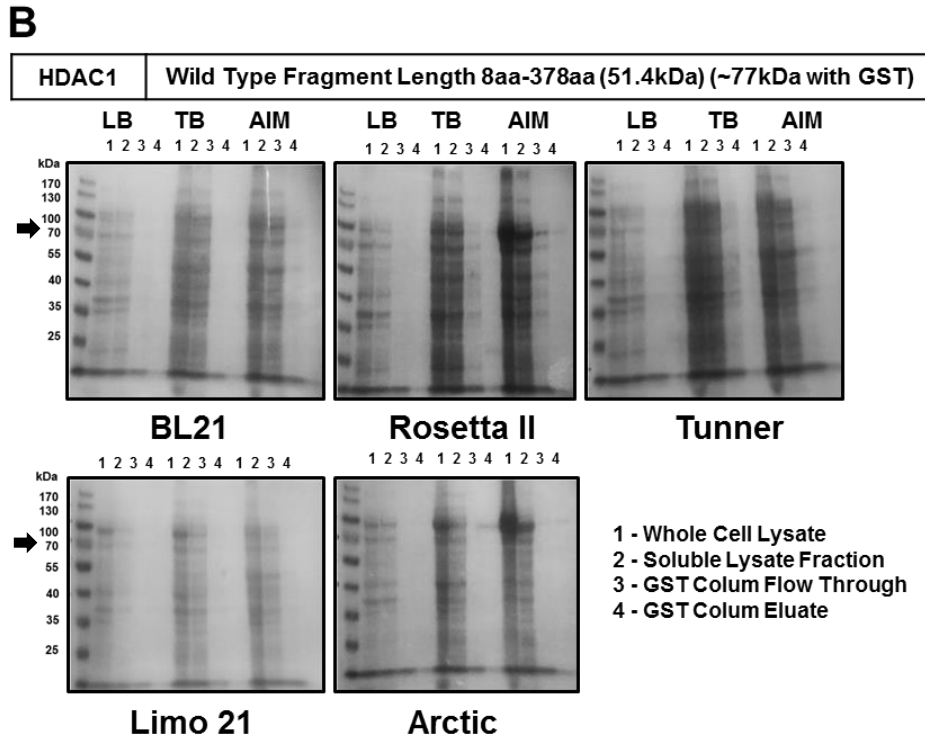
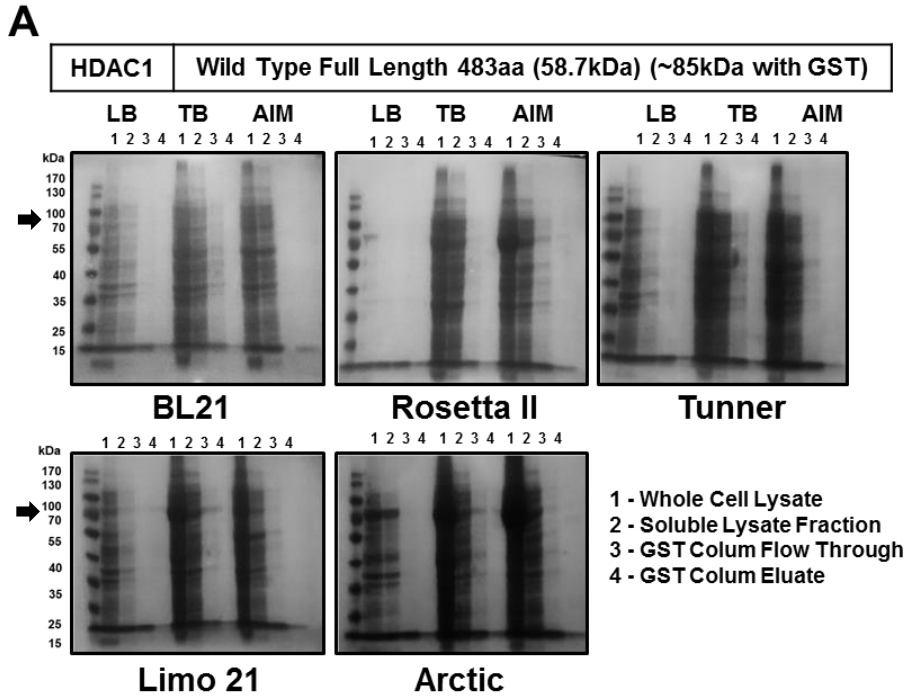


**Figure 4.8 Recombinant Protein Expression Assay for Full and Fragment Length HDAC1**

**A-B.** Coomassie Blue stain of a recombinant expression assay performed in LB, TB or Auto Induction Media (AIM) to determine the viability of selected HDAC1 construct expression in five strains of *E. Coli*. Samples were fractionated by 8% SDS-PAGE. Arrows indicate expected molecular weights of target proteins. More detail in Figure 4.9.

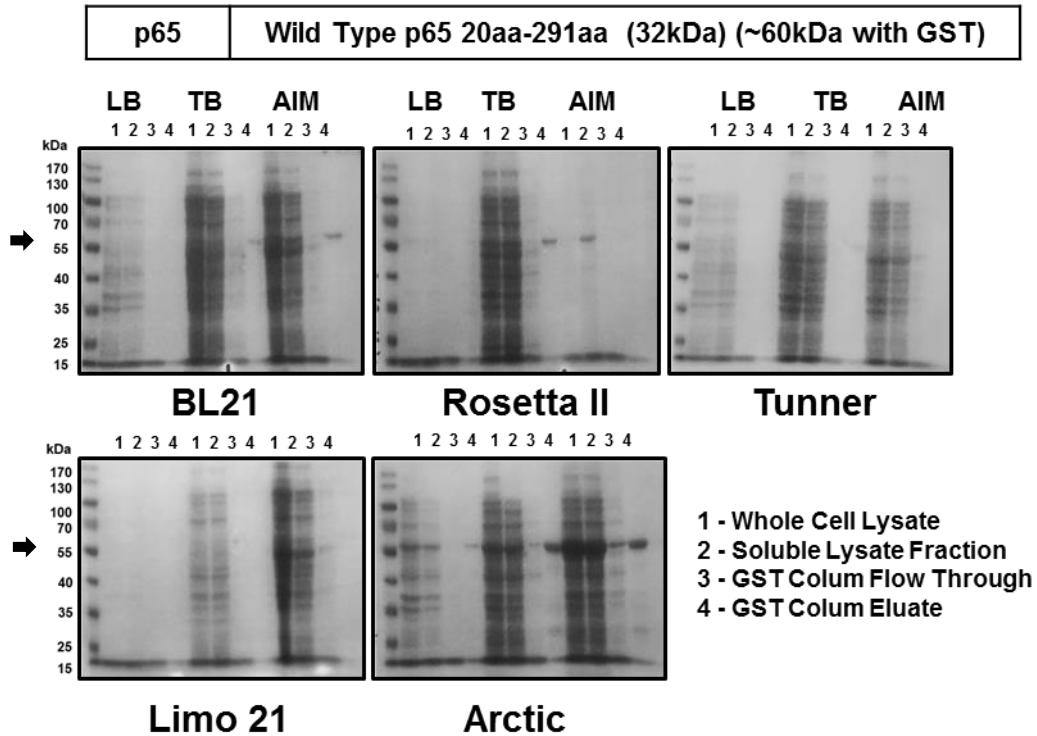


**Figure 4.9 Recombinant Protein Expression Assay of p65**

*Coomassie Blue stain of a recombinant expression assay performed in LB, TB or Auto Induction Media (AIM) to determine the viability of a previously crystallized fragment of p65 expression in five strains of E. Coli. Samples of whole cell lysate, clarified soluble lysate (by centrifugation), GST column flow through filtrate and GST column eluate were fractionated by 8% SDS-PAGE to determine if produced recombinant protein was being lost during purification. Highest yield of recombinant p65 was obtained in Arctic express cells in AIM media after GST purification.*

acids covering the full length of human p50 and HDAC1 were kindly provided by the Kiely Lab (University of Limerick). Firstly, HDAC1 peptide arrays were probed with previously generated recombinant p50 and probed with anti-p50 antibody to determine if p50 formed stable interactions with any fragments of HDAC1. Upon development several specific peptides of HDAC1 were detected to facilitate this p50 interaction (**Figure 4.10A and B**). Positive peptides identified were then mapped to the crystal structure of HDAC1 to determine these locations in three dimensional space. It was determined that only one site of positivity was contained within the crystal structure of HDAC1, however, this site was on an external  $\beta$ -sheet and  $\alpha$ -helix of the globular catalytic core of HDAC1 suggesting it could be suitable as an interacting motif (**Figure 4.10C**). To examine this in more detail, this region was analyzed in relation to the earlier predicted possible binding orientations and it was found that the  $\alpha$ -Helix portion of the identified site would make direct contact with the c-terminal portion of the p50 rel homology domain at a site similar to p50 interactions with I $\kappa$ B's. This observation is visualized in **Figure 4.11A and B** which shows the possible binding orientation of p50 and HDAC1 as well as the sequence in HDAC1 positive for interaction on the peptide array.

In an attempt to confirm this observation, this entire experiment was repeated reciprocally. Recombinant human HDAC1 generated in insect cells and provided commercially was incubated with p50 peptide arrays (**Figure 4.12 A and B**) to determine if HDAC1 would have a specific affinity p50 peptides. **Figure 4.12C** highlights multiple possible points of interaction of HDAC1 along the p50 sequence. These peptides were then examined in the context of the full p50 crystal structure and it was observed that they all exist within the p50 crystal structure with the exception of the far C-terminal end of the more C-terminal positive peptide. Mapped onto the p50 crystal structure these four regions were highlighted and it was observed that while 3 new distinct regions were identified, one of the observed binding peptides lay at the previously identified region of possible interaction as predicted by *in silico* analysis as well as

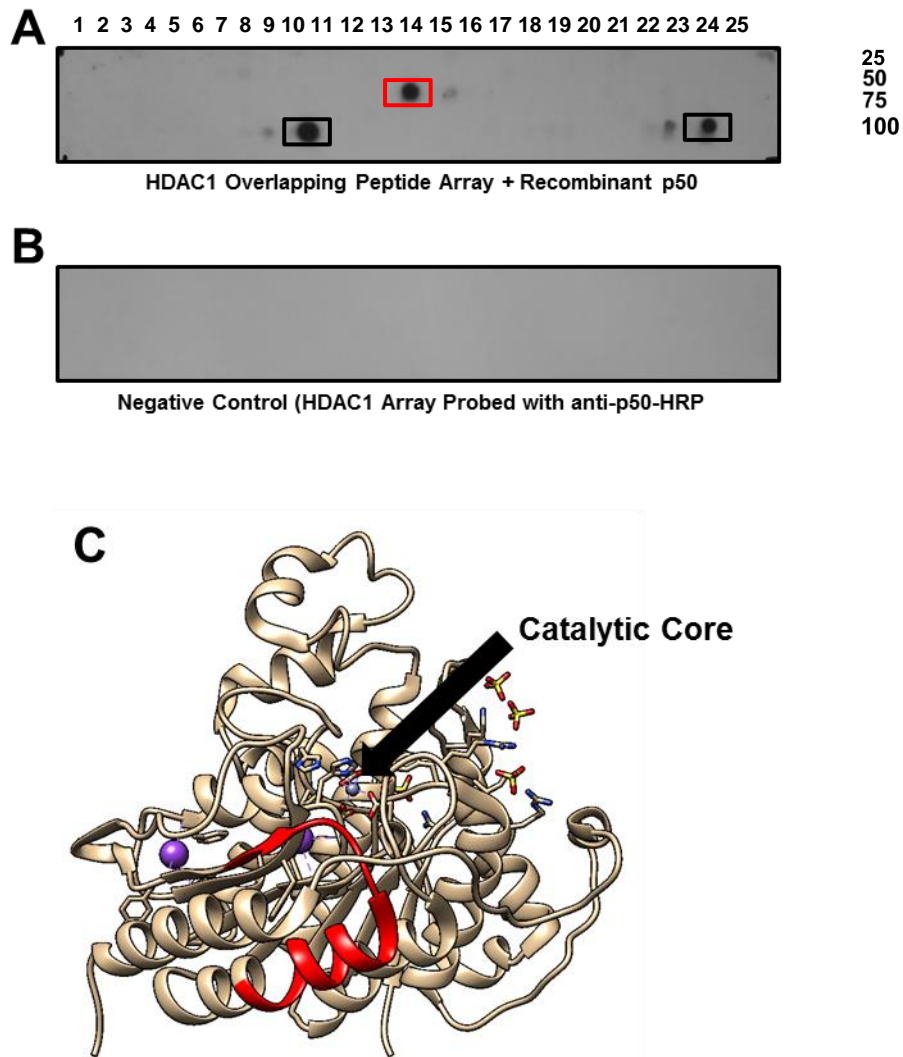


**Figure 4.10 Mapping the p50 Interaction on HDAC1**

**A.** HDAC1 peptide array in which 18 amino acid fragments of wild type HDAC1 hybridized to nitrocellulose probed with generated recombinant wild type p50 followed by anti p50-HRP antibody. **B.** HDAC1 peptide array probed with anti p50-HRP antibody alone. **C.** Crystal structure of HDAC1 highlighting residues positive for p50 interaction (red) in relation to the catalytic core.

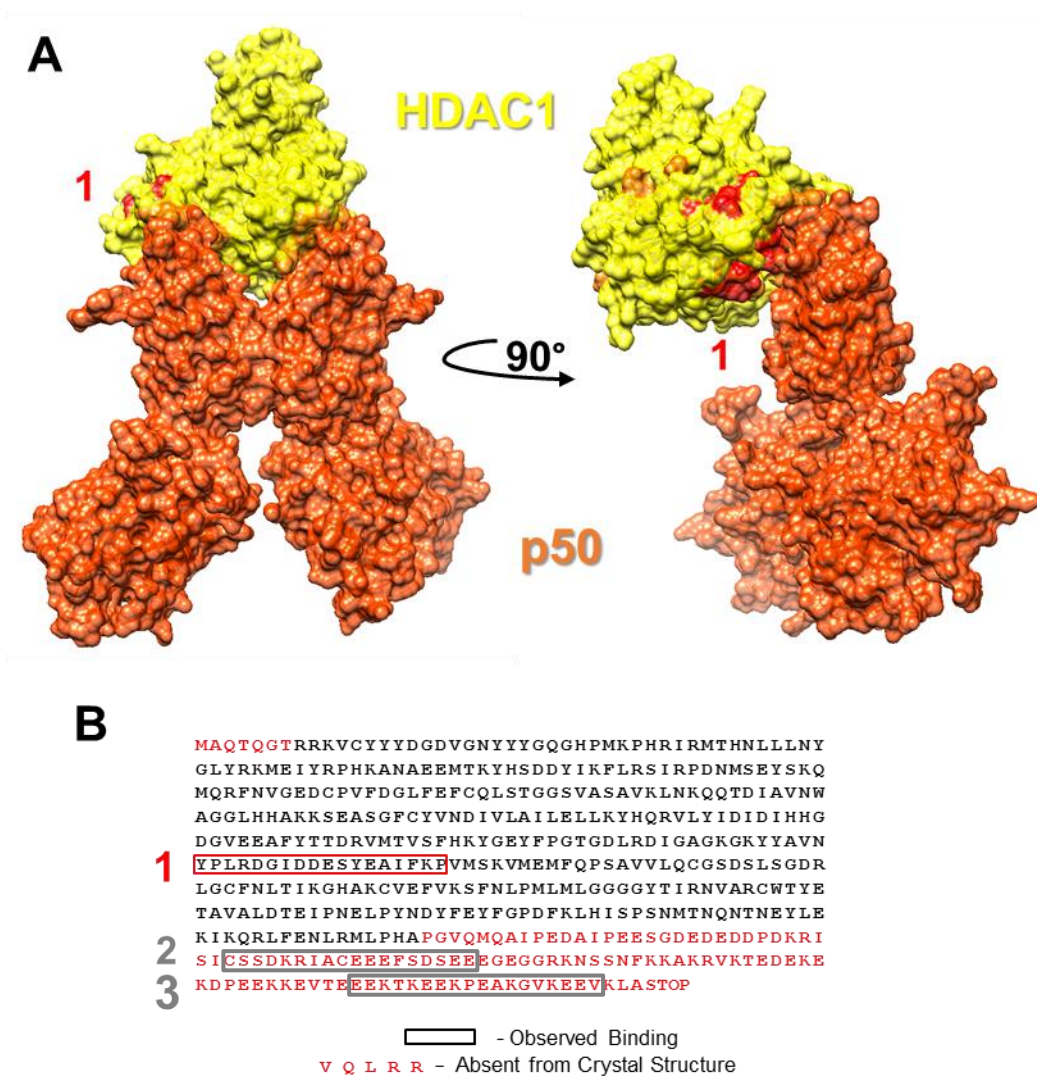


**Figure 4.11 Comparison of Predicted p50-HDAC1 Binding and Peptide Array Data**

**A.** Crystal structure of HDAC1 (yellow) and p50 (orange) in one of the GRAMMX predicted orientations proposed for binding with residues positive in the HDAC1 peptide array highlighted (red). **B.** The location of the peptide array predicted binding motif within the context of the full HDAC1 protein sequence.

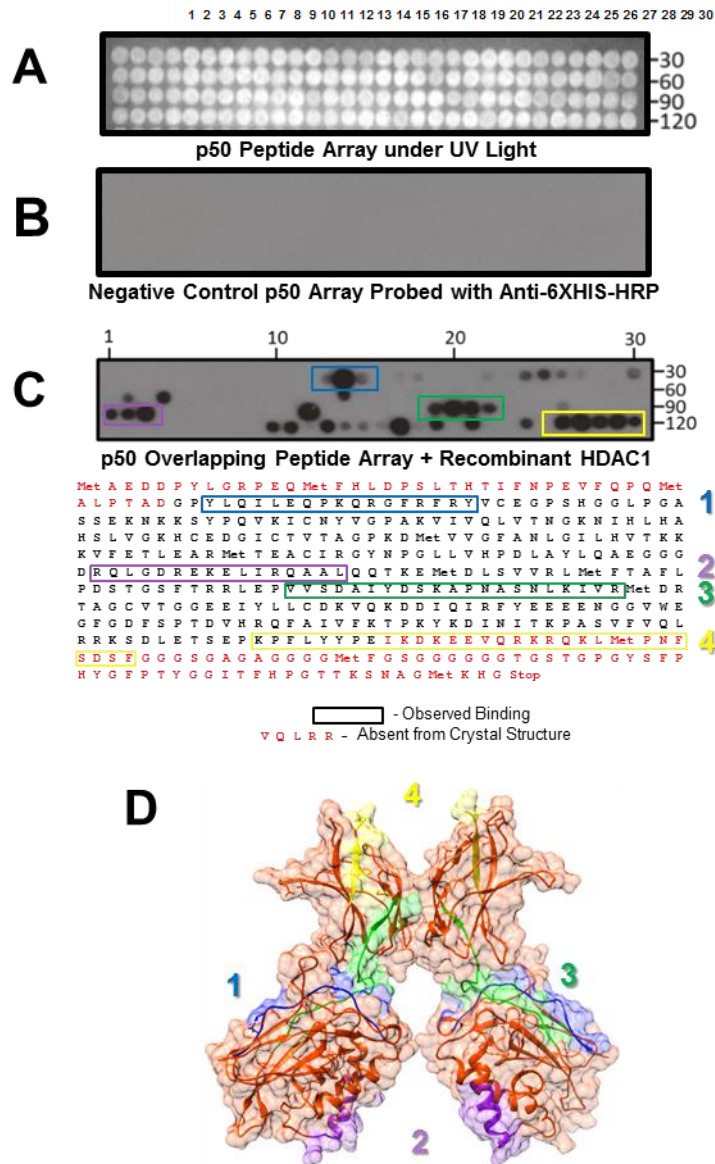


**Figure 4.12 Mapping the HDAC1 interaction on p50**

**A.** p50 peptide array under UV light showing the location of all 120 peptides spanning the length of p50. **B** p50 peptide array probed with anti-HIS-HRP antibody to confirm the absence of non-specific binding. **C.** Peptide array of 120 sequential peptides of 18 amino acids spanning the length of p50 probed with recombinant HDAC1-Hisx3 highlighting multiple sights of potential interaction. **D.** All regions of potential interaction discovered in the peptide array mapped to the crystal structure of the p50 homodimer.

the previous peptide array (**Figure 4.12D**). Together this evidence strongly suggests that p50 interacts with HDAC1 at some portion of the c-terminal region. Therefore, interaction with p50 in the region including the last 7 peptides in the p50 array were further investigated. Sequential alanine substitution was performed on peptides in which each residue had been mutated to an alanine residue to determine the specific contribution of each residue to the interaction as well as identify the exact residues critical in the interaction. Upon re-probing with recombinant HDAC1, several changes in binding to p50 peptides were observed. Namely, variation in the binding of HDAC1 to p50 peptides occurred universally but the most dramatic changes were observed in peptide 120 where changes to the VQRKRQK motif resulted in ablation of the interaction (**Figure 4.13A and B**). This motif, it was observed, was not a part of the crystal structure of p50 however, the residues which showed the greatest change in interaction occurred in the region of p50 previously identified as the nuclear localization signal or NLS (**Figure 4.13C**). Furthermore, it was noted that while two of these residues are conserved in p65, all other nearby residues are unique to p50 (**Figure 4.13D**). Together this strongly suggests that p50 is bound by HDAC1 at its NLS in a manner similar to that of I $\kappa$ B $\alpha$  and may be masking its NLS for the duration of its interaction [124].

#### **4.3.4 Mutation of the p50 NLS Ablates its Interaction with HDAC1**

To confirm this site as the key site of interaction between p50 and HDAC1 a number of mutations were carried out on NLS of p50. pcDNA3.1 mutant p50-Flag constructs were generated by site directed mutagenesis (**Figure 4.14A**). One of these mutants carried the full disruption of the NLS found in the peptide array. These mutant-expressing mammalian constructs were then transfected into Cos7 cells along with their wild type HDAC1-HA fusion expressing pcDNA3.1 constructs and flag immuno-precipitated to determine their ability to bind HDAC1. **Figure 4.14B** shows that HDAC1 is co-precipitated with wild type p50 as well as all mutant constructs with the exception of the total NLS ablation mutant. Interestingly partial

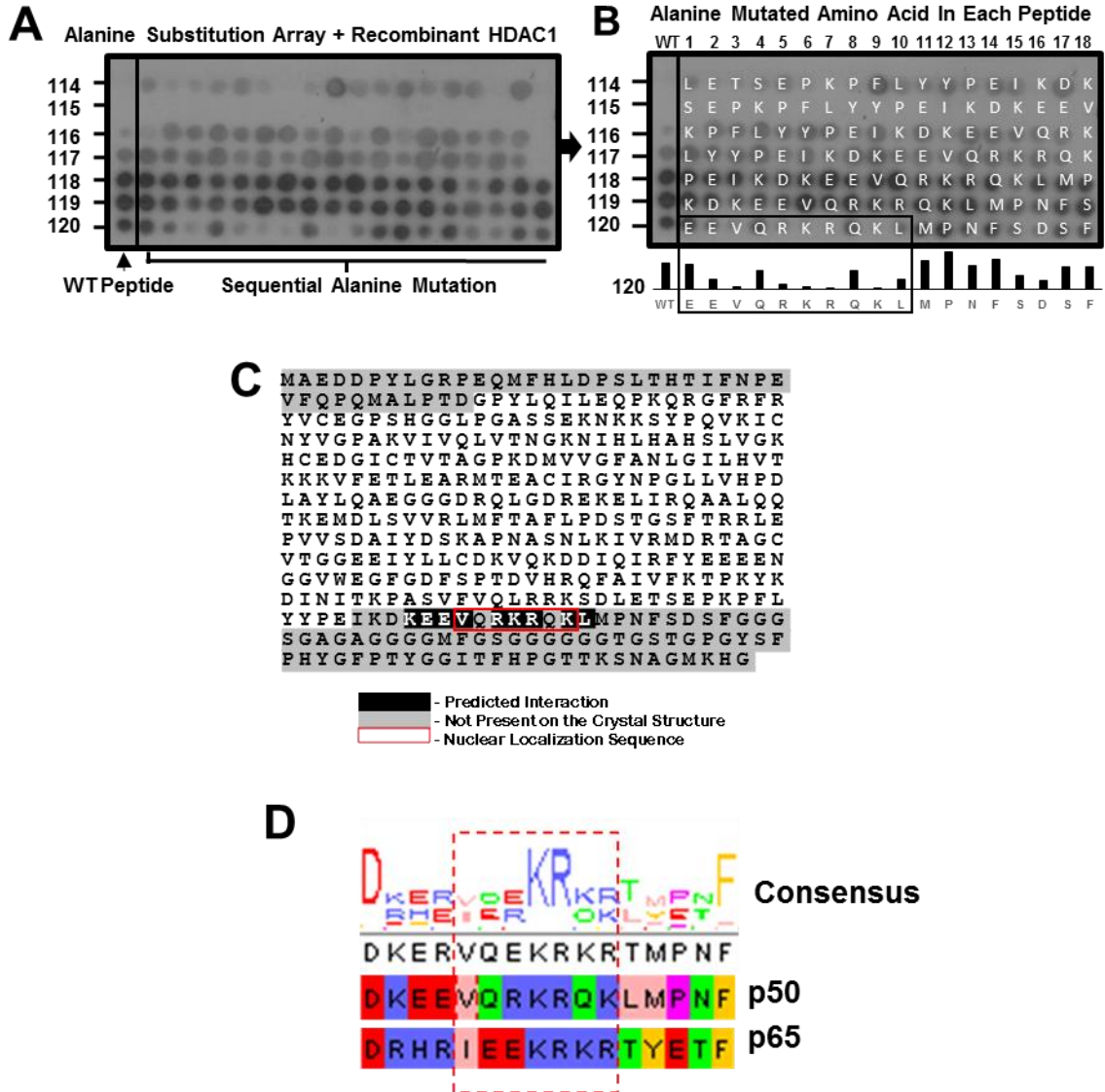


**Figure 4.13 Refinement of Residues Responsible for the p50:HDAC1 Interaction**

**A.** Alanine substitution peptide array of the terminal seven 18aa peptides probed with recombinant HDAC1 displaying differential binding based on specific amino acid changes. **B.** Representation of specific amino acids mutated to alanine and responsible for the apparent loss of interaction. Graph below indicates relative signal of each peptide as measured by densitometry **C.** Residues which attenuate the interaction between HDAC1 and p50 peptides in context of the full-length protein beginning with V360 to L366. **D.** Consensus sequence alignment of p50 and p65 showing distinct residue differences in the region proposed to mediate the p50:HDAC1 interaction.

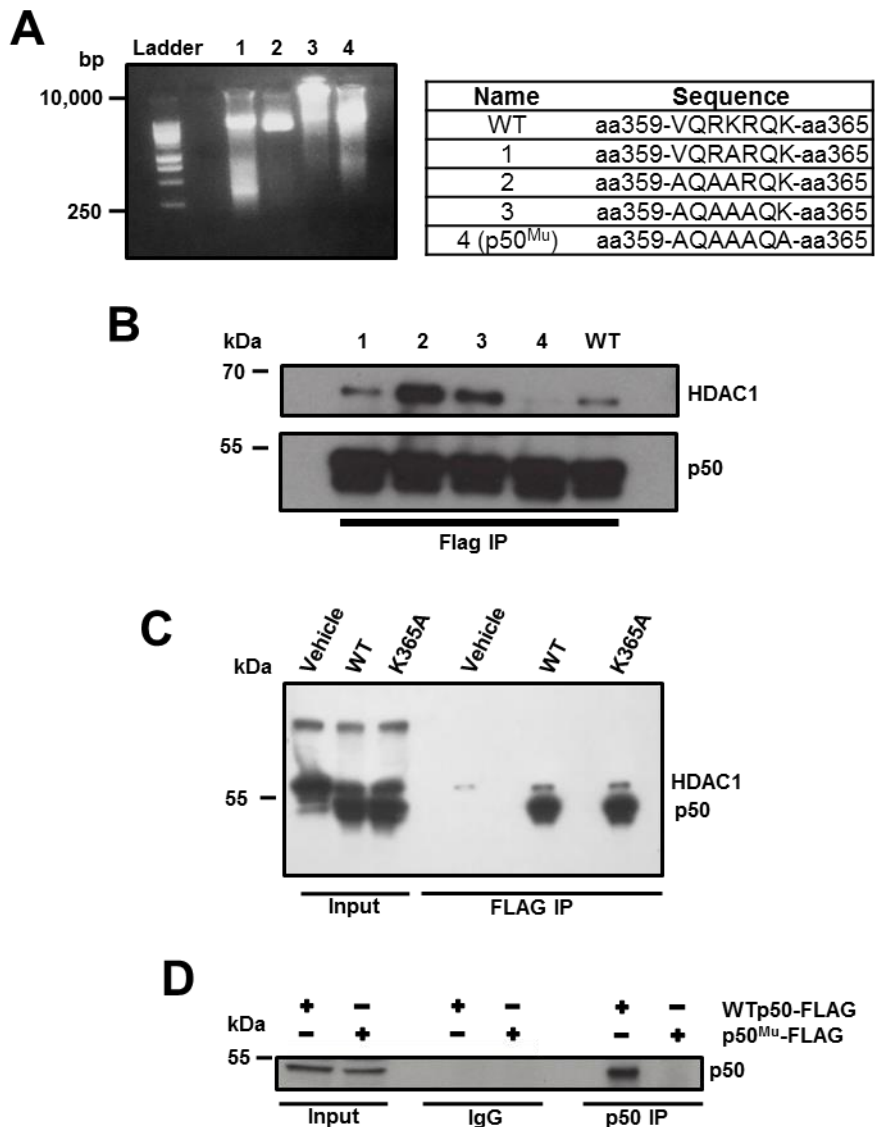


**Figure 4.14 Mutation of Key Residues in the NLS of p50 Ablates the p50:HDAC1 Interaction.**

**A.** DNA gel electrophoresis of four p50 constructs in which increasing mutations were made in the nuclear localization sequence (NLS) of p50 in accordance with peptide array data (left). Table of sequence changes made by site directed mutagenesis to the original wild type p50-FLAG construct (right). **B.** Western blot analysis of a FLAG immunoprecipitation assay of indicated mutant p50 expressed in Cos7 cells transiently transfected along with HDAC1-HA. Complete mutation of the indicated residues (Sequence 4 – p50<sup>Mu</sup>) result in a near total ablation of the p50:HDAC1 interaction in full length transiently transfected proteins. **C.** Western blot analysis of a FLAG Co-IP assay showing no difference of HDAC1 binding between WT or p50<sup>K365A</sup> in Cos-7 cells. **D.** Western blot analysis of an endogenous IP assay with an antibody specific to the nuclear

*localization sequence of p50 showing a loss of p50 pull down in p50<sup>Mu</sup> confirming the presence of a mutation in this region.*

mutants seemed to enhance p50's affinity for HDAC1 however when the terminal lysine residue of the VQRKRQK motif is mutated to alanine the interaction is lost suggesting a crucial role for this lysine in the interaction. Nevertheless, when this amino acid is mutated on its own, and expressed in HeLa cells, there is no observable difference in binding of HDAC1 compared to wild type p50 (**Figure 4.14C**). In addition to this observation it was also confirmed at the protein level that the fully disruptive mutant, here referred to as p50<sup>Mu</sup> did indeed contain a mutated motif by immunoprecipitation. HeLa cells transfected with wild type or p50<sup>Mu</sup> were immuno-precipitated using an NLS specific anti-p50 antibody. In the western blot analysis of this experiment it can be shown that wild type but not p50<sup>Mu</sup> can be precipitated using the NLS specific antibody confirming protein residue changes in this region (**Figure 4.14D**).

As the only evidence for this loss of interaction thus far was in a system where HDAC1 was overexpressed, FLAG constructs of wild type and p50<sup>Mu</sup> were transfected into HeLa cells to determine if mutant p50 would interact with endogenous HDAC1. Positive interaction with wild type but not p50<sup>Mu</sup> with HDAC1 confirmed that this mutant attenuates p50's ability to interact with endogenous HDAC1 in cells (**Figure 4.15A**). Moreover, this experiment was also performed in *nfkb1<sup>-/-</sup>* murine embryonic fibroblasts (MEF) to ensure the interaction was not occurring in wild type controls via interaction with endogenous p50. Therefore MEFs were similarly transfected and similar results obtained where wild type but not p50<sup>Mu</sup> is capable of co-precipitating endogenous HDAC1. Having generated a mutant capable of ablating the HDAC1 interaction, it was prudent to determine the effect this was having on the entire interactome of p50. As such, U2OS cells were transfected with wild type and p50<sup>Mu</sup> and flag IP's performed to co-precipitate p50 and all of its possible binding partners. Samples were then verified by silver stain

after separation by SDS-PAGE (**Figure 4.15B**) and then analyzed by mass spectrometry by the core Mass Spectrometry Facility at Newcastle University. Unfortunately, protein digestion and subsequent analysis did not yield viable data for either the wild type or p50<sup>Mu</sup> sample. Sample was provided on three separate occasions however peptides with weights corresponding to p50 residues were not identified in each case even though the presence of precipitated protein could be detected by western blot. Given the data presented previously, however, this region of p50 identified by peptide array and verified by multiple co-immunoprecipitation experiments suggest it is the site of interaction between p50 and HDAC1.

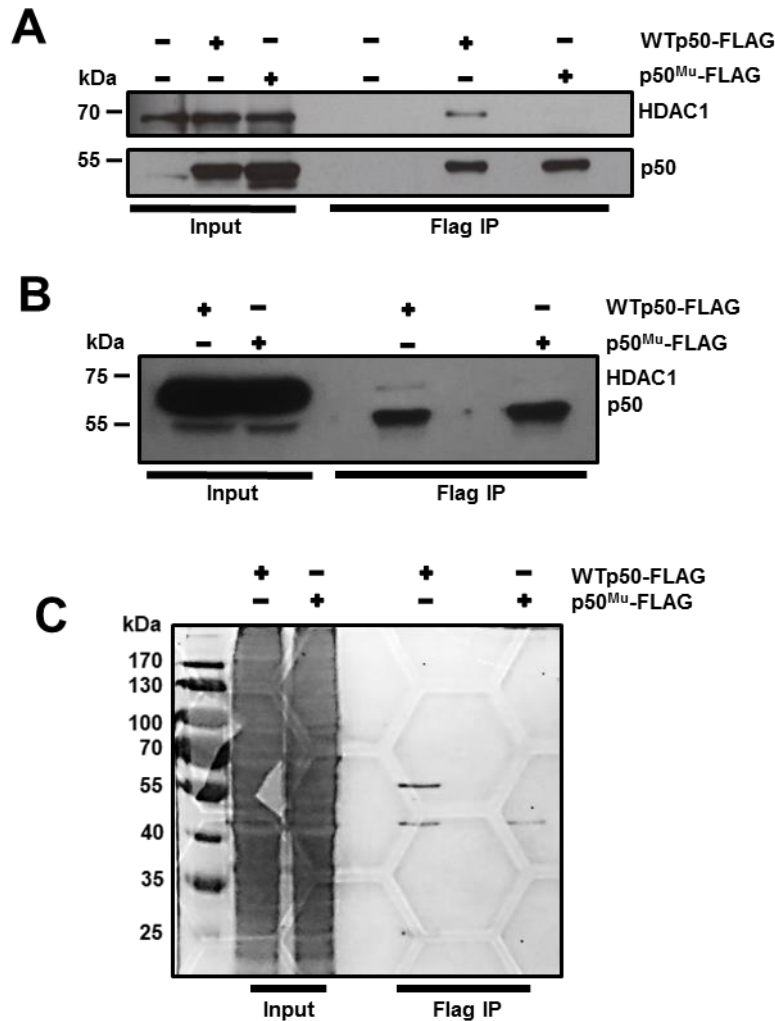


**Figure 4.15 p50<sup>Mu</sup> disrupts endogenous p50:HDAC1 Interaction in Multiple Cell Types.**

**A.** Western blot analysis of a FLAG co-immunoprecipitation assay of HeLa cells transiently transfected with WT or p50<sup>Mu</sup> confirming loss of interaction with endogenous HDAC1 under resting conditions. **B.** Western blot analysis of a FLAG Co-IP assay of *nfk1<sup>-/-</sup>* MEFs showing a loss of interaction with endogenous HDAC1 in p50<sup>Mu</sup> compared to WT. **C.** Silver stain of WT or p50<sup>Mu</sup> FLAG IP showing a loss of co-precipitated targets near 60kDa in p50<sup>Mu</sup> compared to WT.

## 4.4 Discussion

p50/p105 performs numerous complex roles in cells in both its precursor, p105, and p50 forms. In both forms it participates in numerous protein-protein interactions in both the cytoplasm and nucleus of resting and stimulated cells. While as an I $\kappa$ B p105 is known to interact with other NF- $\kappa$ B subunits and in other pathways such as Tpl2 [125], p50's interactions, some of which are known, are rarely investigated with structural detail. Recently, one such interaction has been investigated at this level of detail and provides insights into the mechanisms of how p50 carries out its complex role in cells. Bcl3 has been shown previously to bind p50, however Collins *et. al.* showed that this interaction was at a region in the p50 nuclear localization sequence and share residues that have been previously shown at the site of interaction between p50 and I $\kappa$ B's as well as Importins [73]. Given this information and the uncertainty of whether or not the p50:HDAC1 interaction was direct or mediated by a third party, this investigation into the potential p50:HDAC1 interface was approached in a blinded fashion.

### 4.4.1 Nuclear p50 interacts with HDAC1 in resting cells in a Sin3A independent manner

Having confirmed the p50:HDAC1 *in vivo* and *in vitro* in resting cells particularly, a meaningful question remains regarding other members of this complex. Canonically, HDAC1 is considered an essential component of cellular machinery responsible for general shifts in chromatin organization in all cell types [93]. In this role however, it is most often associated as the catalytic core of complexes such as the NuRD and Sin3A complex and not as a free agent in the nucleus. Data presented in this chapter in the form of *in silico* predictions and peptide arrays do suggest that free HDAC1 could bind p50 with reasonable affinity and in a fashion allosteric to its active site. Moreover, co-IP assays suggest that one of the more well-known HDAC1 complex partners, Sin3A, cannot readily be observed interacting with p50 (**Figure 4.4**). Given that according to peptide array and prediction data, the p50:HDAC1 interaction occurs on an external alpha helix

of HDAC1 on the opposite side of the molecule to the catalytic core of the molecule, p50 could be interacting directly with a free form of HDAC1 and from the basis of a yet understood nuclear remodeling complex. Another important consideration given that the interface on p50 which is implicated as the HDAC1 binding motif is also its nuclear localization signal is that this loss of interaction is not simply due to the proteins existing in different cellular compartments. This specific point is address in chapter five but is an important possible interpretation of observed results.

#### **4.4.2 Loss of p50's NLS Leads to a loss of HDAC1 Interaction**

The VQKRKQK motif which forms a part of the p50 NLS identified as critical to the HDAC1 interaction contains interesting properties. During the course of performing sequential mutation it was observed that loss of some of these residues provided an increase in the p50:HDAC1 interaction by IP while total loss was only achieved after mutation of all K and R residues. Indeed, single mutation of the terminal lysine residue on its own did not seem to have an impact on the interaction when compared to wild type. Given the high concentration of residues which may be acetylated however, one could argue that p50 is a target of HDAC1 and not a complex partner. While these sites have never been reported as acetylated residues, one could argue that acetylation at a protein inhibitor site may be serving a different function. A potential weakness of this study would then be that this possibility was not ruled out experimentally, however this interaction not governed a single amino acid. Additionally, it is unclear if even several continuous deacetylation events at this location would prove enough to retain an HDAC1 signal by co-IP in all of the conditions in which it has been observed. Therefore, using data presented in this chapter one can argue that p50 is recruiting HDAC1 via its nuclear localization signal by direct interaction and independent of other canonical HDAC1 complexes. Moreover, this recruitment, as determined by residue contacts and molecule orientation, is serving to poise HDAC1 as an effector molecule on surrounding proteins such as nearby histones to ensure gene regions bound by

p50 homodimers remain switched off. The molecular orientation indicated by both predictive software and *in vitro* experiments suggest that contacts made between p50 and HDAC1 leave the catalytic core of HDAC1 accessible to nearby proteins. It is conceivable then, that any proteins in the vicinity that can be deacetylated allowing p50 homodimers to locally target genes for three dimensional rearrangement based on their occupancy on DNA sequences.

## Chapter 5 Function of p50<sup>Mu</sup> Mutant in the Context of a Loss of HDAC1 Interaction

---

### 5.1 Introduction

The dogma related to NF- $\kappa$ B activation and signaling pathways converge on the principle that dimers are sequestered in the cytoplasm of resting cells by the I $\kappa$ B's. While others argue a more dynamic system rather than this binary inhibited or active state, it is clear that nuclear localization is the key step for the induction of gene transcription by any transcription factor. As such, the nuclear localization signal of transcription factors plays a major role in gene activation. Data in chapter 4 strongly suggested that p50's nuclear localization sequence serves as the region of interaction between it and HDAC1. Also, it is known from the wider literature that this region is also important for the binding of BCL3, Importin  $\alpha$ , I $\kappa$ B $\alpha$  as well as the ankyrin repeats of p105 during self-inhibition [112]. These studies all suggest that this region of p50 may be acting as a dynamic scaffold for both the cytoplasmic and nuclear control of p50 function. However, more important to understanding the p50:HDAC1 interaction is to determine HDAC1's specific contribution to p50's inhibitory action.

Previous published work has shown that p50 is a potent deactivator of immune cell regulatory and inflammatory genes [38]. In particular, it has been shown that, in addition to canonical pro-inflammatory genes such as IL6, p50 represses genes related closely to the activation of and recruitment of immune cells including genes of the CXCL(cxc motif ligand) and MMP (Matrix metalloprotease) families among others [58]. However, the extent to which this repression relies on the interaction with HDAC1 is not well understood. While Elsarkawy *et al.* showed that MMP13 repression by p50 seemed to be HDAC1 dependent, little has been done to interrogate whether the interaction with HDAC1 provides most if not all of the repressive potential of p50 homodimers [104]. Having generated a tool *in vitro* that seems to interrupt this p50 HDAC1 interaction (p50<sup>Mu</sup>) but lacks the expression challenges of other mutants such as the p50<sup>S343A</sup> previously described, a number

of elusive question regarding the role of HDAC1 in p50 directed NF- $\kappa$ B gene repression can be interrogated.

## **5.2 Aims**

Having identified the major region of interaction between p50 and HDAC1 and generated a construct of p50 that disrupts this interaction, the aims of this chapter are as follows:

- To determine the effect of the p50<sup>Mu</sup> mutation on canonical function of p50 including nuclear localization and binding of I $\kappa$ B $\alpha$  and p65.
- To determine the contribution of HDAC1 to p50 dependent NF- $\kappa$ B gene repression.

## 5.3 Results

### 5.3.1 Mutation of p50 which causes a loss of HDAC1 Interaction Has no Effect on Canonical p50 Interactions

As shown previously, p50<sup>Mu</sup> is unable to bind HDAC1 in a co-IP assay (**Figure 4.15**). Given this result it was important to determine if this loss of HDAC1 provided any functional changes in cells or within the NF- $\kappa$ B signaling pathway. To determine this, multiple cell lines were tested for NF- $\kappa$ B and HDAC1 protein expression. Profiled cell types are shown in **Figure 5.1**. Subsequent to this analysis U2OS cells (cells which displayed proportionate abundant expression of all components) and *nfkb1*<sup>-/-</sup> MEF's (used to determine the mutant's effects specifically) were selected for further experiments. Arguably, one of the most well defined roles of p50 is that of a p50:p65 heterodimer so it was important to determine if this interaction remained intact. Shown in **Figure 5.2A and B**, U2OS and COS7 cells respectively when transfected with either WT or p50<sup>Mu</sup> showed similar levels of p65 interaction as determined by flag co-IP assay. While this confirmed canonical dimer assembly, it is also important to remember that the major factor determining NF- $\kappa$ B activity is the ability of the subunits to be inhibited in the cytoplasm by the I $\kappa$ B's. As such, canonical inhibitor of p65:p50 action, I $\kappa$ B $\alpha$ , was used in a co-IP assay to determine if reconstituted *nfkb1*<sup>-/-</sup> MEFs formed traditional p65:p50:I $\kappa$ B $\alpha$  complexes. Seen in **Figure 5.2C**, when immunoprecipitation is performed using an antibody against I $\kappa$ B $\alpha$ , both p65 and reconstituted wild type and p50<sup>Mu</sup> are observed at similar levels. This evidence suggests that not only is canonical p50:p65 dimer unaffected by the p50 mutation but neither is the ability of I $\kappa$ B $\alpha$  to bind p50, providing strong evidence that the NF- $\kappa$ B pathway is unaffected at this stage.

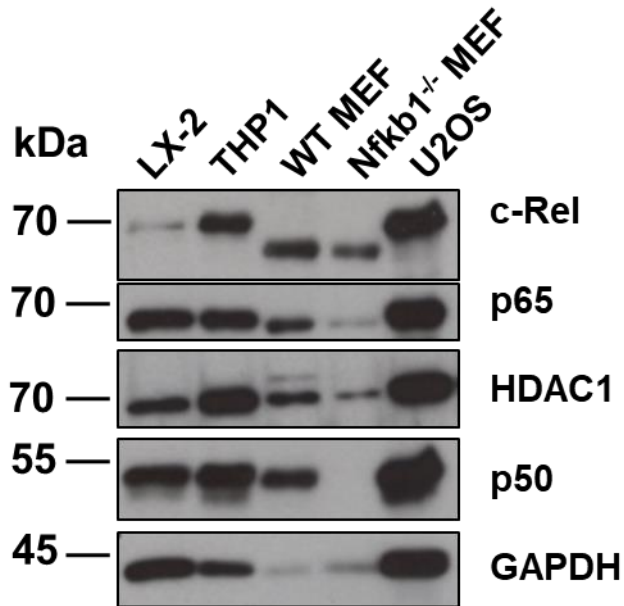


**Figure 5.1 Analysis of various cell types for expression of key complex components.**

*Western blot analysis of multiple cell types for expression of NF- $\kappa$ B components and HDAC1 to determine a suitable system to utilize to interrogate the effect of the p50:HDAC1 complex. LX-2, THP1 and U2OS lines are of human origin compared to murine embryonic fibroblasts and explains the observed differences in molecular weight as proteins are different sizes between species.*

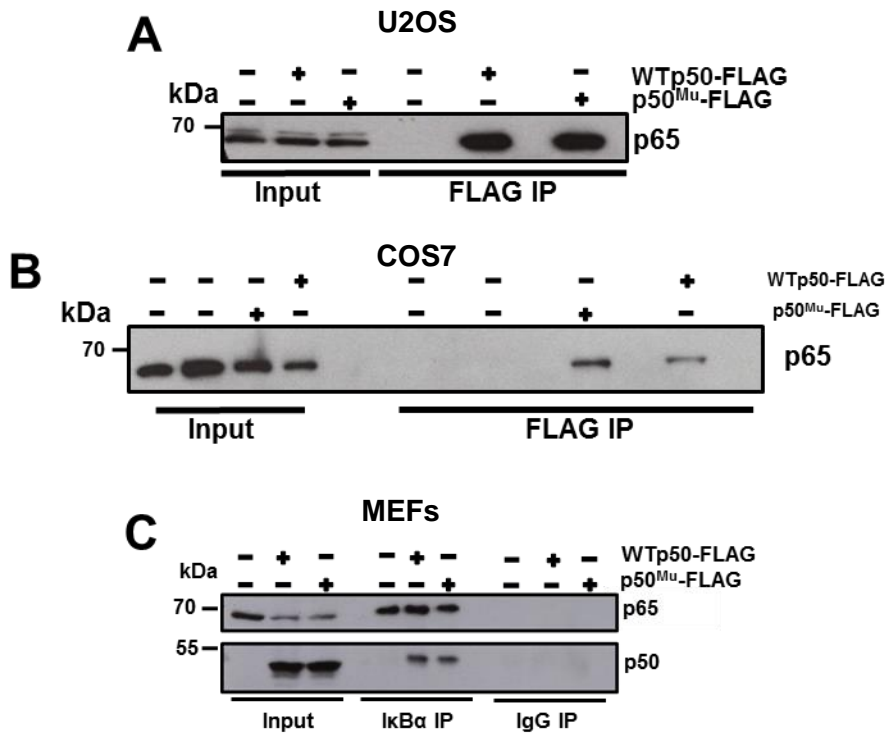


**Figure 5.2** *p50<sup>Mu</sup> does not affect its ability to interact with p65 or IκBα*

**A.** Western blot analysis of a flag co-IP assay in U2OS cells transfected with p50<sup>Mu</sup> or wild type p50 confirming no difference in p65 pull down. **B.** Western blot analysis of a flag co-IP assay in Cos7 cells transfected with p50<sup>Mu</sup> or wild type p50 confirming no difference in p65 pull down. **C.** Western blot analysis of a flag co-IP assay in *nfkb1*<sup>-/-</sup> MEFs transfected with p50<sup>Mu</sup> or wild type p50 showing integrity of the p50:p65:IκBα complex.

### 5.3.2 Mutation of p50 which causes a loss of HDAC1 Interaction Does not Inhibit Nuclear Localization

Another major component of NF- $\kappa$ B signaling is the ability of subunits to, once released from inhibitors, translocate to the nucleus to carry out their transcription-related activity. Since the mutation needed to block p50:HDAC1 interaction occurs predominantly within the nuclear localization sequence of p50, it was prudent to determine if this mutation was having an effect on p50's ability to enter the nucleus. Therefore *nfkb1*<sup>-/-</sup> MEFs (**Figure 5.3A**) and U2OS cells (**Figure 5.3B**) were transfected with either wild type or p50<sup>Mu</sup> and nuclear and cytoplasmic extracts generated to determine the approximate proportions of p50 in each cellular compartment. As can be seen in the relevant figures mentioned above, in both cases, wild type and p50<sup>Mu</sup> are present in both the nuclear and cytoplasmic compartments of the cells examined. Additionally, there appears to be no difference between wild type p50 and p50<sup>Mu</sup> in terms of the ratio of proteins in each compartment which suggests that the proteins are behaving similarly and the mutation is not having an effect on nuclear localization.

Since this finding disagrees with previously reported data suggesting an absolute requirement for p50's nuclear localization sequence for nuclear import, it was decided to show this nuclear localization by a different method. Therefore, U2OS cells were transfected with either wild type or p50<sup>Mu</sup> and probed by confocal immunofluorescence to determine the location of transfected p50 within the cell. Seen in **Figure 5.3C**, a clear nuclear pool of p50 is observed in both wild type and p50<sup>Mu</sup> transfected cells. However, a cytoplasmic pool is only observed in p50<sup>Mu</sup>. This may be a cause for some concern but may be explained by the difference in epitope availability due to the proximity of the mutation to the FLAG tag used in this assay or that the efficiency of nuclear import/shuttling may be slightly impaired in p50<sup>Mu</sup>. Nevertheless, these experiments show that a mutation of this magnitude in the NLS of p50 does not affect its ability to enter the nucleus.

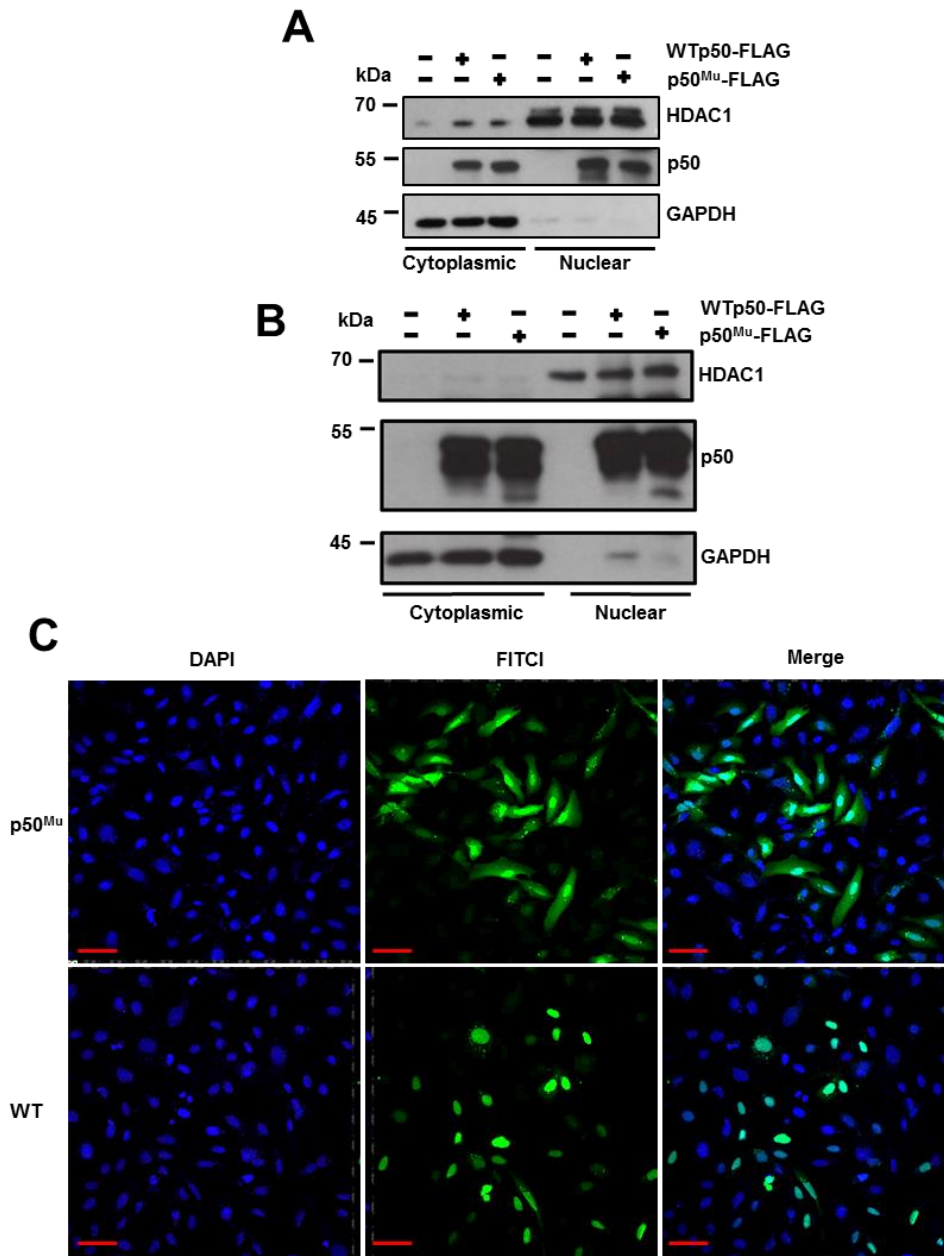


**Figure 5.3 p50Mu does not affect nuclear localization.**

**A.** Western blot of nuclear and cytoplasmic extracts from transiently transfected *nfkb1*<sup>-/-</sup> MEFs showing p50 nuclear translocation is unaffected by the mutation required to disrupt HDAC1 interaction despite its proximity to and inclusion of a portion of the nuclear localization sequence. **B.** Western blot of nuclear and cytoplasmic extracts from transiently transfected U2OS cells also showing p50 nuclear translocation is unaffected by the p50<sup>Mu</sup> mutation. **C.** Immunofluorescence confocal microscopy of U2OS cells transiently transfected with WT-FLAG or p50<sup>Mu</sup>-FLAG detected by anti-FLAG-FITC confirming nuclear localization by both proteins. Scale Bar = 50µm.

### 5.3.3 p50<sup>Mu</sup> Does not alter DNA binding but increases κB Promoter Acetylation

Given that the mutation in p50 established to disrupt the p50:HDAC1 interaction did not cause a significant interruption of canonical dimerization, inhibition and nuclear localization, we next wanted to confirm it maintained its ability to bind DNA and subsequently upregulate κB driven genes. Therefore *nfkb1*<sup>-/-</sup> MEF's were transfected with either wild type or p50<sup>Mu</sup> and one of three luciferase reporter constructs which contained 3x synthetic κB site promoter or the endogenously occurring IκBa or IL-6 promoters. The ability of either wild type or p50<sup>Mu</sup> to bind these sites was then determined by relative luminescence readout. In each case, as seen in **Figure 5.4**, there was no significant difference in relative luminescence observed in any of the three reporters used. While these results have to be interpreted in the context of a p50 reconstitution including reconstitution of the p50:p65 heterodimer, this strongly suggests that p50<sup>Mu</sup> does not affect p50's ability to bind DNA and promote gene transcription.

To gather more evidence in support of this, *nfkb1*<sup>-/-</sup> MEF's were again transfected with wild type or p50<sup>Mu</sup> and a ChIP assay was performed using the FLAG epitope on the transfected proteins. **Figure 5.5** shows that p50<sup>Mu</sup> and wild type p50 both bind known p50 target genes. While there appears to be a slight non-significant reduction in the case of p50<sup>Mu</sup>, this evidence further supports p50<sup>Mu</sup>'s ability to both enter the nucleus of cells and directly bind and drive known target genes. Given these findings, it was then important to determine if this p50 present at known κB promoters was having an effect of the overall acetylation of histones nearby. To test this another ChIP assay was performed using an antibody against pan Histone H3 acetylation in *nfkb1*<sup>-/-</sup> MEF's that had been reconstituted with wild type or p50<sup>Mu</sup> for 48 hours. Highlighted in **Figure 5.6**, previously described p50 target genes *cxcl1* and *cxcl2* display increased acetylation when cells are reconstituted with p50<sup>Mu</sup> and this increase rose to significance in the case of the *cxcl2* promoter. Together these experiments suggest that p50<sup>Mu</sup>, due to its inability

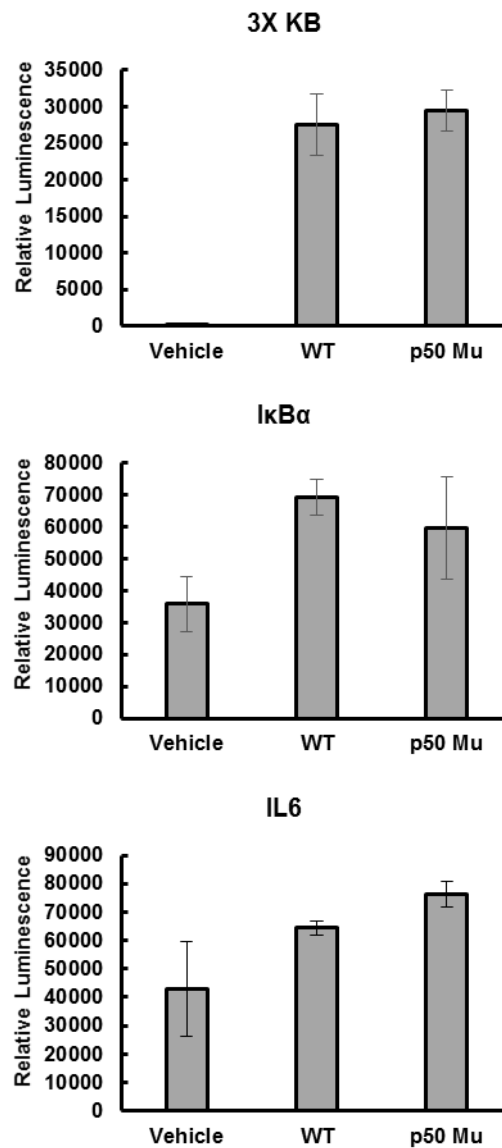


**Figure 5.4 p50<sup>Mu</sup> does not alter DNA binding**

*Luciferase reporter assay for a triple NF-κB promoter and IκBα promoter and IL-6 promoter in MEFs reconstituted with WT or p50<sup>Mu</sup> confirming similar ability to promote NF-κB dependent gene transcription.*

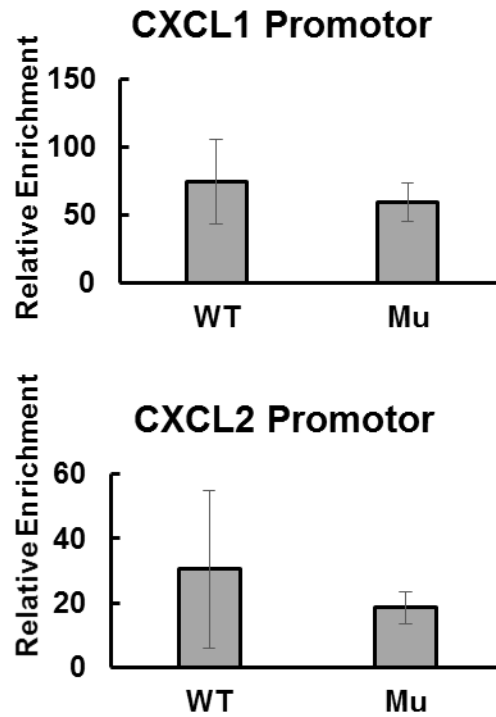


**Figure 5.5 p50<sup>Mu</sup> does not affect p50's ability to bind known target promoters**

*ChIP assay for p50 in nfkb1<sup>-/-</sup> MEFs confirming similar binding at cxcl1 and cxcl2 promoters in cells reconstituted with wild type or p50<sup>Mu</sup>.*

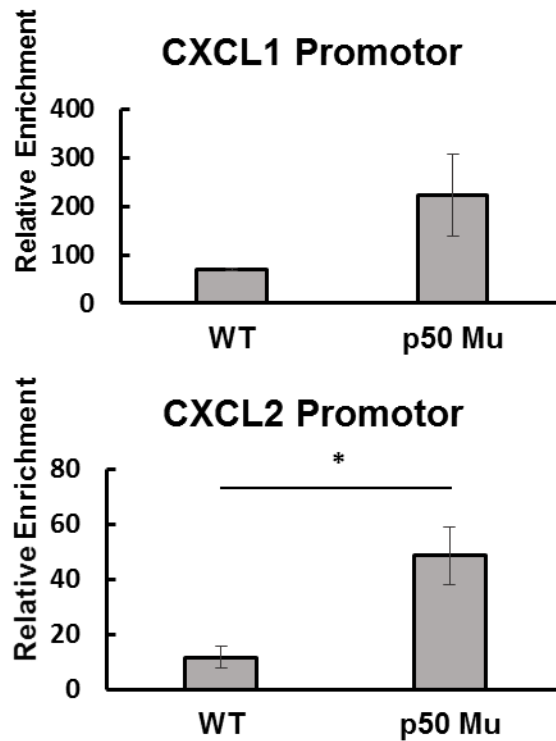


**Figure 5.6 Cells reconstituted with p50Mu possess significantly more acetylation at promoters of known p50 target genes.**

*Pan acetyl Histone 3 ChIP assay qRT-PCR on  $nfkb1^{-/-}$  MEFs demonstrating a significant increase in acetylation of the well-known p50 target gene *cxcl2* when cells are transfected with a version of p50 unable to bind HDAC1 ( $p50^{Mu}$ ) compared to WT (t-test  $p=0.021$ ). The same trend is observed in the target gene *cxcl1*.*

to recruit HDAC1, leads to increased  $\kappa$ B promoter H3 acetylation and the loss of basal gene repression provided in resting cells by p50 homodimers.

#### **5.3.4 p50<sup>Mu</sup> recapitulates the pro-inflammatory phenotype observed when p50 homodimers are lost**

Given this evidence that p50<sup>Mu</sup>'s ability to carry out canonical NF- $\kappa$ B activities appears unimpaired, yet acetylation of  $\kappa$ B driven target genes in cell with p50<sup>Mu</sup> is increased, we hypothesize that this increase in acetylation would be reflected as an increase in pro-inflammatory gene expression in both resting and stimulated cells which have been reconstituted with p50<sup>Mu</sup>. To test this, the response of *nfkb1*<sup>-/-</sup> MEFs to canonical NF- $\kappa$ B activator TNF $\alpha$  at one, three and six hours was observed by RT-qPCR for known pro-inflammatory genes IL-6 and cxcl10. Seen in **Figure 5.7**, significant ( $p=0.042$ ) upregulation of both IL-6 and cxcl10 was observed after one hour of stimulation. This increased to highly significant ( $p=0.0012$ ) after six hours. As such the six-hour time point was chosen for further experiments to both insure capture of late phase genes in the analysis as well as accurately detect any subtle changes in transcripts.

Using this six-hour stimulation regime, *nfkb1*<sup>-/-</sup> MEFs were equally transfected (**Figure 5.8A**) with either wild type or p50<sup>Mu</sup> for 24 hours and then left untreated or treated with TNF $\alpha$ . Relative gene expression under these conditions is shown in **Figure 5.8B**. In each case, the known p50 target genes showed a significant upregulation of gene expression in cells reconstituted with p50<sup>Mu</sup> compared to wild type upon TNF $\alpha$  stimulation. Moreover, this upregulation was also observed in unstimulated cells in the case of IL-6. This data suggests that p50<sup>Mu</sup>, due to its inability to recruit HDAC1, is enhancing gene expression of this subset of pro inflammatory genes. To confirm that this increase in transcript was reflective of a meaningful change in protein expression, an ELISA for IL-6 was performed on supernatant taken from these treated cells. Shown in **Figure 5.9**, a significant increase in secreted IL-6 was also observed in cell reconstituted with p50<sup>Mu</sup> and stimulated with TNF $\alpha$  compared to wild type p50.

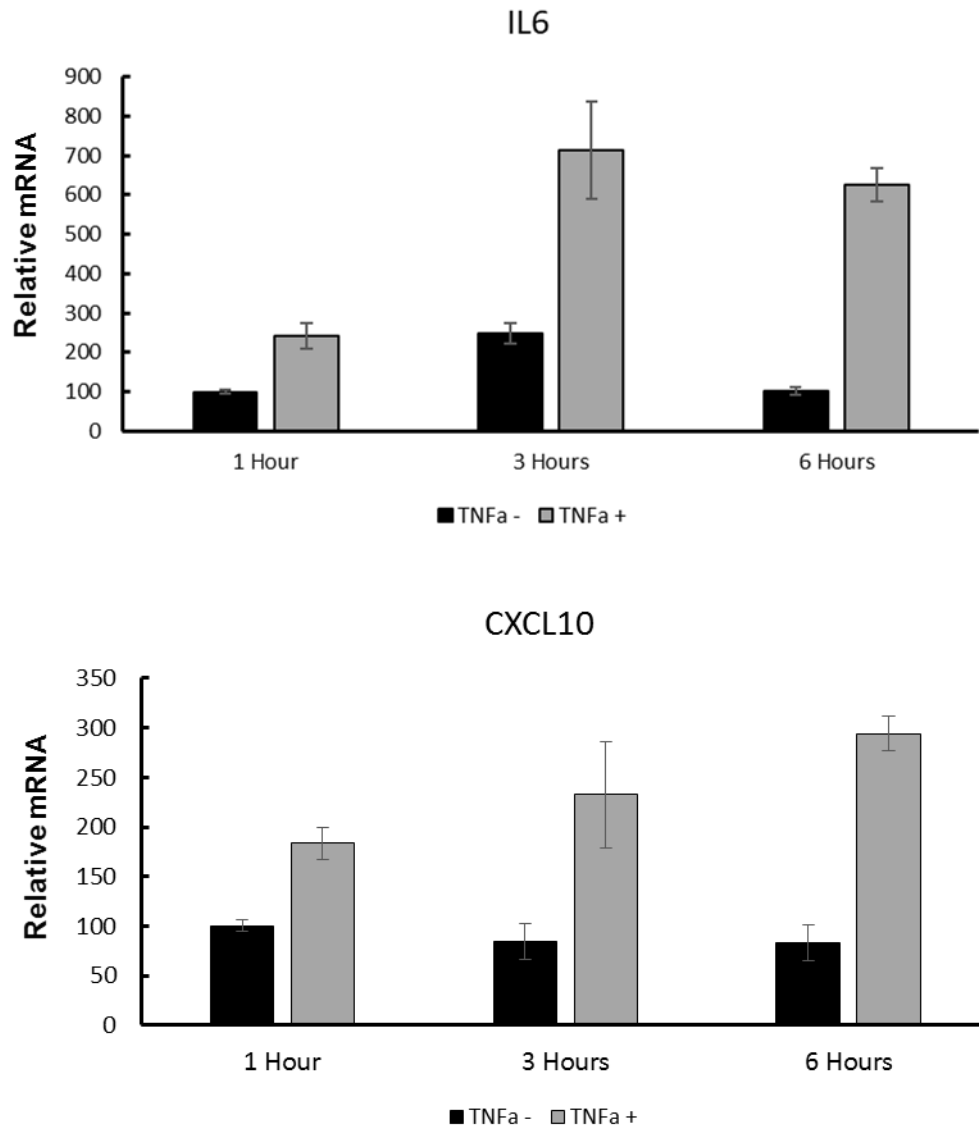


**Figure 5.7 TNFα time course in *nfkb1*<sup>-/-</sup> cells**

*RT-qPCR of two well-known p50 inflammatory target genes cxcl10 and IL-6 untreated or treated with 10ng/ml TNFα at various time points to determine optimal response times for functional characterization. Significant increase in gene transcription is observed at all time points between treated and untreated cells with greatest difference observed at six hours ( $p=0.042$  at 1 hour and  $p=0.0012$  at 6 hours as determined by unpaired students t-test).*

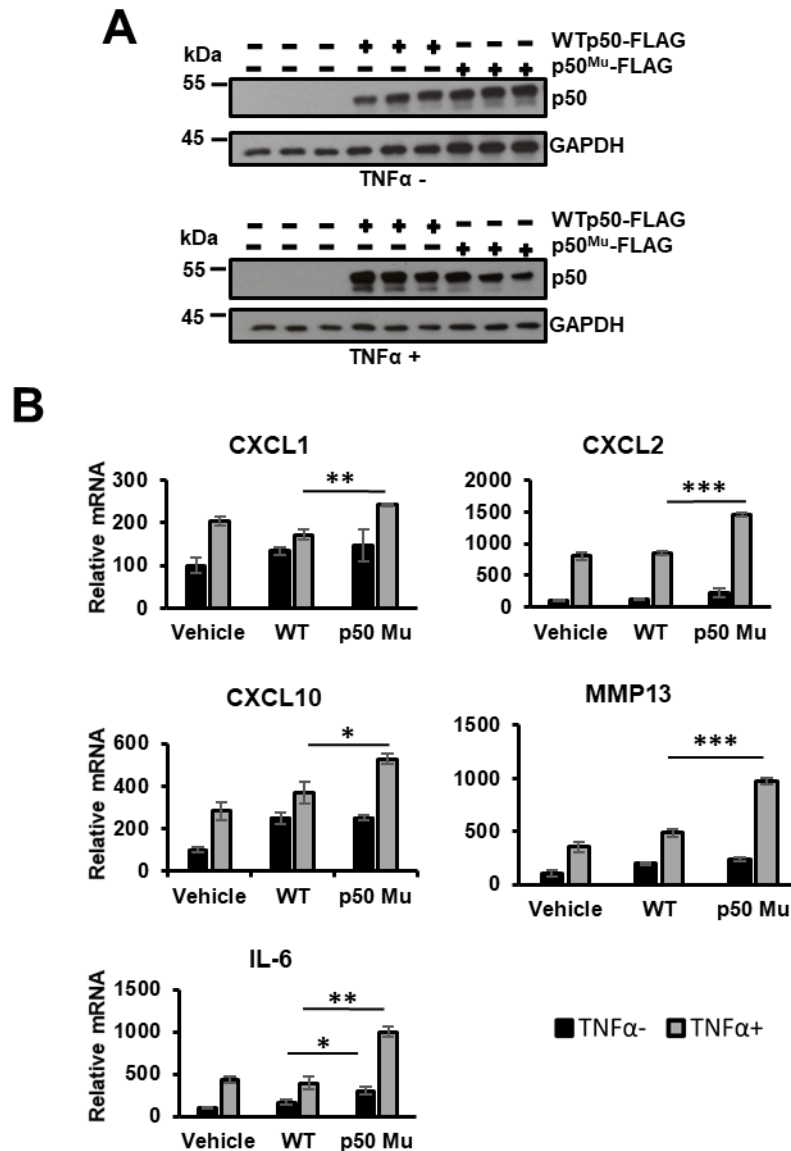


**Figure 5.8 Cells reconstituted with p50<sup>Mu</sup> display a more pro-inflammatory phenotype in comparison to wild type.**

**A.** Western blot analysis confirming equal transient transfection of WT and p50<sup>Mu</sup> in *nfk1<sup>-/-</sup>* MEFs untreated or treated with TNFα. **B.** RT-qPCR demonstrating a significant increase in mRNA expression of well-known p50 repressed genes in the absence of HDAC1 interaction (p50<sup>Mu</sup>). IL-6  $p=0.002$ , *cxcl2*  $p=0.0002$ , *cxcl1*  $p=0.004$ , *cxcl10*  $p=0.048$  and *Mmp13*  $p=0.0004$ . *P* values generated by *t*-test.

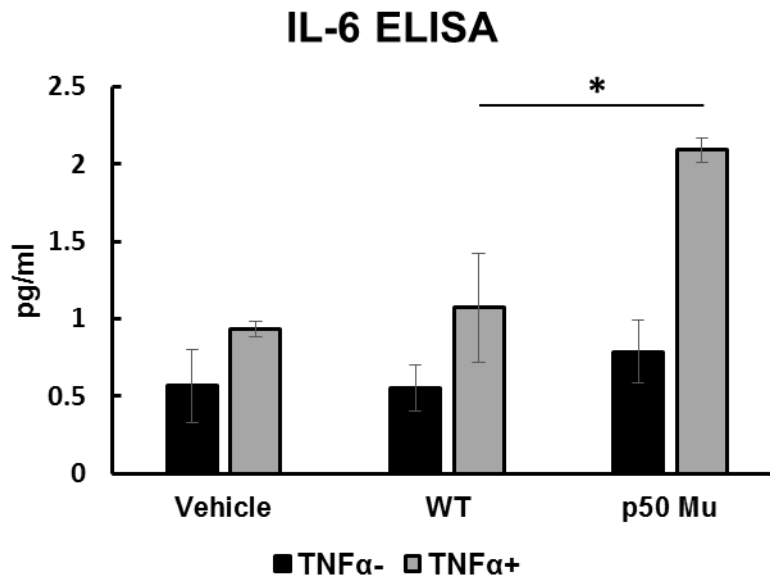


**Figure 5.9 Cells reconstituted with p50Mu secrete more IL-6 than wild type.**

*ELISA analysis of cell media showing a significant increase in released IL-6 in cells stimulated with TNFα ( $p= 0.047$ ) from cells reconstituted with p50<sup>Mu</sup> compared to wild type.*

Finally, to more directly compare the effects of p50<sup>Mu</sup> to that of the known loss of p50 homodimer phenotypes *nfkB1*<sup>-/-</sup> MEF's were reconstituted with wild type or p50<sup>Mu</sup> for 24 hours and then either left untreated or treated with TNF $\alpha$  for six hours. Following this, media was harvested and used to perform a neutrophil chemotaxis assay to determine if cells lacking the p50:HDAC1 interaction provided stronger neutrophil recruitment potential (**Figure 5.10A**). Migrated neutrophil counts show that cells reconstituted with p50<sup>Mu</sup> attracted significantly more neutrophils than wild type p50 when stimulated with TNF $\alpha$  (**Figure 5.10B**). These results, corroborated by representative images (**Figure 5.10C**) and western blot transfection controls (**Figure 5.10D**), suggest that in the absence of the ability to bind HDAC1 p50 loses its innate repressive effect on pro-inflammatory target genes. Taken together with previous findings, a mechanism by which p50 homodimers recruit HDAC1 to  $\kappa$ B sites and silence gene expression there through histone deacetylation is further implicated.

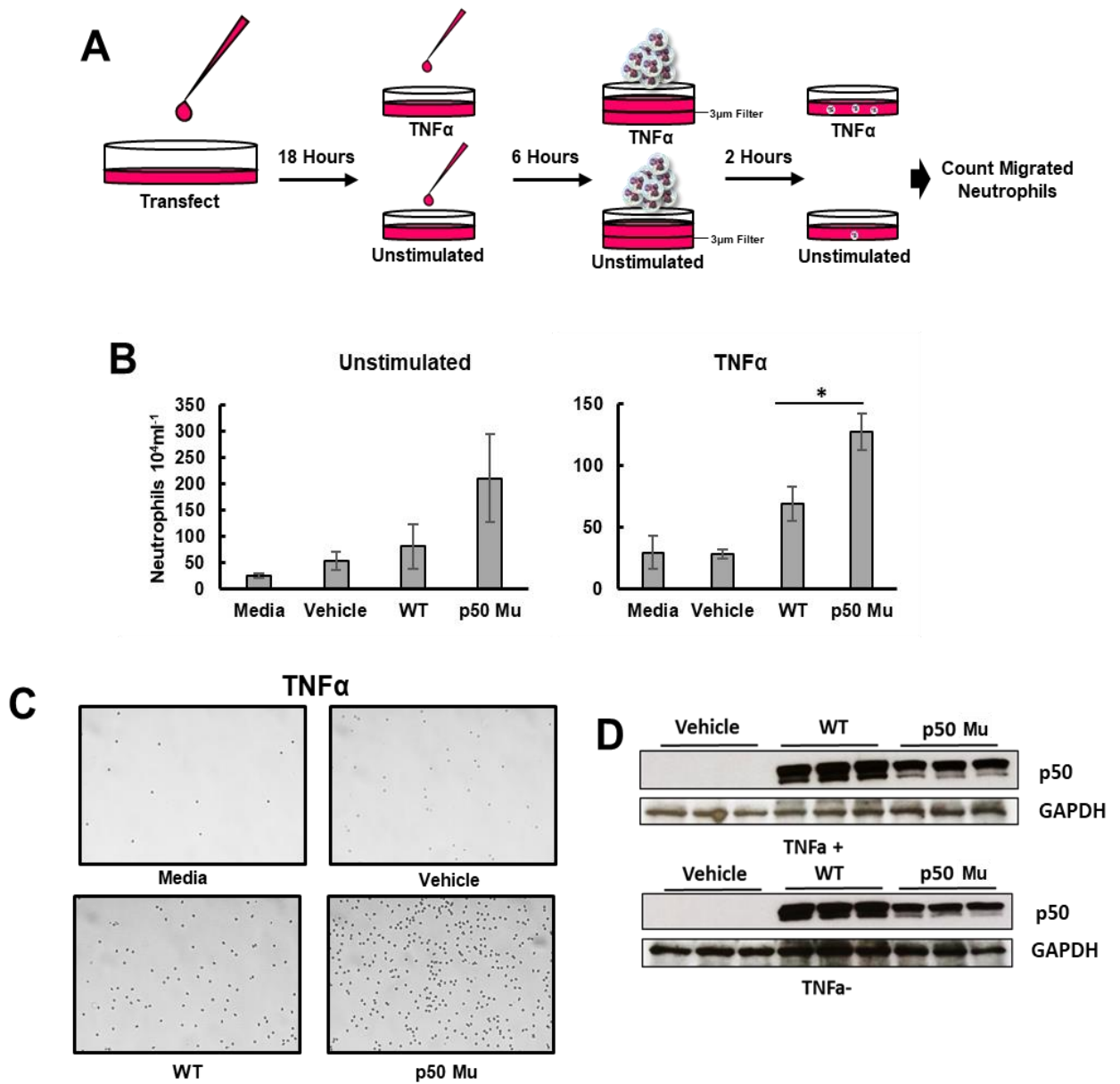


**Figure 5.10 p50Mu promotes significantly more neutrophil chemotaxis**

**A.** Schematic of a neutrophil chemotaxis experiment highlighting timeframes. **B.** Cell counts post chemotaxis of murine neutrophils showing increased chemotaxis toward p50<sup>Mu</sup> conditioned media and significantly more infiltration when MEFs are stimulated with TNF $\alpha$  post transfection ( $p = 0.046$ ). **C.** Representative images of neutrophils post chemotaxis in TNF $\alpha$  treated media. **D.** Western blot showing comparable transfection of WT and p50<sup>Mu</sup> from cells whose supernatant was used in the neutrophil chemotaxis experiment in both the presence and absence of TNF $\alpha$ .

## **5.4 Discussion**

Evidence presented in this chapter strongly implicates HDAC1 as the key effector in p50 driven gene suppression. Additionally, it calls into question the previously reported absolute requirement for the NLS of p50 for nuclear import. These findings advance our understanding of NF- $\kappa$ B inhibition and provide a mechanism by which pro-inflammatory signaling events can be resolved. Data presented here are however not without limitations.

### **5.4.1 p50 Nuclear localization sequence is not essential for nuclear transport.**

Given that p50<sup>Mu</sup> is a drastic ablation of the NLS, expectations were that there would be a severe impact on p50 nuclear import. However, no such loss of nuclear import has been observed as well as no apparent effects on the formation of canonical complexes such as the p50:p65:I $\kappa$ B $\alpha$  complex. While these data strongly suggest these conclusions, in general precautions should be made when interpreting these results. For example, while the p50:p65:I $\kappa$ B $\alpha$  complex appears to be undisturbed, it is hard to rule out the possibility that p50<sup>Mu</sup> is having an impact on I $\kappa$ B $\alpha$  binding in particular. Due to the nature of this complex loss of p50 interacting residues may not be enough on its own to block this interaction and the wild type p65 present is sufficient to keep the complex intact. Similarly, the finding that p50 nuclear localization is unimpaired may be due to the presence of p65 aiding in nuclear import with its own intact NLS. Careful observations such as these have been the crux of the difficulty in teasing apart individual dimer and specific dimer pair functions. Therefore, experiments of this nature will have to always be interpreted in the context that observations are an average of all possible interactions including those with other members of the NF- $\kappa$ B family such as c-Rel.

### **5.4.2 Interaction with HDAC1 is vital to p50's ability to repress NF- $\kappa$ B target genes.**

Previous findings suggest that HDAC1 was required in a certain subset of genes for p50 dependent gene repression. However, data presented here further

corroborate this finding. The original p50 knock out phenotype as observed in *nfkb1<sup>-/-</sup>* is described as a systemic pro-inflammatory condition where systemic levels of chemokines such as IL-6 are elevated [126]. In this chapter, it is seen that cells reconstituted with p50 which is unable to recruit HDAC1 displays a similar phenotype. In addition, it has been shown that neutrophil infiltration is elevated in p50 knock out mice when subject to the carcinogen diethyl nitrosamine [58]. This is again phenocopied *in vitro* where neutrophils are more strongly attracted to supernatant from cells with an impaired p50:HDAC1 complex. These findings strongly suggest HDAC1 as the vital activator of p50 dependent gene repression, however this must be viewed in the context of the wider literature. It is known for example that p50 also binds nuclear Bcl3 which is proposed to protect it from proteasome mediated degradation [127]. Additionally, it has been shown that p50 may recruit p300, a histone acetyl transferase, to directly upregulate gene transcription at the promoter of anti-inflammatory genes such as IL-10 [38]. While these interactions will be context specific and it is not clear how these interactions may co-exist, a potential hypothesis exists. In resting cells p50 homodimers may enter the nucleus and bind kB sites. This would offer the first line of repression as any induced active p50:p65 heterodimers would first have to displace these p50 homodimers. Next, in a context dependent manner, potentially driven by post-translational modifications such as phosphorylation, p50 may associate with HDAC1 or p300 to repress pro-inflammatory gene transcription or enhance anti-inflammatory genes. Once nearby chromatin states have been appropriately modified, HDAC1 may share residency with Bcl3 of p50 homodimers ensuring chromatin remains in a repressed state and p50 homodimers remains in place and protected from premature removal and degradation. This is corroborated by the findings that BCL3 binds p50 via the same NLS region discovered to be critical in the HDAC1 interaction [73]. This model summarized in **Figure 5.11**, best fits with observed experimental data here as well as the published literature whereby p50 is orchestrating the repression of genes to ensure that potent activator signals do not induce unstainable levels of pro-inflammatory signals. This mechanism may

also be vital in the resolution of inflammation. As more I $\kappa$ B is transcribed and free p65 heterodimers are sequestered once more, the balance of dimers may shift to that of p50 homodimers which would then be free to orchestrate the epigenetic changes previously described. While this hypothesis does satisfy previous data more empirical evidence of this order of events is required for firmer claims to be made. What is certain now, however, is that HDAC1 is capable of significant changes to the epigenetic landscape of genes when recruited by p50.

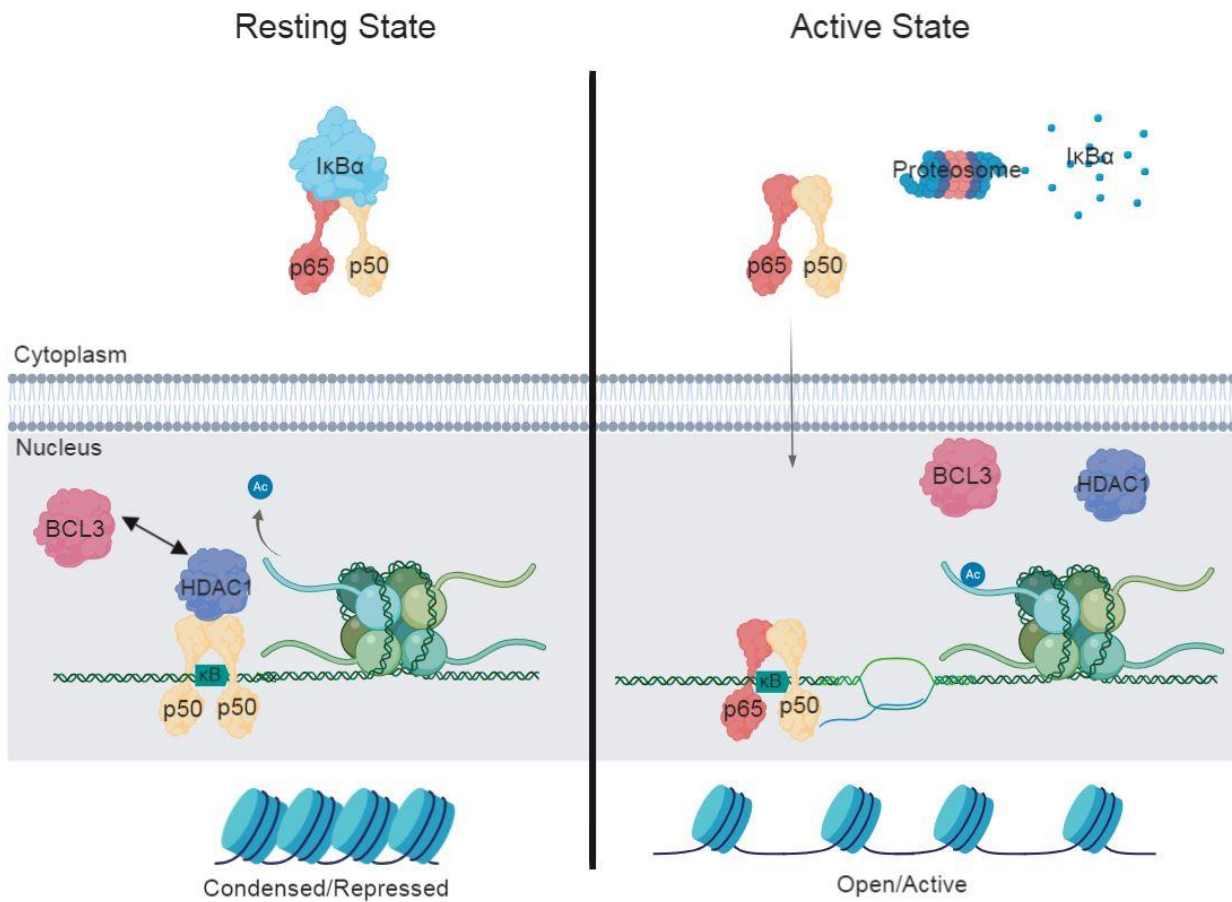


**Figure 5.11 Summary of a proposed mechanism for p50 homodimer and BCL3/HDAC1 mediated NF-κB transcription repression.**

*In resting cells active subunit dimers are sequestered and bound to IκB's in the cytoplasm while repressive p50 homodimers bind κB sites on DNA in the nucleus and through the recruitment of HDAC1 facilitates the deacetylation of histone tails and transcriptional repression. As the HDAC1 and BCL3 sites of interaction on p50 are shared, BCL3 would need to displace HDAC1 from homodimers and maintain their stability through ubiquitination blockade. Once activated by IκB degradation, p50:p65 heterodimers can be transported to the nucleus and displace p50 homodimers and through the recruitment of histone acetyl transferases initiate transcription from the required loci.*

## Chapter 6 General Discussion and Conclusion

---

Data presented in this thesis has added to the growing body of published literature implicating p50 and HDAC1 as critical components of the pro-inflammatory repression machinery in cells. In doing this it has also brought to light some of the complexities involved in studying multifaceted transcription factor families such as the NF- $\kappa$ B family. Teasing apart the intricacies of multiple subunits and the attribution to any observed effects promoted by those subunits must be done with great care.

### **6.1 The complexities of NF- $\kappa$ B dimerization: control of the p50 homodimer**

Discussed in chapter 3, dimer selection remains a poorly characterized area in part due to the complexities described earlier. Not only is it important to understand the context of the system being observed but also, as in the case of the S343A mutation, other unrelated factors that may not be obvious. As more evidence is gathered, it has become apparent that dimerization of subunits in particular is more complicated than previously envisioned. Innate sequence differences, availability of third party interactors as well as environments conducive to certain post-translational modifications along with cell and tissue specific differences most likely all conspire in some way to manipulate appropriate dimer pool balance. As such future work must make all of these considerations when attempting to further deconvolute the myriad of interconnected signals possibly causative of dimer partner selection. Further work on both understanding dimer selection and methods for their manipulation should remain a high priority for the future as specific control of dimers may be the key to more appropriate tuning of NF- $\kappa$ B signaling in disease states. Moreover, direct subunit manipulation offers advantages over potential therapies related to upstream signaling including the reduction of the potential for unwanted off target effects that could exacerbate the underlying condition or have another unintended off target effect [39].

## 6.2 The p50 Nuclear localization sequence as a dynamic scaffold for the control of gene induction and suppression.

In addition to the previously described protein-protein interactions occurring at or near the NLS, data presented here define the NLS of p50 as the major site of interaction with HDAC1. While other possible sites of interaction were predicted *in silico*, the observed near total ablation of p50:HDAC1 interaction upon mutation of the VQKRKQK motif strongly supports this region as the critical site of interaction. Considering this evidence and borrowing from previous published data, the working model proposed here suggests that dimers of p50 at target sites in the nucleus serve as a scaffold for numerous epigenetic events [124,127]. Seen in **Figure 6.1**, loops of the ankyrin repeats of I $\kappa$ B $\alpha$  bind a p65 homodimer near the region of the p65 NLS. Moreover, the flexibility of the terminal amino acids on this end of p50, if similar to p65, may serve as a tether to bind freed epigenetic remodeling complexes. The crystal structure of HDAC1 bound to metastasis associated protein 1 (Mta1) suggests this is a reasonable assumption as in this resolved structure the unstructured tail of Mta1 wraps around the catalytic core of HDAC1 and makes several contacts along grooves created by external alpha helices of [95]. In a similar way the unstructured tail of p50 may be created multiple points of contacts around not just HDAC1 but other components of the nuclear epigenetic machinery. With this stated, however, the possibility of third party mediators within the p50:HDAC1 or other interactors has not been experimentally disproven. Further evidence and investigation is needed to ascertain two important unknowns raised here. First, is p50 capable of direct recruitment of these numerous co-factors to  $\kappa$ B sites or are there further intermediates? Secondly, of the many complexes potentially capable of being formed on a p50 scaffold, how many of them provide meaningful changes to the function of cell in which they are found. Evidence for Bcl3 and now HDAC1 strongly suggests these as two direct interactors but whether these represent the end of a list or a small subsection of a much larger pool is yet to be determined.

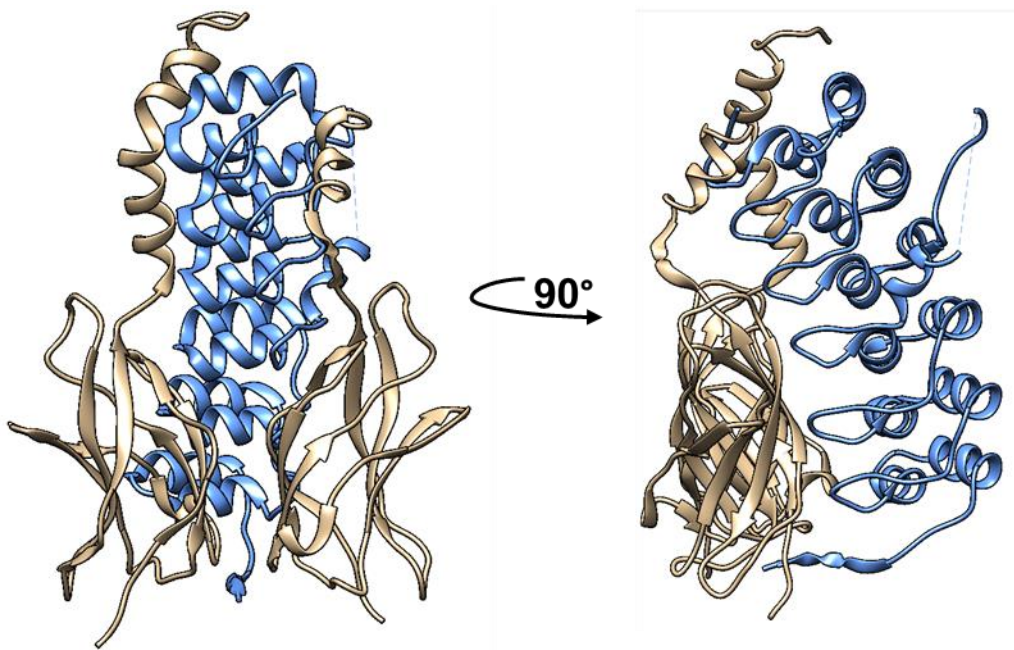


**Figure 6.1 Crystal structure of p65 homodimer bound to IκBβ**

*Crystal structure of a p65 homodimer (beige) dimerization domain bound to IκBβ (blue) highlighting the nature of the interaction between the ankyrin repeats as well as the unstructured tails of p50 and p65 (PDB ID 1OY3) [124].*

### **6.3 Interaction with HDAC1 is critical to the active gene repression of p50 homodimers**

Evidence provided for the direct interaction of p50 with HDAC1 while suggested by two methods relies either on *in vitro* observation or overexpression. This evidence on its own, however, does make a strong case that the site identified is indeed where p50 binds HDAC1. Moreover, functional tests by RT-qPCR and chemotaxis assay all suggest important regulation by p50 of pro-inflammatory genes in an HDAC1-dependent manner. While conclusions in this regard may be strengthened by further *in vivo* work including the verification of a pro-inflammatory, cell specific phenotype in genetically modified mice, the data presented robustly supports the arguments made regarding the importance and observed effects of a loss of HDAC1. One potential weakness in the functional data regarding an upregulation of pro-inflammatory genes (**Figure 5.8**), is that p50 WT is seen activating transcription. There is, however, little evidence that suggests that a p50 overexpression would cause complete suppression of gene transcription in WT cells much less the p50 knock outs used in this experiment. What is clear is that p50 is not just a simple repressive molecule but tends toward active repression in the absence of signal and that these results are being interpreted as the result of the reconstitution of both p50 and the p50:p65 heterodimer which will have potent effects on gene transcription.

### **6.4 Conclusion**

This collection of work has driven our understanding of NF- $\kappa$ B repression and made several advances in our appreciation of the biochemistry of p50. Shown through the use of *in silico* molecular dynamics simulations, p50 may be phosphorylated at serine 343 but this residue is also critical for protein stability and homodimerization [58]. This collection of data also further elucidates the conserved difference in the interfaces of p50 and p65 and demonstrated that mutation in interfacial residues may have a significant impact on the affinities of dimers

[113,116]. This work has also described the VQKRKQK motif in the NLS of p50 as the region responsible for the p50:HDAC1 interaction which exists primarily in resting cells. Additionally, loss of most residues due to mutation of the NLS seemed to have little to no effect on p50 nuclear localization and calls into question previous studies which report this region as essential [112]. Another major observation includes the fact that the loss of HDAC1 interaction and its NLS does not seem to impact the function of p50 in any way, including its ability to form canonical complexes and drive DNA transcription along with p65 in addition to not influencing localization. Finally loss of p50:HDAC1 leads to increased promoter acetylation, increased transcription of pro-inflammatory genes and increased neutrophil chemotaxis all of which cementing HDAC1 as a critical effector in NF- $\kappa$ B signaling repression.

## **6.5 Future Work**

Given the complexities underscored here and in the literature concerning the various intricacies of subunit and cascade activation that leads to multiple transcriptional programs, it is clear that there is much still left to be uncovered. Two important and related questions that warrant further examination is the role of interface residues highlighted in chapter 3 in the section of dimer partners and the regulation of interaction factors (such as HDAC1, BCL3, HAT's etc.) on those base line possible subunit combinations.

Dimerization has always posed a challenge in the NF- $\kappa$ B field as many tools and systems developed to date made it impossible to determine the specific contributions of each subunit to a particular transcriptional profile. While others have noted subunit specific sequence changes that facilitate different dimer affinities as well as potential posttranslational modifications which do the same, emerging powerful techniques such as CRISPR gene editing may provide an alternative method for dissecting the lone and combinatorial effect of residues in subunits such as those interface and sites of posttranslational modification described in this work. Uncovering the contribution of each subunit and post

translational modification and subsequent enzymes responsible would not only lead to better understanding of this important transcription factor system but could highlight therapeutic targets for many inflammation associated diseases.

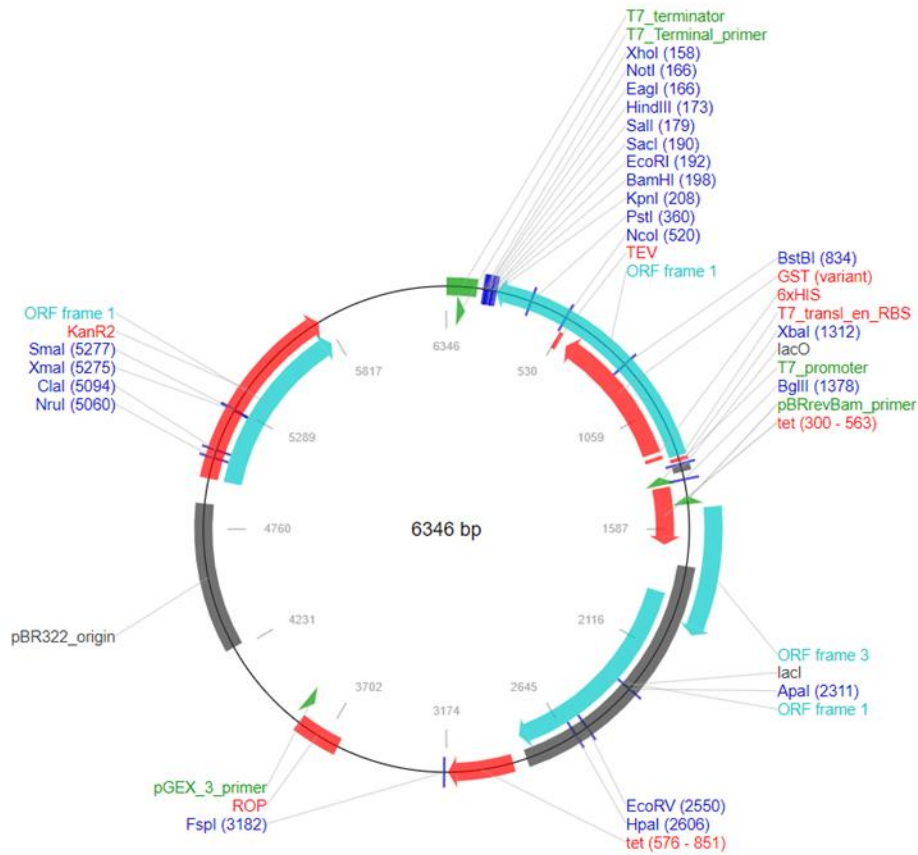
In a similar manner the emerging network surrounding third party interactors with subunits still needs exploration. Previously described in the most detail, BCL3 has been added to the list of p50 homodimer interactors that enhance their function [73]. This work now also adds HDAC1 to that list in a similarly robust way. As discussed earlier, however, much still needs to be understood regarding the relationship these two proteins have with regards to p50 homodimers including the conditions of their occupancy on binding sites. In addition, there are undoubtedly more third party interactors that adds more specificity to the function of not only p50 dimers but those of the other subunit combinations as well. While not an easy challenge, mapping this dimer specific interactome of all possible combination would provide true insight in the tightly controlled way that NF- $\kappa$ B promotes and repressed gene transcription. This understanding would especially be of importance to those designing therapeutic to fully understand the wider implications of altering pathways or pathways outcomes in an attempt to treat disease.

## 6.6 Summary

- Serine 343 (human) is critical to the stability of p50 and may be a site of post translational modification involved in dimer selection.
- Four conserved differences in the interface of the p50:p65 heterodimer impart partial dimer stability and specificity.
- p50 interacts with HDAC1 via its VQKRKQK NLS motif.
- Mutation of the p50 NLS motif does not affect DNA binding, dimerization or nuclear localization.
- In the absence of HDAC1, p50 bound promoters show increased acetylation.
- In the absence of HDAC1, p50 bound pro-inflammatory target genes show increased expression.
- Loss of p50:HDAC1 stimulates cells to increase neutrophil chemotaxis signals and enhance a pro-inflammatory environment.

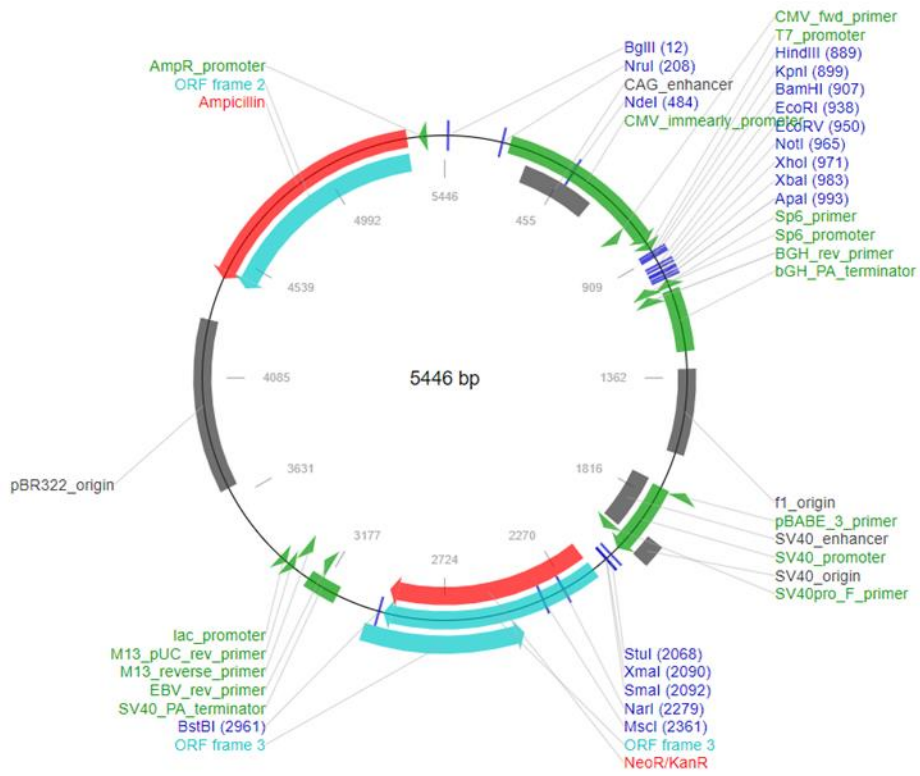
# Chapter 7 Appendices

## PetM30 – Kanamycin Resistance



Appendix 7.1 petM30 Vector Map

# pcDNA3 – Ampicillin Resistance



Appendix 7.2 pcDNA3 Vector Map

<b>Mutagenesis Primers</b>		<b>Tm</b>
AQAAAQA Forward	agctcaggcgCTCATGCCCAATTTTTCG	60
AQAAAQA Reverse	gccgcctgcgcTTCTTCTTTATCTTTGATTT CAGG	60
AQAAAQK Forward	agctcagaagCTCATGCCCAATTTTTCG	60
AQAAAQK Reverse	gccgcctgcgcTTCTTCTTTATCTTTGATTT CAGG	60
AQAARQK Forward	acgtcagaagCTCATGCCCAATTTTTCG	60
AQAARQK Reverse	gccgcctgcgcTTCTTCTTTATCTTTGATTT CAGG	60
VQAARQK Forward	acgtcagaagCTCATGCCCAATTTTTCG	60
VQAARQK Reverse	gccgcctgcacTTCTTCTTTATCTTTGATTT CAGG	60
VQRARQK Forward	acgtcagaagCTCATGCCCAATTTTTCG	60
VQRARQK Reverse	gccctctgcacTTCTTCTTTATCTTTGATTT CAGG	60
<b>qRT-PCR Primers</b>		
mIL-6 Forward	GAGGATACCACTCCCAACAGA	60
mIL-6 Reverse	AAGTGCATCATCGTTGTT CATA	60
mCXCL1 Forward	CTGGGATTCACCTCAAGAACATC	60
mCXCL1 Reverse	CAGGGTCAAGGCAAGCCTC	60
mCXCL2 Forward	CCAACCACCAGGCTACAGG	60
mCXCL2 Reverse	GCGTCACACTCAAGCTCTG	60
mCXCL10 Forward	AAGTGCTGCCGTCATTTCT	57
mCXCL10 Reverse	GTGGCAATGATCTCAACACG	57
mMMP13 Forward	CTTCTTCTTGTTGAGCTGGACTC	57
mMMP13 Reverse	CTGTGGAGGTCACTGTAGACT	57
<b>ChIP Primers</b>		
mCXCL1 Forward	GTTGGCAAAGCAAACCACC	57
mCXCL1 Reverse	ACTACAGTGATTTGCGGGGA	57
mCXCL2 Forward	GACATCCCAGGGTCCCATAG	57
mCXCL2 Reverse	TGCACGATGTCTGGAAAAGC	57

### Appendix 7.3 Primers used in SDM, RT-qPCR and ChIP Assays

Cloning Primers		Tm
HDAC1 Full (Gibson) F	CTTTATTTTCAGGGCGCCATG GCG CAG ACG CAG GGC AC	72
HDAC1 Full (Gibson) R	GGTGCTCGAGTGCGGGCCGCATCAGGCCAACTTGACCTCC	72
HDAC1 Frag (Gibson) F	GAATCTTTATTTTCAGGGCGCCCGAGGAAAGTCTGTTACTAC	72
HDAC1 Frag (Gibson) R	GGTGGTGCTCGAGTGCGGGCCGCACTAAGAATCGGAGAACTCTTCCTC	72
p50 Full (Gibson) F	GAGAATCTTTATTTTCAGGGCGCCATGGCAGAAGATGATCCATATTTGG	72
p50 Full (Gibson) R	GGTGGTGCTCGAGTGCGGGCCGCATCATCCATGCTTCATCCCAGCATTAG	72
p50 Frag (Gibson) F	GAGAATCTTTATTTTCAGGGCGCCGCAGATGGCCCATACCTTCAAATAT	72
p50 Frag (Gibson) R	TGGTGGTGCTCGAGTGCGGGCCGCACTAAGGATAGTAGAGGAAAGGTTTTGG	72
p65 Frag (Gibson) F	TACGACGTACCAGATTACGCTCAATATGTGGAGATCATTGAGCAGC	72
p65 Frag (Gibson) R	GCAGCTCGAGCTCGATGGATCTAATCTGGCAGGTACTIONGGAATTCC	72
Sequencing Primers		
pet-M30 F	TGCGGCCGCACTCGAGCACC	na
pet-M30R	GCGCCCTGAAAATAAAGATTC	na

**Appendix 7.4 Primers used in petM30 cloning and sequencing for crystallography constructs.**

<b>Bacterial Strain</b>	<b>Source</b>
NEB Ultra Competent DH5 $\alpha$	New England Biolabs C2987H
Rosetta 2(DE3)pLysS	Novagen 71401
BL21 DE3	New England Biolabs C2527H
Lemo21	New England Biolabs C2528J
Tunner	Novagen 70623
Arctic Express	Agilent 230191
In-lab generated DH5 $\alpha$	Originally New England Biolabs C2987H

### **Appendix 7.5 Bacterial strains used in production of recombinant protein.**

<b>Backbone</b>	<b>Insert</b>	<b>Tags</b>
pcDNA3.1	p50 WT	Flag
pcDNA3.1	p50 VQRARQK	Flag
pcDNA3.1	p50 VQAARQK	Flag
pcDNA3.1	p50 AQAARQK	Flag
pcDNA3.1	p50 AQAAAQK	Flag
pcDNA3.1	p50 AQAAAQA	Flag
pcDNA3.1	p50 K365A	Flag
petM30	HDAC1 WT	TEV-GST-6xHIS
petM30	HDAC1 8-378aa	TEV-GST-6xHIS
petM30	p65	TEV-GST-6xHIS
petM30	p50 WT	TEV-GST-6xHIS
petM30	p50 40-353aa	TEV-GST-6xHIS

### **Appendix 7.6 List of Plasmids Used and Generated**

## References

---

1. Sen R, Baltimore D (1986) Multiple nuclear factors interact with the immunoglobulin enhancer sequences. *Cell* **46**: 705–716.
2. Ghosh S, May MJ, Kopp EB (1998) NF-kappa B and Rel proteins: evolutionarily conserved mediators of immune responses. *Annu Rev Immunol* **16**: 225–260.
3. Perkins ND (2007) Integrating cell-signalling pathways with NF-kappaB and IKK function. *Nat Rev Mol Cell Biol* **8**: 49–62.
4. Vu D, Huang D-B, Vemu A, Ghosh G (2013) A structural basis for selective dimerization by NF- $\kappa$ B RelB. *J Mol Biol* **425**: 1934–1945.
5. Kunsch C, Ruben SM, Rosen C a (1992) Selection of optimal kappa B/Rel DNA-binding motifs: interaction of both subunits of NF-kappa B with DNA is required for transcriptional activation. *Mol Cell Biol* **12**: 4412–4421.
6. Savinova O V, Hoffmann A, Ghosh G (2009) The Nfkb1 and Nfkb2 proteins p105 and p100 function as the core of high-molecular-weight heterogeneous complexes. *Mol Cell* **34**: 591–602.
7. Kravtsova-Ivantsiv Y, Shomer I, Cohen-Kaplan V, Snijder B, Superti-Furga G, Gonen H, Sommer T, Ziv T, Admon A, Naroditsky I, et al. (2015) KPC1-Mediated Ubiquitination and Proteasomal Processing of NF- $\kappa$ B1 p105 to p50 Restricts Tumor Growth. *Cell* **161**: 333–347.
8. Moorthy AK, Savinova O V, Ho JQ, Wang VY-F, Vu D, Ghosh G (2006) The 20S proteasome processes NF-kappaB1 p105 into p50 in a translation-independent manner. *EMBO J* **25**: 1945–1956.
9. Lin L, DeMartino GN, Greene WC (1998) Cotranslational biogenesis of NF-kappaB p50 by the 26S proteasome. *Cell* **92**: 819–828.
10. Oeckinghaus A, Ghosh S (2009) The NF-kappaB family of transcription factors and its regulation. *Cold Spring Harb Perspect Biol* **1**: a000034.
11. Viatour P, Merville MP, Bours V, Chariot A (2005) Phosphorylation of NF- $\kappa$ B and

- I $\kappa$ B proteins: Implications in cancer and inflammation. *Trends Biochem Sci* **30**: 43–52.
12. Kato T, Delhase M, Hoffmann A, Karin M (2003) CK2 is a C-terminal I kappa B kinase responsible for NF-kappa B activation during the UV response. *Mol Cell* **12**: 829–839.
  13. Scott ML, Fujita T, Liou HC, Nolan GP, Baltimore D (2007) The p65 subunit of NF-kappa B regulates I kappa B by two distinct mechanisms. *Genes Dev* **7**: 1266–1276.
  14. Laín de Lera T, Folgueira L, Martín AG, Dargemont C, Pedraza M-A, Bermejo M, Bonay P, Fresno M, Alcami J (1999) Expression of I $\kappa$ B $\alpha$  in the nucleus of human peripheral blood T lymphocytes. *Oncogene* **18**: 1581–1588.
  15. Nelson DE, Ihekweba AEC, Elliott M, Johnson JR, Gibney CA, Foreman BE, Nelson G, See V, Horton CA, Spiller DG, et al. (2004) Oscillations in NF-kappaB signaling control the dynamics of gene expression. *Science* **306**: 704–708.
  16. Collins P, Mitxitorena I, Carmody R (2016) The Ubiquitination of NF- $\kappa$ B Subunits in the Control of Transcription. *Cells* **5**: 23.
  17. Collins PE, Kiely P a., Carmody RJ (2014) Inhibition of transcription by B cell leukemia 3 (Bcl-3) protein requires interaction with nuclear factor  $\kappa$ B (NF- $\kappa$ B) p50. *J Biol Chem* **289**: 7059–7067.
  18. Zhang Q, Didonato JA, Karin M, McKeithan TW (1994) BCL3 encodes a nuclear protein which can alter the subcellular location of NF-kappa B proteins. *Mol Cell Biol* **14**: 3915–3926.
  19. Rosenfeld ME, Prichard L, Shiojiri N, Fausto N (2000) Prevention of hepatic apoptosis and embryonic lethality in RelA/TNFR-1 double knockout mice. *Am J Pathol* **156**: 997–1007.
  20. Deng J, Miller S a, Wang H-Y, Xia W, Wen Y, Zhou BP, Li Y, Lin S-Y, Hung M-C (2002) beta-catenin interacts with and inhibits NF-kappa B in human colon and breast cancer. *Cancer Cell* **2**: 323–334.

21. Fazal F, Minhajuddin M, Bijli KM, McGrath JL, Rahman A (2007) Evidence for actin cytoskeleton-dependent and -independent pathways for RelA/p65 nuclear translocation in endothelial cells. *J Biol Chem* **282**: 3940–3950.
22. Akiyama M, Hideshima T, Hayashi T, Tai Y-T, Mitsiades CS, Mitsiades N, Chauhan D, Richardson P, Munshi NC, Anderson KC (2003) Nuclear factor-kappaB p65 mediates tumor necrosis factor alpha-induced nuclear translocation of telomerase reverse transcriptase protein. *Cancer Res* **63**: 18–21.
23. Chen L-F, Williams S a, Mu Y, Nakano H, Duerr JM, Buckbinder L, Greene WC (2005) NF-kappaB RelA phosphorylation regulates RelA acetylation. *Mol Cell Biol* **25**: 7966–7975.
24. Kiernan R, Brès V, Ng RWM, Coudart M-P, El Messaoudi S, Sardet C, Jin D-Y, Emiliani S, Benkirane M (2003) Post-activation turn-off of NF-kappa B-dependent transcription is regulated by acetylation of p65. *J Biol Chem* **278**: 2758–2766.
25. Moles A, Sanchez AM, Banks PS, Murphy LB, Luli S, Borthwick L, Fisher A, O'Reilly S, van Laar JM, White SA, et al. (2013) Inhibition of RelA-Ser536 phosphorylation by a competing peptide reduces mouse liver fibrosis without blocking the innate immune response. *Hepatology* **57**: 817–828.
26. Kontgen F, Grumont RJ, Strasser a., Metcalf D, Li R, Tarlinton D, Gerondakis S (1995) Mice lacking the c-rel proto-oncogene exhibit defects in lymphocyte proliferation, humoral immunity, and interleukin-2 expression. *Genes Dev* **9**: 1965–1977.
27. Lu H, Yang X, Duggal P, Allen CT, Yan B, Cohen J, Nottingham L, Romano RA, Sinha S, King KE, et al. (2011) TNF- $\alpha$  promotes c-REL/ $\Delta$ Np63 $\alpha$  interaction and TAp73 dissociation from key genes that mediate growth arrest and apoptosis in head and neck cancer. *Cancer Res* **71**: 6867–6877.
28. Martin a G, Fresno M (2000) Tumor necrosis factor-alpha activation of NF-kappa B requires the phosphorylation of Ser-471 in the transactivation domain of c-Rel. *J Biol Chem* **275**: 24383–24391.
29. Huang DB, Chen YQ, Ruetsche M, Phelps CB, Ghosh G (2001) X-ray crystal

structure of proto-oncogene product c-Rel bound to the CD28 response element of IL-2. *Structure* **9**: 669–678.

30. Clark JM, Aleksiyadis K, Martin A, McNamee K, Tharmalingam T, Williams RO, Mémet S, Cope AP (2011) Inhibitor of kappa b epsilon ( $\text{ikB}\epsilon$ ) is a non-redundant regulator of c-rel-dependent gene expression in murine T and B cells. *PLoS One* **6**.
31. Garbati MR, Alço G, Gilmore TD (2010) Histone acetyltransferase p300 is a coactivator for transcription factor REL and is C-terminally truncated in the human diffuse large B-cell lymphoma cell line RC-K8. *Cancer Lett* **291**: 237–245.
32. Meyer CF, Wang X, Chang C, Templeton D, Tan TH (1996) Interaction between c-Rel and the mitogen-activated protein kinase kinase 1 signaling cascade in mediating  $\kappa\text{B}$  enhancer activation. *J Biol Chem* **271**: 8971–8976.
33. Dephoure N, Zhou C, Villén J, Beausoleil S a, Bakalarski CE, Elledge SJ, Gygi SP (2008) A quantitative atlas of mitotic phosphorylation. *Proc Natl Acad Sci U S A* **105**: 10762–10767.
34. Betts JC, Nabel GJ (1996) Differential regulation of NF-kappaB2(p100) processing and control by amino-terminal sequences. *Mol Cell Biol* **16**: 6363–6371.
35. Jacque E, Billot K, Authier H, Bordereaux D, Baud V (2012) RelB inhibits cell proliferation and tumor growth through p53 transcriptional activation. *Oncogene* **32**: 2661–2669.
36. Vogel CFA, Sciallo E, Matsumura F (2007) Involvement of RelB in aryl hydrocarbon receptor-mediated induction of chemokines. *Biochem Biophys Res Commun* **363**: 722–726.
37. Cartwright T, Perkins ND, L. Wilson C (2016) NFKB1: a suppressor of inflammation, ageing and cancer. *FEBS J* **283**: 1812–1822.
38. Cao S, Zhang X, Edwards JP, Mosser DM (2006) NF-kappaB1 (p50) homodimers differentially regulate pro- and anti-inflammatory cytokines in macrophages. *J Biol Chem* **281**: 26041–26050.

39. Lodish MB (2013) Clinical review: kinase inhibitors: adverse effects related to the endocrine system. *J Clin Endocrinol Metab* **98**: 1333–1342.
40. Lu ZY, Yu SP, Wei JF, Wei L (2006) Age-related neural degeneration in nuclear-factor  $\kappa$ B p50 knockout mice. *Neuroscience* **139**: 965–978.
41. Jhaveri K a, Ramkumar V, Trammell R a, Toth L a (2006) Spontaneous, homeostatic, and inflammation-induced sleep in NF-kappaB p50 knockout mice. *Am J Physiol Regul Integr Comp Physiol* **291**: R1516–R1526.
42. Sha WC, Liou HC, Tuomanen EI, Baltimore D (1995) Targeted disruption of the p50 subunit of NF-kappa B leads to multifocal defects in immune responses. *Cell* **80**: 321–330.
43. Campbell IK, Gerondakis S, O'Donnell K, Wicks IP (2000) Distinct roles for the NF-kappaB1 (p50) and c-Rel transcription factors in inflammatory arthritis. *J Clin Invest* **105**: 1799–1806.
44. Gerondakis S, Grossmann M, Nakamura Y, Pohl T, Grumont R (1999) Genetic approaches in mice to understand Rel/NF-kappaB and IkappaB function: transgenics and knockouts. *Oncogene* **18**: 6888–6895.
45. Parameswaran N, Pao CS, Leonhard KS, Dong SK, Kratz M, Ley SC, Benovic JL (2006) Arrestin-2 and G protein-coupled receptor kinase 5 interact with NF $\kappa$ B1 p105 and negatively regulate lipopolysaccharide-stimulated ERK1/2 activation in macrophages. *J Biol Chem* **281**: 34159–34170.
46. Minami M, Shimizu K, Okamoto Y, Folco E, Ilasaca ML, Feinberg MW, Aikawa M, Libby P (2008) Prostaglandin E receptor type 4-associated protein interacts directly with NF- $\kappa$ B1 and attenuates macrophage activation. *J Biol Chem* **283**: 9692–9703.
47. Hirai H, Fujisawa J, Suzuki T, Ueda K, Muramatsu M, Tsuboi A, Arai N, Yoshida M (1992) Transcriptional activator Tax of HTLV-1 binds to the NF-kappa B precursor p105. *Oncogene* **7**: 1737–1742.
48. Beinke S, Deka J, Lang V, Belich MP, Walker P a, Howell S, Smerdon SJ, Gamblin SJ, Ley SC (2003) NF-kappaB1 p105 negatively regulates TPL-2 MEK

- kinase activity. *Mol Cell Biol* **23**: 4739–4752.
49. Ghosh G, Duyne G Van, Ghosh S, Sigler PB (1995) Structure of NF-[kappa]B p50 homodimer bound to a [kappa]B site. *Nature* **373**: 303–310.
  50. Müller C, Rey F, Sodeoka M (1995) Structure of the NF- $\kappa$ B p50 homodimer bound to DNA. *Nature*.
  51. Demarchi F, Bertoli C, Sandy P, Schneider C (2003) Glycogen synthase kinase-3 $\alpha$  regulates NF- $\kappa$ B1/p105 stability. *J Biol Chem* **278**: 39583–39590.
  52. Lang V, Janzen J, Fischer GZ, Soneji Y, Beinke S, Salmeron A, Allen H, Hay RT, Ben-Neriah Y, Ley SC (2003) betaTrCP-mediated proteolysis of NF-kappaB1 p105 requires phosphorylation of p105 serines 927 and 932. *Mol Cell Biol* **23**: 402–413.
  53. Salmerón A, Janzen J, Soneji Y, Bump N, Kamens J, Allen H, Ley SC (2001) Direct Phosphorylation of NF- $\kappa$ B1 p105 by the I $\kappa$ B Kinase Complex on Serine 927 Is Essential for Signal-induced p105 Proteolysis. *J Biol Chem* **276**: 22215–22222.
  54. Demarchi F, Bertoli C, Sandy P, Schneider C (2003) Glycogen synthase kinase-3 beta regulates NF-kappa B1/p105 stability. *J Biol Chem* **278**: 39583–39590.
  55. Marshall, He; Stamler J (2001) Inhibition of NF- $\kappa$ B by S-nitrosylation. *Biochemistry* **40**: 1688–1693.
  56. Furia B, Deng L, Wu K, Baylor S, Kehn K, Li H, Donnelly R, Coleman T, Kashanchi F (2002) Enhancement of nuclear factor- $\kappa$ B acetylation by coactivator p300 and HIV-1 Tat proteins. *J Biol Chem* **277**: 4973–4980.
  57. Hou S, Guan H, Ricciardi RP (2003) Phosphorylation of serine 337 of NF-kappaB p50 is critical for DNA binding. *J Biol Chem* **278**: 45994–45998.
  58. Wilson CL, Jurk D, Fullard N, Banks P, Page a, Luli S, Elsharkawy a M, Gieling RG, Chakraborty JB, Fox C, et al. (2015) NF $\kappa$ B1 is a suppressor of neutrophil-driven hepatocellular carcinoma. *Nat Commun* **6**: 6818.
  59. Qiaozhen L, Xiaoyang Z, McIntosh T, Davis H, Nemeth JF, Pendley C, Wu SL, Hancock WS (2009) Development of different analysis platforms with LC-MS for

pharmacokinetic studies of protein drugs. *Anal Chem* **81**: 8715–8723.

60. Crawley CD, Raleigh DR, Kang S, Voce DJ, Schmitt AM, Weichselbaum RR, Yamini B (2013) DNA damage-induced cytotoxicity is mediated by the cooperative interaction of phospho-NF- $\kappa$ B p50 and a single nucleotide in the kb-site. *Nucleic Acids Res* **41**: 764–774.
61. Fliegau M, L. Bryant V, Frede N, Slade C, Woon ST, Lehnert K, Winzer S, Bulashevskaya A, Scerri T, Leung E, et al. (2015) Haploinsufficiency of the NF- $\kappa$ B1 Subunit p50 in Common Variable Immunodeficiency. *Am J Hum Genet* **97**: 389–403.
62. Tu YC, Huang DY, Shiah SG, Wang JS, Lin WW (2013) 1DUMMY Regulation of c-Fos gene expression by NF- $\kappa$ B: A p65 homodimer binding site in mouse embryonic fibroblasts but not human HEK293 cells. *PLoS One* **8**: 1–14.
63. Lee SK, Kim JH, Lee YC, Cheong J, Lee JW (2000) Silencing mediator of retinoic acid and thyroid hormone receptors, as a novel transcriptional corepressor molecule of activating protein-1, nuclear factor- $\kappa$ B, and serum response factor. *J Biol Chem* **275**: 12470–12474.
64. He B, Weber GF (2004) Synergistic activation of the CMV promoter by NF- $\kappa$ B P50 and PKG. *Biochem Biophys Res Commun* **321**: 13–20.
65. Rudders S, Gaspar J, Madore R, Volland C, Grall F, Patel A, Pellacani A, Perrella M a., Libermann T a., Oettgen P (2001) ESE-1 is a Novel Transcriptional Mediator of Inflammation that Interacts with NF- $\kappa$ B to Regulate the Inducible Nitric-oxide Synthase Gene. *J Biol Chem* **276**: 3302–3309.
66. Drew PD, Franzoso G, Carlson LM, Biddison WE, Siebenlist U, Ozato K (1995) Interferon regulatory factor-2 physically interacts with NF- $\kappa$ B in vitro and inhibits NF- $\kappa$ B induction of major histocompatibility class I and beta 2-microglobulin gene expression in transfected human neuroblastoma cells. *J Neuroimmunol* **63**: 157–162.
67. Uskoković A, Dinić S, Mihailović M, Grdović N, Arambašić J, Vidaković M, Bogojević D, Ivanović-Matić S, Martinović V, Petrović M, et al. (2012) STAT3/NF-

- κB interactions determine the level of haptoglobin expression in male rats exposed to dietary restriction and/or acute phase stimuli. *Mol Biol Rep* **39**: 167–176.
68. YU Z, ZHANG W, KONE BC (2002) Signal transducers and activators of transcription 3 (STAT3) inhibits transcription of the inducible nitric oxide synthase gene by interacting with nuclear factor κB. *Biochem J* **367**: 97–105.
  69. Wang D, Paz-Priel I, Friedman AD (2009) NF-kappa B p50 regulates C/EBP alpha expression and inflammatory cytokine-induced neutrophil production. *J Immunol* **182**: 5757–5762.
  70. Paz-Priel I, Houg S, Doohar J, Friedman a. D (2011) C/EBP and C/EBP oncoproteins regulate nfkb1 and displace histone deacetylases from NF- B p50 homodimers to induce NF-kB target genes. *Blood* **117**: 4085–4094.
  71. Oakley F, Mann J, Nailard S, Smart DE, Mungalsingh N, Constandinou C, Ali S, Wilson SJ, Millward-Sadler H, Iredale JP, et al. (2005) Nuclear factor-kappaB1 (p50) limits the inflammatory and fibrogenic responses to chronic injury. *Am J Pathol* **166**: 695–708.
  72. Wessells J, Baer M, Young H a., Claudio E, Brown K, Siebenlist U, Johnson PF (2004) BCL-3 and NF-kB p50 attenuate lipopolysaccharide-induced inflammatory responses in macrophages. *J Biol Chem* **279**: 49995–50003.
  73. Collins PE, Grassia G, Colleran A, Kiely P a., Ialenti A, Maffia P, Carmody RJ (2015) Mapping the interaction of B cell leukaemia 3 (Bcl-3) and nuclear factor κB (NF-κB) p50 identifies a Bcl-3-mimetic anti-inflammatory peptide. *J Biol Chem* **3**: jbc.M115.643700.
  74. Mariño-Ramírez L, Kann MG, Shoemaker BA, Landsman D (2005) Histone structure and nucleosome stability. *Expert Rev Proteomics* **2**: 719–729.
  75. Ghirlando R, Felsenfeld G (2016) CTCF: Making the right connections. *Genes Dev* **30**: 881–891.
  76. Moore LD, Le T, Fan G (2013) DNA methylation and its basic function. *Neuropsychopharmacology* **38**: 23–38.

77. Zhang Y, Reinberg D (2001) Transcription regulation by histone methylation: Interplay between different covalent modifications of the core histone tails. *Genes Dev* **15**: 2343–2360.
78. Rossetto D, Avvakumov N, Côté J (2012) Histone phosphorylation: A chromatin modification involved in diverse nuclear events. *Epigenetics* **7**: 1098–1108.
79. Eberharter A, Becker PB (2002) Histone acetylation: A switch between repressive and permissive chromatin. Second in review on chromatin dynamics. *EMBO Rep* **3**: 224–229.
80. Yan C, Boyd DD (2006) Histone H3 Acetylation and H3 K4 Methylation Define Distinct Chromatin Regions Permissive for Transgene Expression. *Mol Cell Biol* **26**: 6357–6371.
81. Gates LA, Shi J, Rohira AD, Feng Q, Zhu B, Bedford MT, Sagum CA, Jung SY, Qin J, Tsai MJ, et al. (2017) Acetylation on histone H3 lysine 9 mediates a switch from transcription initiation to elongation. *J Biol Chem* **292**: 14456–14472.
82. Karmodiya K, Krebs AR, Oulad-Abdelghani M, Kimura H, Tora L (2012) H3K9 and H3K14 acetylation co-occur at many gene regulatory elements, while H3K14ac marks a subset of inactive inducible promoters in mouse embryonic stem cells. *BMC Genomics* **13**:
83. Kurdistani SK, Tavazoie S, Grunstein M (2004) Mapping global histone acetylation patterns to gene expression. *Cell* **117**: 721–733.
84. Majumder S, Alinari L, Roy S, Miller T, Datta J, Sif S, Baiocchi R, Jacob ST (2010) Methylation of histone H3 and H4 by PRMT5 regulates ribosomal RNA gene transcription. *J Cell Biochem* **109**: 553–563.
85. Bauer UM, Daujat S, Nielsen SJ, Nightingale K, Kouzarides T (2002) Methylation at arginine 17 of histone H3 is linked to gene activation. *EMBO Rep* **3**: 39–44.
86. Activity G, Wang L, Joshi P, Miller EL, Higgins L, Slattery M, Simon JA (2018) A Role for Monomethylation of Histone H3-K27 in. **208**: 1023–1036.
87. Warren E, Temple B, Grewal SIS, Strahl BD (2005) Histone H3 K36 Methylation Is

Associated with Transcription Elongation in. *Microbiology* **4**: 1446–1454.

88. Rossodivita AA, Boudoures AL, Mecoli JP, Steenkiste EM, Karl AL, Vines EM, Cole AM, Ansbro MR, Thompson JS (2014) Histone H3 K79 methylation states play distinct roles in UV-induced sister chromatid exchange and cell cycle checkpoint arrest in *Saccharomyces cerevisiae*. *Nucleic Acids Res* **42**: 6286–6299.
89. Sawicka A, Seiser C (2012) Histone H3 phosphorylation - a versatile chromatin modification for different occasions. *Biochimie* **94**: 2193–2201.
90. Dokmanovic M, Clarke C, Marks P a (2007) Histone deacetylase inhibitors: overview and perspectives. *Mol Cancer Res* **5**: 981–989.
91. Oh YM, Kwon YE, Kim JM, Bae SJ, Lee BK, Yoo SJ, Chung CH, Deshaies RJ, Seol JH (2009) Chfr is linked to tumour metastasis through the downregulation of HDAC1. *Nat Cell Biol* **11**: 295–302.
92. Choudhary C, Kumar C, Gnad F, Nielsen ML, Rehman M, Walther TC, Olsen J V, Mann M (2009) Lysine acetylation targets protein complexes and co-regulates major cellular functions. *Science* **325**: 834–840.
93. Pflum MKH, Tong JK, Lane WS, Schreiber SL (2001) Histone Deacetylase 1 Phosphorylation Promotes Enzymatic Activity and Complex Formation. *J Biol Chem* **276**: 47733–47741.
94. Liu Y, Smith PW, Jones DR (2006) Breast cancer metastasis suppressor 1 functions as a corepressor by enhancing histone deacetylase 1-mediated deacetylation of RelA/p65 and promoting apoptosis. *Mol Cell Biol* **26**: 8683–8696.
95. Millard CJ, Watson PJ, Celardo I, Gordiyenko Y, Cowley SM, Robinson C V., Fairall L, Schwabe JWR (2013) Class I HDACs share a common mechanism of regulation by inositol phosphates. *Mol Cell* **51**: 57–67.
96. Sommer A, Hilfenhaus S, Menkel A, Kremmer E, Seiser C, Loidl P, Lüscher B (1997) Cell growth inhibition by the Mad/Max complex through recruitment of histone deacetylase activity. *Curr Biol* **7**: 357–365.

97. Basta J, Rauchman M (2015) The nucleosome remodeling and deacetylase complex in development and disease. *Transl Res* **165**: 36–47.
98. You A, Tong JK, Grozinger CM, Schreiber SL (2001) CoREST is an integral component of the CoREST- human histone deacetylase complex. *Proc Natl Acad Sci* **98**: 1454–1458.
99. Perkins ND, Gilmore TD (2006) Good cop, bad cop: the different faces of NF- $\kappa$ B. *Cell Death Differ* **13**: 759–772.
100. Arenzana-Seisdedos F, Turpin P, Rodriguez M, Thomas D, Hay RT, Virelizier JL, Dargemont C (1997) Nuclear localization of I kappa B alpha promotes active transport of NF-kappa B from the nucleus to the cytoplasm. *J Cell Sci* **110** ( Pt 3): 369–378.
101. Laín de Lera T, Folgueira L, Martín AG, Dargemont C, Pedraza M-A, Bermejo M, Bonay P, Fresno M, Alami J (1999) Expression of I $\kappa$ B $\alpha$  in the nucleus of human peripheral blood T lymphocytes. *Oncogene* **18**: 1581–1588.
102. Bandyopadhyaya A, Tsurumi A, Rahme LG (2017) NF- $\kappa$ Bp50 and HDAC1 interaction is implicated in the host tolerance to infection mediated by the bacterial quorum sensing signal 2-aminoacetophenone. *Front Microbiol* **8**: 1–11.
103. Zhong H, May MJ, Jimi E, Ghosh S (2002) The Phosphorylation Status of Nuclear NF- $\kappa$ B Determines Its Association with CBP/p300 or HDAC-1. *Mol Cell* **9**: 625–636.
104. Elsharkawy AM, Oakley F, Lin F, Packham G, Mann D a, Mann J (2010) The NF- $\kappa$ B p50:p50:HDAC-1 repressor complex orchestrates transcriptional inhibition of multiple pro-inflammatory genes. *J Hepatol* **53**: 519–527.
105. Pettersen EF, Goddard TD, Huang CC, Couch GS, Greenblatt DM, Meng EC, Ferrin TE (2004) UCSF Chimera -A visualization system for exploratory research and analysis. *J Comput Chem* **25**: 1605–1612.
106. Berkowitz B, Huang D Bin, Chen-Park FE, Sigler PB, Ghosh G (2002) The X-ray crystal structure of the NF- $\kappa$ B p50-p65 heterodimer bound to the interferon  $\beta$ - $\kappa$ B site. *J Biol Chem* **277**: 24694–24700.

107. Fusco A, Huang DB, Miller D, Vu D, Ghosh G NF-kappaB p52:RelB heterodimer uses different binding modes to recognize different kappaB DNA. *TO BE Publ.*
108. Tovchigrechko A VI (2006) GRAMM-X public web server for protein-protein docking. *Nucleic Acids Res* **34**: 310–304.
109. Cavallo L, Kleinjung J, Fraternali F (2003) POPS: A fast algorithm for solvent accessible surface areas at atomic and residue level. *Nucleic Acids Res* **31**: 3364–3366.
110. Preparation of Chemical Competent Cells, Last updated 2008, Accessed on 2008.
111. Kramer A, Schneider-Mergener J (1998) Synthesis and Screening of Peptide Libraries on Continuous Cellulose Membrane Supports BT - Combinatorial Peptide Library Protocols. In Cabilly S (ed.) pp 25–39. Humana Press, Totowa, NJ.
112. Fagerlund R, Kinnunen L, Köhler M, Julkunen I, Melén K (2005) NF- $\kappa$ B Is Transported into the Nucleus by Importin  $\alpha$ 3 and Importin  $\alpha$ 4. *J Biol Chem* **280**: 15942–15951.
113. Sengchanthalangsy LL, Datta S, Huang DB, Anderson E, Braswell EH, Ghosh G (1999) Characterization of the dimer interface of transcription factor NFkappaB p50 homodimer. *J Mol Biol* **289**: 1029–1040.
114. Cartwright T, Perkins ND, L. Wilson C (2016) NFKB1: a suppressor of inflammation, ageing and cancer. *FEBS J* **283**: 1812–1822.
115. Ganchi P a, Sun SC, Greene WC, Ballard DW (1993) A novel NF-kappa B complex containing p65 homodimers: implications for transcriptional control at the level of subunit dimerization. *Mol Cell Biol* **13**: 7826–7835.
116. Huang D Bin, Huxford T, Chen YQ, Ghosh G (1997) The role of DNA in the mechanism of NFk $\kappa$ B dimer formation: Crystal structures of the dimerization domains of the p50 and p65 subunits. *Structure* **5**: 1427–1436.
117. Wan F, Lenardo MJ (2009) Specification of DNA binding activity of NF-kappaB proteins. *Cold Spring Harb Perspect Biol* **1**: a000067.

118. Wang VY-F, Huang W, Asagiri M, Spann N, Hoffmann A, Glass C, Ghosh G (2012) The Transcriptional Specificity of NF- $\kappa$ B Dimers Is Coded within the  $\kappa$ B DNA Response Elements. *Cell Rep* **2**: 824–839.
119. Jacque E, Tchenio T, Piton G, Romeo P-H, Baud V (2005) RelA repression of RelB activity induces selective gene activation downstream of TNF receptors. *Proc Natl Acad Sci U S A* **102**: 14635–14640.
120. Huxford T, Ghosh G (2009) A structural guide to proteins of the NF-kappaB signaling module. *Cold Spring Harb Perspect Biol* **1**: a000075.
121. Tsui R, Kearns JD, Lynch C, Vu D, Ngo KA, Basak S, Ghosh G, Hoffmann A (2015) I $\kappa$ B $\beta$  enhances the generation of the low-affinity NF[ $\kappa$ ]B/RelA homodimer. *Nat Commun* **6**:
122. Ashkenazi S, Plotnikov A, Bahat A, Ben-Zeev E, Warszawski S, Dikstein R (2016) A Novel Allosteric Mechanism of NF- $\kappa$ B Dimerization and DNA Binding Targeted by an Anti-Inflammatory Drug. *Mol Cell Biol* **36**: 1237–1247.
123. Zhong H, May MJ, Jimi E, Ghosh S (2002) The Phosphorylation Status of Nuclear NF-KB Determines Its Association with CBP/p300 or HDAC-1. *Mol Cell* **9**: 625–636.
124. Malek S, Huang D Bin, Huxford T, Ghosh S, Ghosh G (2003) X-ray crystal structure of an I $\kappa$ B $\beta$ ·NF- $\kappa$ B p65 homodimer complex. *J Biol Chem* **278**: 23094–23100.
125. Cho J, Tschlis PN (2005) Phosphorylation at Thr-290 regulates Tpl2 binding to NF-kappaB1/p105 and Tpl2 activation and degradation by lipopolysaccharide. *Proc Natl Acad Sci U S A* **102**: 2350–2355.
126. Jurk D, Wilson C, Passos JF, Oakley F, Correia-Melo C, Greaves L, Saretzki G, Fox C, Lawless C, Anderson R, et al. (2014) Chronic inflammation induces telomere dysfunction and accelerates ageing in mice. *Nat Commun* **2**: 4172.
127. Collins PE, Kiely P a, Carmody RJ (2014) Inhibition of transcription by B cell Leukemia 3 (Bcl-3) protein requires interaction with nuclear factor  $\kappa$ B (NF- $\kappa$ B) p50. *J Biol Chem* **289**: 7059–7067.